

## Review

## Need and vision for global medium-resolution Landsat and Sentinel-2 data products



Volker C. Radeloff<sup>a,\*</sup>, David P. Roy<sup>b</sup>, Michael A. Wulder<sup>c</sup>, Martha Anderson<sup>d</sup>, Bruce Cook<sup>e</sup>, Christopher J. Crawford<sup>f</sup>, Mark Friedl<sup>g</sup>, Feng Gao<sup>d</sup>, Noel Gorelick<sup>h</sup>, Matthew Hansen<sup>i</sup>, Sean Healey<sup>j</sup>, Patrick Hostert<sup>k,l</sup>, Glynn Hulley<sup>m</sup>, Justin L. Huntington<sup>n</sup>, David M. Johnson<sup>o</sup>, Chris Neigh<sup>e</sup>, Alexei Lyapustin<sup>e</sup>, Leo Lymburner<sup>p</sup>, Nima Pahlevan<sup>e</sup>, Jean-Francois Pekel<sup>q</sup>, Theodore A. Scambos<sup>r</sup>, Crystal Schaaf<sup>s</sup>, Peter Strobl<sup>q</sup>, Curtis E. Woodcock<sup>g</sup>, Hankui K. Zhang<sup>t</sup>, Zhe Zhu<sup>u</sup>

<sup>a</sup> SILVIS Lab, Department of Forest and Wildlife Ecology, University of Wisconsin-Madison, 1630 Linden Drive, Madison, WI 53706, USA<sup>b</sup> Department of Geography, Environment, and Spatial Sciences, & Center for Global Change and Earth Observations, Michigan State University, MI 48824, USA<sup>c</sup> Canadian Forest Service, Pacific Forestry Centre, Natural Resources Canada, 506 West Burnside Road, Victoria, British Columbia V8Z 1M5, Canada<sup>d</sup> USDA-ARS, Hydrology and Remote Sensing Laboratory, 10300 Baltimore Avenue, Beltsville, MD 20705, USA<sup>e</sup> NASA, Goddard Space Flight Center, Science and Exploration Directorate, Greenbelt, MS 20771, USA<sup>f</sup> USGS, Earth Resources Observation and Science (EROS) Center, 47914 252<sup>nd</sup> Street, Sioux Falls, SD 57198, USA<sup>g</sup> Department of Earth and Environment, Boston University 675 Commonwealth Avenue, Boston, MA 02215, USA<sup>h</sup> Google Switzerland, Brandschenkestrasse 110, Zurich 8002, Switzerland<sup>i</sup> Department of Geographical Sciences, University of Maryland, 7251 Preinkert Drive, College Park, MD 20742, USA<sup>j</sup> US Forest Service, Rocky Mountain Research Station, 4919 S 1500 W, Riverdale, UT 84405, USA<sup>k</sup> Geography Department, Humboldt-Universität zu Berlin, Unter den Linden 6, 10099 Berlin, Germany<sup>l</sup> Integrative Research Institute on Transformations of Human-Environment Systems (IRI THESys), Humboldt-Universität zu Berlin, Unter den Linden 6, 10099 Berlin, Germany<sup>m</sup> Jet Propulsion Laboratory, California Institute of Technology, 4800 Oak Grove Drive, Pasadena, CA 91109, USA<sup>n</sup> Division of Hydrologic Sciences, Desert Research Institute, Reno, NV 89512, USA<sup>o</sup> USDA, National Agricultural Statistics Service, 1400 Independence Ave., SW, Washington, DC 20250, USA<sup>p</sup> National Earth and Marine Observation Group, Geoscience Australia, 101 Jerrabomberra Ave, Symonston, ACT 2609, Australia<sup>q</sup> Joint Research Center, European Commission, Via Enrico Fermi 27149, 21027 Ispra, VA, Italy<sup>r</sup> Earth Observation Center, CIRES, University of Colorado Boulder, Boulder, CO 80301, USA<sup>s</sup> School for the Environment, University of Massachusetts Boston, 100 Morrissey Blvd, Boston, MA 02125, USA<sup>t</sup> Geospatial Sciences Center of Excellence, Department of Geography and Geospatial Sciences, South Dakota State University, Brookings, SD 57007, USA<sup>u</sup> Department of Natural Resources and the Environment, University of Connecticut, Storrs, CT 06269, USA

## ARTICLE INFO

Edited by Jing M. Chen

## Keywords:

High-level data products  
Analysis Ready Data  
global change monitoring  
Harmonized Landsat Sentinel-2 data

## ABSTRACT

Global changes in climate and land use are threatening natural ecosystems, biodiversity, and the ecosystem services people rely on. This is why it is necessary to track and monitor spatiotemporal change at a level of detail that can inform science, management, and policy development. The current constellation of multiple Landsat and Sentinel-2 satellites collecting imagery at predominantly  $\leq 30\text{-m}$  spatial resolution affords an opportunity for the generation of global medium-resolution products every few days. Our goal is to both identify the information needs and provide direction towards the generation of a suite of global, high-level, systematically-generated, medium-resolution products designed for both management and science. Our vision builds on the success of the NASA MODIS/VIIRS product suite, while recognizing the unique strengths of medium-resolution satellite data given their higher spatial resolution and longer time series. We propose a suite of 13 essential products that enable the characterization of the current state and changes in the biosphere, cryosphere, and hydrosphere, and would fill information needs identified by the Committee on Earth Observation Satellites for the Global Climate Observing System and the Global Terrestrial Observing System, by the National Research Council of the US National Academies in the decadal survey, and by others. These products are: land cover, land cover change,

\* Corresponding author.

E-mail address: [radeloff@wisc.edu](mailto:radeloff@wisc.edu) (V.C. Radeloff).

burned area, forest loss, vegetation indices, phenology, dynamic habitat indices, albedo, land surface temperature, snow cover, ice extent, surface water extent, and evapotranspiration. Furthermore, we provide a list of desirable products poised for addition to the essential products (e.g., crop type, emissivity, and ice sheet velocity). Lastly, we suggest aspirational products requiring further algorithm development (e.g., forest structure and crop yield). For the identified essential products, algorithms are in place, making it feasible to begin generating products systematically. These products should be accompanied by quality and accuracy assessments undertaken following consensus protocols. Five decades after the first Landsat satellite, and two decades after the MODIS products were first produced, it is time now for readily available, standardized, and consistent high-level products built upon medium-resolution imagery, thereby fulfilling the promise and the vision that inspired the Landsat program since its inception.

## 1. Introduction

Humans rely on the benefits of natural ecosystems, but climate and land-use change threaten many of these benefits (IPCC, 2021; MA, 2005). Human population increase and activity since the agrarian and industrial revolutions have caused global changes beyond natural variability (Foley et al., 2005; Steffen et al., 2015). Scientific understanding, monitoring, modeling, and management of the Earth system and of global change processes requires free and nondiscriminatory distribution of accurate, consistent and unbiased monitoring data, for which satellite observations are fundamentally important. There has long been recognition of the need and utility of satellite data for studying global change (Justice et al., 1985; Kaufman et al., 1998; NASA et al., 1986; NRC, 1990; Sellers et al., 1995). To date, high-level global products derived consistently and systematically from satellite data have been generated at coarse (100-1,000 m) spatial resolution. However, coarse spatial resolution data may not resolve many global change processes and terrestrial phenomena apparent at medium (10 m to 100 m) and high (<10 m) spatial resolution. High spatial and temporal resolution data with global coverage are becoming available from commercial satellite constellations, but currently these data are collected with a smaller number of multi-spectral bands that are not rigorously calibrated and corrected for atmospheric effects and sun-sensor geometry without cross-calibration with other satellites (Roy et al., 2021). Gridded, medium-resolution ‘higher-level’ global products that have been subject to geophysical transformations and processed to derive environmental variables over different time periods (weekly, monthly, seasonal, annual) are needed by the user community, as has been suggested by the Landsat Science Team (Roy et al., 2014b). The products should be generated on a systematic basis and subject to routine quality assessment and validation, with reprocessing as needed. The continued availability of Landsat observations, initiated in 1972 with Landsat-1 through the 2021 Landsat-9 mission (Masek et al., 2020), combined with the Landsat-like Sentinel-2A, -2B and planned Sentinel-2C and -2D missions (Drusch et al., 2012), provide a unique opportunity to generate such products.

The widespread use of existing coarse-resolution data products demonstrates the strong demand for systematically derived, high-level products. The Advanced Very High Resolution Radiometer (AVHRR) sensor series have been in operation since 1978 and provide global daily coverage at coarse to very-coarse spatial resolution (1 - 15 km, (Cracknell, 1997)). The AVHRR data, particularly in the first several decades, were suboptimal for terrestrial monitoring due to a number of factors, including lack of visible wavelength calibration and substantial orbit drift (Giglio and Roy, 2020). Despite this, AVHRR data were used with substantial investment to generate the first global coverage land products (Townshend, 1994). The NASA Moderate Resolution Imaging Spectroradiometer (MODIS) program built on this heritage to systematically generate a suite of high-level, global land, ocean, and atmospheric data products that have revolutionized global change research and applications (Justice et al., 1998), with instrumentation evolution and continuity provided by the Visible Infrared Imaging Radiometer Suite (VIIRS). However, the MODIS record started in 2000 whereas the Landsat record began in 1972, and full global repeat Landsat 30-m

coverage has been available since the 1990s (Wulder et al., 2016), which means that longer-term trends can be captured. The Sentinel-2 systems, launched in 2015 and 2017, provide 10-, 20- and 60-m multispectral reflective wavelength observations that complement Landsat capabilities, and together provide high temporal global coverage for common visible to short wavelength infrared (VSWIR) bands until at least the early 2030s.

While there are only a few large-area data products derived systematically from medium-resolution satellite imagery, those that are available support key applications and scientific advances. At national scale, examples include the United States Geological Survey’s (USGS) National Land Cover Data (NLCD) (Homer et al., 2020) and the United States Department of Agriculture’s (USDA) Crop Data Layer (CDL) (Boryan et al., 2011), which are both generated on a systematic basis. At global scale, several medium-resolution products have been developed such as global land cover (Chen et al., 2015), forest dynamics (Hansen et al., 2013), and surface water dynamics (Pekel et al., 2016). The uptake of these existing medium-resolution data products attests to their relevance, but also highlights the lack of a full suite of other products needed to inform global change and terrestrial, cryosphere, and aquatic applications.

Substantial advances in computing provide new and timely opportunities to produce global, medium-resolution products. These include increasing storage capabilities, multi-core processing, graphical processing units, cloud computing, and high bandwidth internet. Landsat data distribution via the internet, which once was a limitation for many users (Roy et al., 2010), has now become the norm (Zhu et al., 2019b). Analysis Ready Data (ARD) have been developed to reduce the pre-processing burden on users and provide direct access to user-friendly products. For example, the USGS provides Landsat tiled, top-of-atmosphere and atmospherically corrected ARD defined in a common equal area projection, accompanied by spatially explicit quality assessment and cloud mask information over the conterminous United States (CONUS), Alaska, and Hawaii for the Landsat-4/5/7/8/9 30-m archive (Dwyer et al., 2018). Methods to improve the harmonization among Landsat sensors, for example, to account for differences in the spectral response functions of similar bands on different Landsat sensors (Berner et al., 2020; Roy et al., 2016a), and between Landsat and Sentinel-2 sensors (Chastain et al., 2019; Wulder et al., 2021) have been developed. Furthermore, planning is underway to extend the ARD products to include Landsat-1 to Landsat-5 Multispectral Scanner System (MSS) data (Crawford et al., 2023), and the generation of global coverage Landsat ARD products is being considered (Wulder et al., 2022). For example, multi-sensor ARD are being developed by the NASA Harmonized Landsat Sentinel-2 (HLS) project, which generates products similar to the Landsat ARD but harmonizes Landsat-8 (and since May 2022, Landsat-9), Sentinel-2A and -2B data to a common 30-m product from 2015 onwards in the Sentinel-2 tile grid (Claverie et al., 2018), and the European Space Agency’s (ESA) Sen2Like algorithms is designed for a common 10-m product (Saunier et al., 2022). In addition, the two sensors complement each other well in that Landsat provides thermal measurements, whereas Sentinel-2 has additional reflective wavelength bands, for example red edge bands, which allow plant functional traits such as leaf chlorophyll content to be estimated.

Our goal in this paper is to both synthesize the information needs and articulate a vision for a suite of medium-resolution, high-level, global, systematically generated products derived from Landsat and Sentinel-2 data. First, we highlight the *information needs* for global change science and management that require medium-resolution products. Second, we provide a *vision for a suite of high-level products*, which we categorize as either (a) essential, of highest importance, and for which algorithms are mature (land cover, land cover change, burned area, forest loss, vegetation indices, phenology, dynamic habitat indices, albedo, land surface temperature, snow cover, ice extent, surface water extent, and evapotranspiration), (b) desirable, also technically feasible now, but for which demand is not quite as pressing and user communities are smaller, or (c) aspirational, that are in need of further research and algorithm development.

## 2. Information needs for sustainable management, societal benefit, and global change challenges

Mitigating and adapting to global change requires consistent, long-term monitoring and modelling of the Earth System (land, cryosphere, ocean, and atmosphere). Globally, the need for such monitoring has been identified by the Millennium Ecosystem Assessment (MA, 2005), the Rio+20 United Nations Conference on Sustainable Development (UN, 2012), and the assessment of planetary boundaries by the Stockholm Resilience Center (Steffen et al., 2015). The United Nations Framework Convention on Climate developed the requirements and recommendations for a Global Climate Observing System (GCOS, 2016, 2021). In its latest implementation plan, GCOS highlighted the need for systematic and consistent observation as the basis for long time series, but also urgency to provide near-real time information (GCOS, 2022). In support of GCOS, the Global Terrestrial Observing System (GTOS) was set up to facilitate the observation, modeling, and analysis of terrestrial ecosystems. Similarly, the Committee on Earth Observation Satellites (CEOS), and especially its virtual constellation on Land Surface Imaging (LSI-VC) with its thematic subgroups on Forests & Biomass, and on Global Agricultural Monitoring (GEOGLAM), have defined information needs for terrestrial land monitoring. Within the US, the latest Decadal Survey of the National Research Council (NRC, 2018) identified 35 key science and applications priorities including key geophysical observables and measurement parameters.

Prior conventions and committees have established general information needs for management and global change science, but often without explicit consideration of the necessary data characteristics to meet those needs. Our contribution here is to highlight the extent to which those established information needs can and should be met via systematic satellite data products derived from medium-resolution Landsat and Sentinel-2 imagery (Table 1). We group these information needs into five thematic areas: climate change, biodiversity conservation, sustainable management and ecosystem services, food security,

and natural hazards.

Information needs related to *climate change* fall broadly into two main categories. First, there is information needed to better understand the drivers of climate change, especially the global carbon cycle, including sources of carbon emissions and sequestration stores. For example, carbon loss due to deforestation and emissions from biomass burning are important information needs, which motivate the GOFC-GOLD program (<https://gofcgold.umd.edu/>). Accordingly, the Paris Agreement of the United National Framework Convention on Climate Change mandates an assessment of progress towards its goals called the global stocktake for which satellite observations are essential (Hegglin et al., 2022; Ochiai et al., 2023). Second, there is a need to monitor the effects of climate change. For example, the United Nations Framework Convention on Climate Change highlights information needs for the cryosphere, including snow cover, the speed at which glaciers and ice sheets flow, and the distribution of sea ice (GCOS, 2016). The critical information needs related to climate change have led to the development of the Essential Climate Variables (ECVs), many of which require satellite data to monitor, but are currently only starting to become available at medium resolution.

Global *biodiversity* declines were the impetus for the UN Convention on Biological Diversity, which was passed at the UN Conference on Environment and Development in Rio de Janeiro in 1992. Since then, 15 meetings of the Conference of Parties have taken place, including the 15<sup>th</sup> meeting in Kunming-Montreal where the Global Biodiversity Framework was passed (UNCBD, 2022) that include a target to effectively conserve at least 30% of terrestrial, inland water, and coastal and marine areas (Target 3). The strategic plan of the framework stated the need for global biodiversity monitoring (Target 20) with the Global Biodiversity Information Facility (GBIF, 2022) focused on *in situ* observations, and the GEO-Biodiversity Observation Network (GEO-BON, 2022) emphasizing satellite-derived indicators and the Essential Biodiversity Variables (EBVs) (Pereira et al., 2013; Pettorelli et al., 2016) to quantify change in the state of biodiversity (Scholes et al., 2012; Turner et al., 2003).

To address *food security*, the Group of Twenty (G20) countries met in 2011 in France and ratified a declaration regarding food security called Actional Plan on Food Price Volatility and Agriculture (G20, 2011) in response to agricultural commodity price fluctuations that began during the 2007-2008 global financial crisis. Out of this came a major initiative called the Global Agricultural Geo-Monitoring (GLAM) with the goal of “strengthening global agricultural monitoring by improving the use of remote sensing tools for crop production projections and weather forecasting.” Ultimately, this became organized within the United Nations (UN) Group on Earth Observations (GEO) and is known fully as GEOGLAM. Over the past decade GEOGLAM has evolved from establishing best practices and satellite needs for crop production monitoring, particularly in terms of spatial resolution and revisit rate, to understanding how this imagery can help in meeting UN

**Table 1**

Information needs for the five major thematic areas related to sustainable management, societal benefits, and global change challenges. ‘High’ means that there is a strong information need for a given societal benefit of global change challenge.

Societal benefit or global change challenge		Climate change	Biodiversity conservation	Food security	Sustainable management and ecosystem services	Natural hazards
Information needs						
Biosphere	Land cover and land use	High	High	High	High	Medium
	Vegetation condition and phenology	High	High	High	High	High
	Biodiversity and faunal habitat	Low	High	Low	High	Low
	Disturbances	High	High	High	High	High
Cryosphere	Surface energy balance	High	Medium	High	Low	Medium
	Snow cover	High	Medium	Medium	Medium	Medium
Hydrosphere	Ice sheets and glaciers	High	Low	Medium	Low	Low
	Freshwater and marine ecosystems	High	High	High	High	High
	Evapotranspiration	High	Low	High	High	Medium

Sustainable Development Goals (Whitcraft et al., 2022). A number of regional- to continental-scale crop monitoring programs exist (Fritz et al., 2019), which typically have supranational or governmental support, for example from the European Commission, or from U.S. and Chinese agencies. Crop monitoring data have proven invaluable for rapid, synoptic assessment of regional areas. However, the majority of these crop monitoring programs are based on satellite data with coarse spatial resolution, limiting their value for more localized food security initiatives. This is particularly true in those parts of the world where food security is lower, and where fields are typically small, intercropped, and surrounded by complex landscapes. Medium-resolution crop monitoring data are essential to ensure food security in these environments.

Regarding *sustainable management and ecosystem services*, the UN's Sustainable Development Goals (SDG) (UN, 2017) highlight manifold and urgent information needs for management and continued provisioning of ecosystem services. For example, land cover maps are essential for SDG 6, the protection and restoration of water-related ecosystems including mountains, forests, and wetlands, and the monitoring of aquatic ecosystems, and for SDG 15.1, the conservation, restoration and sustainable use of ecosystems and their services. Closely related are maps of forest area, and ideally maps of forest structure that are necessary for SDG 15.2., the sustainable management for forests. Similarly, maps of urban land cover and form are required for SDG 11.3, inclusive and sustainable urbanization. Evapotranspiration (ET), as a metric of consumptive water use and ecosystem health, is a information need for many SDGs. Both monitoring of management and decision support aimed at ensuring the continued provisioning of ecosystem services would greatly benefit from medium-resolution data products because medium-resolution satellite data match the scale of land management units such as crop fields, forest stands, or urban subdivisions in many parts of the world, while coarse-resolution imagery does not.

Several *natural hazards* have important information needs that can be met with moderate-resolution data. For example, desertification is a natural hazard with clearly established information needs (UNCCD, 2013) that is best monitored with medium-resolution satellite data. Wildfires are another important natural hazard, both because of the risk they pose to human lives, homes, and livelihoods (Schug et al., 2023), and the impacts they have on ecosystems and climate (GCOS, 2016). Medium-resolution satellite data do not currently have the temporal frequency to adequately capture active fires (Wooster et al., 2021), but can map burned areas more accurately than coarse resolution satellite data (Chuvieco et al., 2019). Frequent medium-resolution satellite imagery is required to capture the spatial extents of flooding events (Heimhuber et al., 2018), as well as damage from hurricanes, tornadoes,

and hailstorms. Anomalies in evapotranspiration derived from thermal infrared imagery have proven to be an effective early signal of developing flash drought (Otkin et al., 2013), with medium-resolution imagery revealing drought impacts of fields (Yang et al., 2021a) or forest stands (Yang et al., 2021b). Understanding the extent and impacts of natural hazards is especially important given that more frequent extreme weather fluctuations are expected due to climate change.

### 3. The proposed suite of high-level, medium-resolution products

Based on the above articulated information needs for the five major thematic areas related to sustainable management, societal benefits, and global change challenges, we identified a suite of products that can be derived from medium-resolution satellite imagery (Table 2). In many cases, a given product meets the information needs for more than one of the five thematic areas. For example, land cover data are essential for food security, land management, climate change, and biodiversity assessments. Among all products, we separated those that are essential, and required by large user communities, from others that are desirable, but have smaller user communities. High-level derived products should preferably be generated using community-endorsed algorithms, i.e., ones that have been selected competitively by scientific peer review and/or that are published in the literature. We do not advocate specific algorithms but rather outline the required characteristics of the resulting products. Similarly, it is beyond the scope and intent of this paper to prescribe computational solutions and procedures for higher level product generation. We assume that some form of global ARD similar to the USGS Landsat ARD or the NASA global HLS are available, because systematic product generation requires radiometrically and geometrically calibrated satellite data including cloud masking, atmospheric correction, and addressing bi-directional reflectance effects as detailed in Claverie et al. (2018), Roy et al. (2019) and Saunier et al. (2022). As new satellite data are acquired, they should be subject to the same ARD processing and characterization to ensure that they are temporally consistent. We also assume that, following standard practice, per-pixel quality assessment information is part of all products to help ensure correct product utility.

As products are generated, routine quality assessment should be undertaken, typically by product examination at different temporal and spatial scales, which is necessary given the large number of factors that can adversely affect product quality (for a detailed discussion see Roy et al., 2002). In addition, each product's accuracy needs to be validated periodically to ensure appropriate scientific use. Validation should follow community-endorsed procedures that are necessarily product-specific but are typically undertaken by comparison with a

**Table 2**

Medium-resolution satellite image-based products that meet the identified information needs for sustainable management, societal benefits, and global change challenges.

Product categories		Essential products	Desirable products	Aspirational products
Information need				
Biosphere	Land cover	- Land cover - Land cover change	- Crop types - Irrigated fields - Abandonment - Forest loss agent	- Forest types, and tree species - Urban structure  - Forest recovery
	Disturbances	- Burned area - Forest loss	- LAI/FAPAR - Green vegetation cover fraction	- Crop yield - Forest Biomass - Habitat heterogeneity - Winter habitat indices - Net radiation
	Vegetation condition and phenology	- Vegetation indices - Phenology	- Dynamic habitat indices	
	Biodiversity	- Albedo - Land surface temperature	- Emissivity	
	Surface energy balance	- Snow cover - Ice extent	- Ice sheet velocity	- Snow and ice sheet surface melt - Ice sheet and glacier melt ponds - Sea ice motion
	Cryosphere	Lakes and river conditions Evapotranspiration	- Surface water extent - Evapotranspiration	- Surface water quality - Evaporative stress  - Evaporation and transpiration

representative sample of independent reference data collected at finer spatial resolution and with minimal error (Baret et al., 2006; Morisette et al., 2002). The results of the quality assessment, and sometimes the validation, may result in the need for product reprocessing.

### 3.1. Land cover, land use, and land cover change

Mapping and monitoring of land cover and land use was a key motivation for the launch of the first Landsat in 1972 (Goward et al., 2017). While often grouped together, land cover, land use, and changes in these properties are distinct quantities. Land cover defines the physical properties at the surface of the Earth, while land use describes the social, economic, and cultural utility of the land (Loveland et al., 2000). For example, a land cover class could be grassland and the land uses could include pastureland or parkland, but satellite data do not always suffice to distinguish land uses. Land cover, land use, and land cover change maps that capture human activity and many ecological processes are more appropriately resolved at medium than coarse spatial resolution (Gutman et al., 2008; Townshend and Justice, 1988). For example, processes, such as fire spread, forest edge effects, or habitat selection, operate at scales that require medium-resolution land cover maps. Similarly, impact evaluation of land management actions and policies requires monitoring of changes at sub-watershed scale and with respect to parcels, stands of trees or agricultural fields. Coarse-resolution satellite imagery are not able to monitor parcel-scale processes, and so miss important human-environment interactions that provide insights needed to improve management and foster improved environmental stewardship.

**Land cover** is an essential climate variable in the global climate observation system (GCOS) (Bojinski et al., 2014). Land cover products are important for characterizing anthropogenic activity and biogeographical and eco-climatic diversity (Cihlar, 2000; Townshend et al., 1992; Wulder et al., 2018). Detailed, accurate, and up-to-date land cover products are required by resource managers and decision-makers to develop and monitor land management policies, and to satisfy reporting requirements from local to global scales (Erb et al., 2017; Foley et al., 2005; Roe et al., 2019).

Global land cover maps were initially derived from coarse-resolution AVHRR data (DeFries and Townshend, 1994; Hansen et al., 2000; Loveland et al., 2000). With the availability of improved data provided by MODIS, land cover has been mapped globally at 500-m resolution on a systematic annual basis, initially based on the International Geosphere Biosphere Program (IGBP) and University of Maryland land cover classification legends (Friedl et al., 2002; Hansen and Reed, 2000). The most recent Collection 6 MODIS land cover product includes six distinct classification legends (Sulla-Menashe et al., 2019) including a hierarchical scheme based on the FAO's Land Cover Classification System (LCCS; (Di Gregorio, 2016)). Rather than define discrete land cover classes, continuous estimates of physiognomic or structural attributes (DeFries et al., 1999), such as percent vegetative cover, have also been derived, which, if needed, can sometimes be transformed into land cover classes (Hansen et al., 2011).

There is a long recognized need for medium-resolution land cover products generated over large areas (e.g., Cihlar, 2000; Townshend et al., 1992). The availability of free and open Landsat data has enabled systematic land cover mapping at medium-resolution with national products generated at regular frequency and with relatively low latency. For example, the USGS National Land Cover Database (NLCD) has produced 30-m CONUS land cover maps with 8 and 20 classes every 2–3 years since 2001, with a 3–5 year latency (Homer et al., 2020). The USGS Land Change Monitoring, Assessment, and Projection (LCMAP) project generates annual 30-m land cover maps for CONUS with 8 classes since 1985 with 2 year latency (Brown et al., 2020a). European medium-resolution land cover products include the 5 and 15 class 100-m CORINE Land Cover product (Büttner et al., 2004) with a 3-year latency (Inglada et al., 2017).

Recently, global land cover maps have been generated using Landsat, often supplemented with MODIS and AVHRR data to compensate for limited cloud free Landsat availability prevalent in many regions of the world (Kovalskyy and Roy, 2013). Global Landsat 30-m land cover products include the Finer Resolution Observation and Monitoring of Global Land Cover (FROM-GLC) product generated for 2010, 2015 and 2017 (Gong et al., 2013), the Globeland30 product generated for 2000, 2010 and 2020 (Chen et al., 2015), the iMap World 1.0 product generated annually from 1985 to 2020 (Liu et al., 2021), and the Global Land Cover Estimation (GLanCE) products generated annually from 2001 to 2020 (Friedl et al., 2022). Global land cover products derived from 10-m Sentinel-2 data include ESA WorldCover 2020 (Zanaga et al., 2021), the Environmental Systems Research Institute (ESRI) Land Cover (Karra et al., 2021), and the Google Dynamic World (Brown et al., 2022) products.

**Land use** products are needed, particularly as the area of land dominated by humans expands and land resource competition has increased (Goldewijk, 2001; Ramankutty and Foley, 1999). Certain land uses can have profoundly negative impacts on ecosystem services including water supply (Li et al., 2007; Spera et al., 2016), carbon sequestration (Erb et al., 2018), and biodiversity (Felipe-Lucia et al., 2020; Haines-Young, 2009; Powers and Jetz, 2019). Global land use classification schemes have been developed but typically include a mixture of both land cover (e.g., Forest land, Grassland, Wetlands) and land use (e.g., Cropland, Settlements) classes (Milne et al., 2003). As noted above, medium-resolution data have sufficient spatial resolution to map land cover, but finer spatial resolution (<10 m) data are typically required to accurately discriminate spatially fragmented land use classes. For example, infrastructure (e.g., buildings, roads) and agricultural fields in many regions are not resolved at medium resolution (White and Roy, 2015).

Large-area agricultural land use mapping has received significant attention reflecting the critical role of agriculture. Notably, the USDA on an annual basis systematically generates the 30-m US Crop Data Layer (CDL) for the conterminous United States using Landsat and other sensor data, and benefits from extensive training data collected as part of the US agricultural census to provide approximately 110 classes (Boryan et al., 2011). Global agricultural cropland maps have been produced (Fritz et al., 2015; Thenkabail et al., 2009; Yu et al., 2013), but are not generated systematically. In addition, there is a growing body of research on mapping agricultural practices, for example, irrigated versus rainfed (Deines et al., 2017; Xie and Lark, 2021), tilled versus no-till agriculture (Azzari et al., 2019; Zheng et al., 2014), and mapping of crop rotation and fallow periods (Dara et al., 2018; Sahajpal et al., 2014; Yin et al., 2020). Lastly, maps of built-up land reflecting the distribution of human settlements and associated infrastructure have been developed from MODIS (Schneider et al., 2009) and Landsat data (Esch et al., 2017). Because built-up land is a land use defined by spatial context, newer deep learning classification methods are promising for mapping and monitoring urban land use (Chen et al., 2020).

**Land cover change** is an essential information need. Land cover change mapping in the last decade has evolved to using Landsat time series instead of single-date images, to better characterize the type and timing of change, and to gain insights on the directionality and persistence of change trends (Hansen and Loveland, 2012; Woodcock et al., 2020; Zhu, 2017). The analysis of temporal metrics, combined with ancillary data, allows different types of land cover and land cover change products to be generated (Wulder et al., 2018). However, changes may not manifest themselves in the data for some time after the event that caused the change, and changes in surface condition can occur without a change in land cover. For example, trees can persist yet appear spectrally different over time due to insect activity or drought stress, causing a change in vegetation condition without a change in land cover (Coops et al., 2020). Mapping change in a binary change/no-change manner for some phenomena may thus be restrictive. For example, forests are defined by physiognomic or structural attributes

including potential mature tree height and canopy cover. Therefore, change mapping based on sub-pixel fractional cover can be advantageous (Ye et al., 2021b).

Land cover and land cover change mapping algorithms are mature, and a wide range of methodological options are available. We suggest to adopt a land cover class catalog that is hierarchical and supports different levels of detail (e.g., UN LCCS; (Di Gregorio, 2016)). A global land cover map will necessarily require some level of simplicity and generalization (Milne et al., 2003), but should allow for additional detail on a local to regional basis (Tulbure et al., 2021). Integrating new capabilities in a research-to-operations mode while maintaining a core record consistent with historical data is desirable. The current state-of-the-practice approach for large area land cover classification is based on the application of ensemble tree-based classifiers, such as random forests (Breiman, 2001), to satellite time series to take advantage of spectral differences among classes over time (Brown et al., 2020b; Sulla-Menashe et al., 2019; Wulder et al., 2018). Deep learning-based algorithms have advantages for land cover classifications (Kussul et al., 2017; Zhang et al., 2020). Deep learning models can exploit spatial relationships among pixels in contrast to conventional classification approaches that are applied independently to individual pixel locations, and that is beneficial, for example, when classifying urban areas. While deep learning requires large training data sets and considerable computer resources for the derivation of the classification model, once generated, the model can be applied quite efficiently, allowing for rapid classification updates. Land cover and land cover *change* mapping should ideally be based on a single integrated mapping process. Generation of change features (where, when), and metrics describing the nature of changes detected (e.g., change magnitude and persistence), is recommended, and can support the generation of land use maps (Wulder et al., 2018).

With the advent of free and easily obtainable ARD, sharing classification models for on-demand classification applications has considerable potential. The development of interoperable machine learning models and training data standards would be helpful in this respect. At present, reliable global land cover product generation requires substantial human interaction and is not purely a data science issue. This is due to the aforementioned need for training data and because of irregular temporal cadence of satellite time series and factors that reduce input product quality. Training data collection is a bottleneck but there are a number of methodologies to reduce this (Wulder et al., 2018). Training data collection is particularly challenging for change product generation because high spatial resolution imagery in archives such as Google Earth are often spatially and temporally sparse (Lesiv et al., 2018). Recent constellation satellite imagery, such as the PlanetScope constellation, which provides 3–4 m imagery with a global median average revisit interval of only 30 hours (Roy et al., 2021), may be useful for training data collection. Human inspection will almost certainly continue to be necessary for the foreseeable future, with classification iteration as appropriate. In particular, classes consisting of mixed life forms (shrubs versus trees), or sparse cover (semi-arid grasslands), can be challenging to consistently discriminate and characterize, particularly with temporally sparse satellite data. Rigorous accuracy assessments are a key element of any land cover and land cover change product, including independent assessments and reporting on the accuracy of both maps and changes (Tsutsumida and Comber, 2015; Zhang and Roy, 2017). Validation data (i.e., independently collected land cover and change samples) are as challenging to collect as training data. Obtaining globally representative independent land cover reference data is essential, which is particularly complex for change classes because both the spatial and temporal distribution of change should be sampled (Boschetti et al., 2015) and accuracy assessments need to follow best statistical practices (Olofsson et al., 2014; Olofsson et al., 2012).

### 3.2. Disturbance

Disturbance refers to events that disrupt ecosystem, community, or population structure but typically do not result in a land cover change (Zhu et al., 2022). Change in disturbance regimes, for example, changes in the spatial and temporal dynamics of disturbance, or in disturbance severity, may have profound effects on ecosystems (Senf and Seidl, 2021; Turner, 2010).

We propose two essential disturbance products, burned area and forest loss, because algorithms for both are mature and have established requirements, and given their importance for the global carbon cycle, ecosystems, and biodiversity. Accurate disturbance mapping is highly dependent on the temporal resolution of the available satellite data. However, the temporal cadence of satellite observations is often irregular in space and time due to cloud and shadow contamination and different overlapping swath geometries (Egorov et al., 2019), which present substantial detection challenges (Brown et al., 2020b; Roy et al., 2019). The free and open policy of Landsat has made the use of dense Landsat time series possible, allowing disturbance mapping intervals to shrink from a decade (Masek et al., 2008) to every 2–3 years (Jin et al., 2017), annual (Hansen et al., 2013; Hermosilla et al., 2015; Vancutsem et al., 2021), sub-annual (Zhu et al., 2012), 8–16 day (Pasquarella et al., 2017; Ye et al., 2021a), and owing to the launch of Sentinel-2 and the creation of harmonized Landsat Sentinel-2 data ca. 3 days (Claverie et al., 2018; Li and Roy, 2017).

#### 3.2.1. Burned area

Fire is a widespread disturbance occurring on all continents except Antarctica (Giglio et al., 2018). In addition to loss of life and property (Radeloff et al., 2023) and the deleterious impacts of frequent and intense fires on ecosystems, fire is a major source of greenhouse gases (equivalent to ~25% of fossil fuel emissions) (van der Werf et al., 2017). Active fire detection algorithms require middle-infrared (~4 μm) wavelengths to reliably detect the location of small and cool fires (Wooster et al., 2021). Landsat sensors have no middle-infrared bands and only a 16-day repeat, and so Landsat data are of limited use for systematic active fire detection, despite algorithms developed for this purpose using the near-infrared (NIR) and short-wave infrared (SWIR) bands (Kumar and Roy, 2018; Schroeder et al., 2016). In contrast, Landsat data have been used widely for mapping burned area (Arino et al., 2001; Boschetti et al., 2015; Chuvieco et al., 2019).

Fire transforms living and dead leaf and woody material into char and ash that typically is identified by reduced reflectance post-fire, particularly in the NIR, which may persist for weeks (in savannas and grasslands) to decades (in boreal forests) (Melchiorre and Boschetti, 2018; Trigg and Flasse, 2000). Prior to the free availability of Landsat, burned area mapping was undertaken using a small number of cloud-free images, typically by thresholding spectral reflectance or by visual interpretation (Hall et al., 1980; Minnich, 1983). Subsequently, spectral band ratios such as the Normalized Burn Ratio (NBR), defined as the NIR minus the SWIR reflectance divided by their sum (López García and Caselles, 1991), and others (Chuvieco et al., 2002) were developed and used to map burned areas. The NBR has also been used to map burn severity, including systematically across the U.S. (Picotte et al., 2020), although relationships to ground assessments of severity are often imperfect (French et al., 2008; Roy et al., 2006).

In the last decade, Landsat and Sentinel-2 time series based burned area mapping algorithms have been developed to take advantage of the temporal persistency of fire effects. The change in reflectance post-fire depends on several factors but predominantly on the fraction of the pixel that burned and on the combustion completeness, which is the fraction of fuel exposed to the fire that actually burned (Roy and Landmann, 2005). Factors including post-fire vegetation recovery, the degree of char and ash dissipation by wind and rain, and pre-fire and post-fire vegetation structure, soil and understory reflectance, also affect burned area mapping (Disney et al., 2011; Kokaly et al., 2007; Lentile

et al., 2006; Roy and Landmann, 2005; Trigg et al., 2005). In addition, burned area algorithms must differentiate between spectral changes due to fire and similar spectral changes that are not fire related (Giglio et al., 2018; Roy et al., 2005). There is no consensus burned area mapping approach, although most algorithms are applied to reflectance or spectral band ratio time series and many are supplemented with active fire detections, such as Landsat and MODIS active fire detections (Boschetti et al., 2015), Sentinel-2 and MODIS active fire detections (Roteta et al., 2019), using only Landsat (Hawbaker et al., 2017), or both Landsat and Sentinel-2 (Roy et al., 2019).

An outstanding issue is the need to rigorously validate medium-resolution burned area products. Previously, 30-m burned area maps interpreted from hundreds of globally distributed Landsat image pairs were used to validate coarser spatial resolution global MODIS burned area products (Boschetti et al., 2019; Padilla et al., 2014). Currently, high spatial resolution (<10 m) independent burned area data are needed to assess the accuracy of Landsat and Sentinel-2 burned areas products, and this, with ongoing algorithm development, is an area of active research and development.

We consider burned area an essential medium-resolution product that should preferably map the approximate day of burning given the ephemeral nature of fire and the utility of higher temporal resolution information for natural resource and fire management applications. The product should include per pixel quality information with flags to denote if there were insufficient satellite time series data to detect the burned/unburned status, the approximate detected day of burning, the acquisition dates of the images bounding the change, and a measure of the confidence of burn detection.

### 3.2.2. Forest loss

Forest loss accounts for >10% of human-induced greenhouse gas emissions mainly due to deforestation of humid tropical forests (Houghton, 2013) with rising emissions over the last two decades (Feng et al., 2022). In addition to carbon sequestration, forests provide many

ecosystem services, including habitat for terrestrial biodiversity and maintenance of hydrologic services (Chiabai et al., 2011; Schwaab et al., 2021), and provide key commodities, such as timber, pulp for paper, rubber, and cacao. Monitoring forests, in particular the conversion of natural forests to forestry or non-forest land uses, is required to assess the effects of these changes on environmental sustainability.

The main way to assess national- to global-scale forest change has been through the use of time-series satellite data. Landsat data have been key for the mapping of forest loss in the Brazilian Amazon (Nelson et al., 1994), North America (Masek et al., 2008; White et al., 2017; Zhao et al., 2018; Egorov et al., 2023), Europe (Potapov et al., 2015; Senf and Seidl, 2021), and Asia (Grogan et al., 2015). At global scale, the Global Forest Change product (Hansen et al., 2013; Kim et al., 2014) identifies 30-m pixels with >50% of canopy cover loss annually since 2000. We consider annual forest loss an essential dataset, for which feasibility at global scale have been demonstrated by the Global Forest Change product (Fig. 1). There is a range of approaches to map forest loss, including classification approaches based on image metrics (Potapov et al., 2015), or the analysis of Landsat time series (Zhu, 2017) including temporal segmentation (Hermosilla et al., 2015; Kennedy et al., 2010) or other types of fitted time series models (Verbesselt et al., 2010; Zhu et al., 2012). An ensemble of forest disturbance algorithms aggregated through ensemble learning (Healey et al., 2018) can overcome differences in the results of different forest disturbance detection algorithms (Cohen et al., 2017).

In addition to accurately identifying the timing and extent of forest loss, future forest loss products would ideally attribute forest loss to specific agents, such as harvest (Healey et al., 2006; Wilson and Sader, 2002; Wulder et al., 2004), fire (Hawbaker et al., 2020; Roy et al., 2019), wind (Baumann et al., 2014), hydrology (Castaneda et al., 2005; Pekel et al., 2016), landslide (Barlow et al., 2003; Chen et al., 2019; Lacroix et al., 2019), insect infestation (Goodwin et al., 2008; Ye et al., 2021b), pathogens (Chen et al., 2017; He et al., 2019), or multiple disturbance agents (Kennedy et al., 2015; Schroeder et al., 2017). Recovery

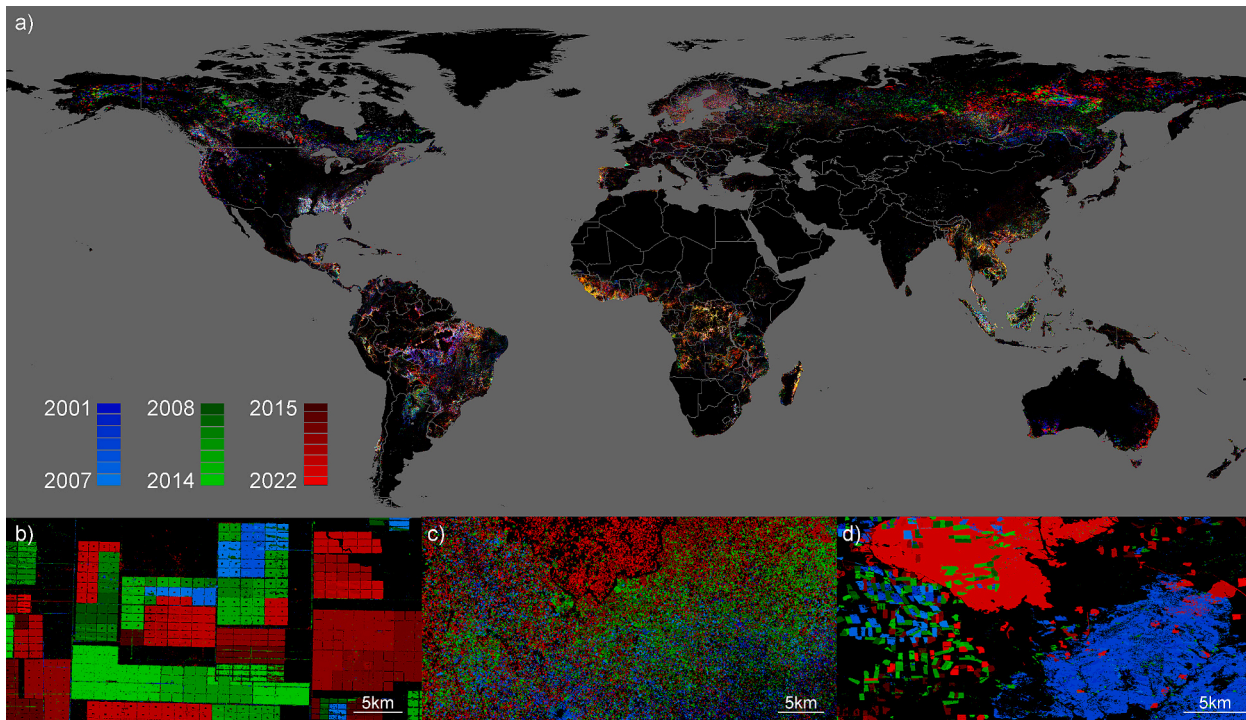


**Fig. 1.** (a) Global forest cover loss, 2001-2022, derived from annual multi-temporal Landsat metrics, shown averaged at a 0.05 degree resolution in red, green and blue by epoch. Insets are full resolution zooms of (b) Chaco woodland clearing in Paraguay centered at 60°40'16"W, 20°41'47"S, (c) shifting cultivation expansion in humid tropical forest of the Democratic Republic of the Congo centered at 29°19'19"E, 0°57'14"N, and (d) boreal forest logging and fire in Siberia, Russia centered at 103°22'44"E, 55°49'02"N (after Hansen et al., 2013).

information characterizing the condition and structure of vegetation after disturbance is another desirable attribute (Pflugmacher et al., 2014; White et al., 2018). Forest degradation remains challenging to quantify, due to its ephemeral nature particularly in tropical systems (Souza et al., 2005), and differing definitions and measurable attributes, but is possible (Bullock et al., 2020; Maticardi et al., 2020). Forest loss alerts are a monitoring application intended to provide near-real time information on disturbances that on the ground land managers and other interested parties may use to interdict or deter potential illicit activity. Landsat and Sentinel-1 and 2 based alerts (Hansen et al., 2016; Reiche et al., 2021) are part of the Global Forest Watch project (<https://www.globalforestwatch.org/blog/data-and-research/integrated-deforestation-alerts/>), and have decreased the probability of deforestation in Africa with attendant carbon benefits (Moffette et al., 2021).

Forest loss validation is challenging but validation and area estimation of forest loss is possible through the use of random sampling designs and unbiased estimators (Penman et al., 2003). Good practice approaches to forest loss accuracy assessment and area estimation can be made using “reference data sources that provide sufficient spatial and temporal representation to accurately label each unit in the sample” (Olofsson et al., 2014). In this manner, a map of forest extent and change is used to stratify a study area, with accurately mapped classes affording a sampling efficiency that improves the precision of area estimates (Hansen et al., 2008). Importantly, probability-based stratified sampling of the reference data allows unbiased estimation of the forest cover loss accuracy metrics and associated standard errors (Olofsson et al., 2014). In addition, reference data may also allow to assess forest type, causes of forest loss, and land cover and land use outcomes (Tyukavina et al.,

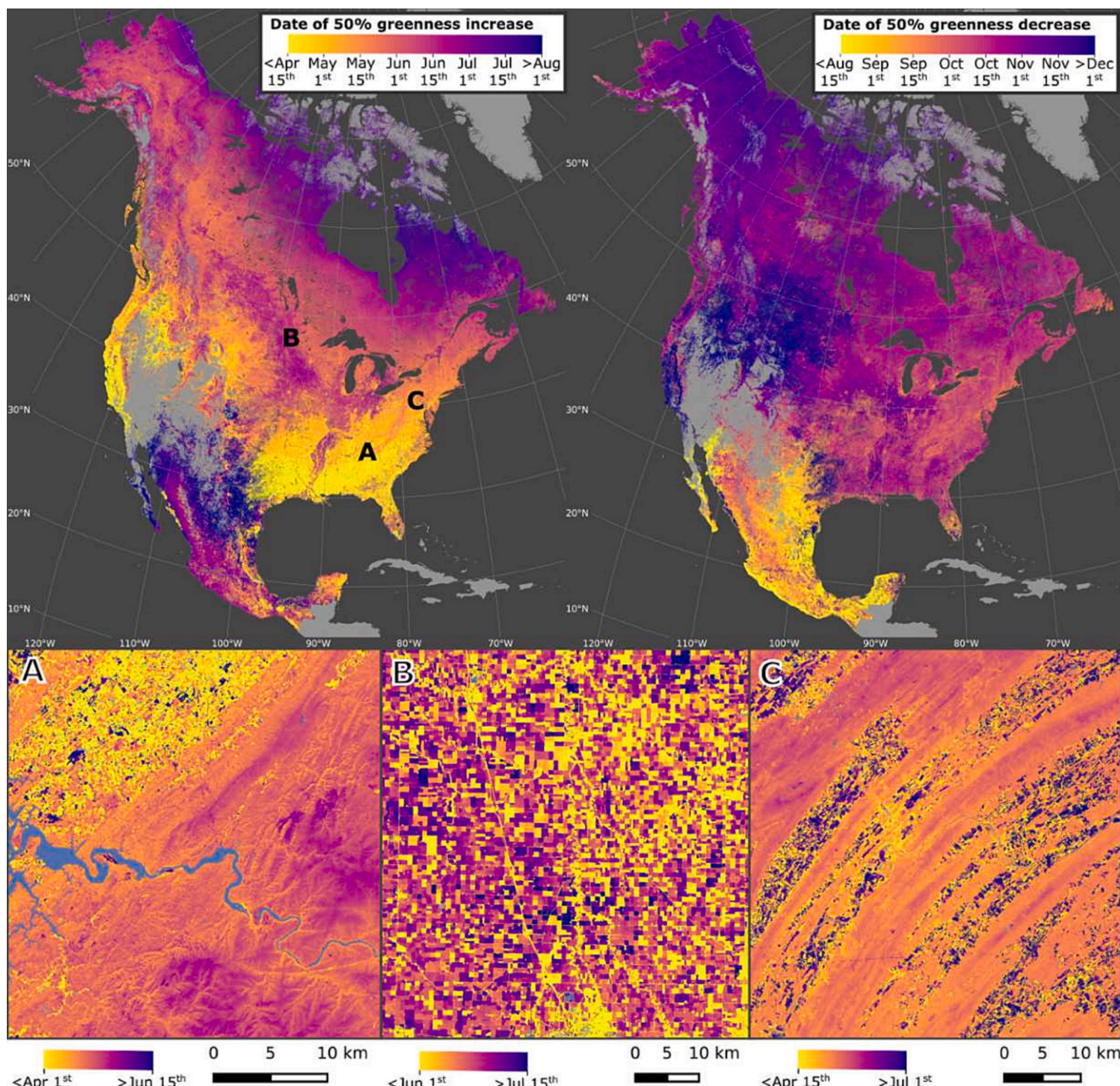


**Fig. 2.** Continental land surface phenology at 30-m spatial resolution from Harmonized Landsat Sentinel-2 imagery (Bolton et al., 2020). The top row shows the day of year for green-up (left) and green-down (right) in 2019. Lower panel shows zoom in for specific locations for green-up: (A) mix of natural vegetation and land use in central Tennessee with higher elevation Smokey Mountains in the eastern portion of the image; (B) agriculture in North Dakota; (C) Appalachian ridge and valley system in Pennsylvania.

2018; Tyukavina et al., 2017). Such approaches enable the assessment of commodity driven deforestation, such as the role of soybean expansion in South America deforestation (Song et al., 2021). Sample-based estimates currently remain the most precise way to summarize forest extent and change dynamics. Validation is key to build confidence in the use of mapped products in downstream applications.

### 3.3. Vegetation condition and phenology

Measures of vegetation condition reflect the overall health of vegetation (e.g., drought stress) and generally require a historical baseline to quantify changes (i.e., long-term average and trend). In addition to changes arising from external forcing, variation in phenology arising from natural variation in weather can drive changes in vegetation that are distinct from changes in condition. Time series of medium-resolution imagery allow both vegetation condition and phenology to be monitored at scale (Fig. 2). Typically this is undertaken using vegetation indices, which serve as proxies for canopy properties (Huete et al., 2002).

In natural ecosystems, the timing of phenological events is a key indicator of the effects of climate change on growing seasons (Korner and Basler, 2010; Penuelas et al., 2009; Piao et al., 2019) and characterizes the sensitivity of ecosystem processes to climate variability and change (Friedl et al., 2014; Keenan et al., 2014). In agro-ecosystems, phenology is diagnostic of management practices (e.g., sowing and harvest dates, irrigation), crop types, and crop yields (Bolton and Friedl, 2013; Sacks et al., 2010). Intra-annual time series of vegetation indices capture patterns in land surface phenology, providing information related to crop development and ecosystem function (de Beurs and Henebry, 2004; Gao et al., 2020). Phenological information resolved at medium resolution is particularly relevant for agricultural systems, both within large agro-industrial fields and in regions where smallholder agriculture with small fields and mixed cropping prevails (Griffiths et al., 2019).

Long-term average land surface phenology can be estimated from multi-year Landsat time series (Elmore et al., 2012; Fisher et al., 2006), as can the timing of leaf emergence and fall senescence (Melaas et al., 2016), and (in combination with MODIS) additional phenology dates such as canopy maturity or dormancy in forests (Baumann et al., 2017) and crops (Gao et al., 2017). The launch of Sentinel 2A and 2B, in combination with Landsat 8 and 9, provides the capability to monitor vegetation phenology and condition at medium resolution, but with MODIS-like temporal sampling.

We consider vegetation condition and phenology products that map the timing and variability in vegetation indices at sub-seasonal time scale to be essential medium-resolution products. The products should include quality assurance information quantifying uncertainty in vegetation condition and phenology metrics. Specifically, we suggest development of 30-m Normalized Difference Vegetation Index (NDVI) and Enhanced Vegetation Index (EVI) products, along with a separate phenology product derived from these vegetation indices. In cloudy regions, image compositing approaches (Qiu et al., 2023) can be applied to produce cloud and atmospheric artifact-free gap-filled data sets (Griffiths et al., 2019; Potapov et al., 2020). Gap-filled products provide user-friendly ARD, and would also provide reproducibility and transparency for analyses based on these data. Analyses of HLS data have generated medium-resolution land surface phenology (Bolton et al., 2020) and crop phenology (Gao et al., 2020; Gao et al., 2021) products at scale.

The land surface phenology metric product should capture three key characteristics of vegetation development: (i) timing of key phenological dates (e.g., the start of the season, peak growth, and the end of the season); (ii) productivity (e.g., seasonal mean, or the growing season integral of the vegetation index time series); and (iii) seasonality (i.e., the magnitude of within-season variability). Global maps of such metrics can only be produced at medium resolution using both Landsat and Sentinel-2 data. Vegetation condition products for the pre-Sentinel-2 era

should focus on composite vegetation indices and on a reduced set of phenological descriptors insensitive to sparser time series data. Alternatively, the combination of Landsat observations from multiple years can be used to produce multi-year average phenology products (Baumann et al., 2017), and, where there is sufficient data density, annual start and end of growing season metrics for stable land cover types (Melaas et al., 2016).

Several factors influence the quality of phenological metrics: the temporal cadence of the satellite observations (i.e., the density and distribution of observations) during the annual phenological cycle, the quality of cloud, shadow and snow flagging, and the appropriateness of the model used to fit the observations. Per-pixel product quality information should reflect factors such as the maximum gap between observations during each phenophase (e.g., greenup) during the growing season, and the coefficient of determination ( $R^2$ ) between interpolated and observed values during different periods in the growing season (Bolton et al., 2020; Zhang et al., 2018).

In addition to the vegetation index and phenology essential products identified above, desirable vegetation condition products include medium-resolution Leaf Area Index (LAI) and the fraction of photosynthetically active radiation absorbed by the canopy (FAPAR). Both can be derived in multiple ways including radiative transfer modelling (Ganguly et al., 2012), downscaling MODIS/VIIRS LAI (Gao et al., 2012), or using machine learning (Kang et al., 2021). For example, the Sentinel-2 Level 2 LAI and FAPAR products use the physically-based PROSAIL model to simulate surface reflectance and retrieve LAI and FAPAR using trained neural networks (Fernandes et al., 2014; Weiss and Baret, 2016). Another desirable product is the fraction of green vegetation cover. Spectral mixture analysis can estimate fractional cover estimates globally from coarse resolution data (Filipponi et al., 2018), and is likely straightforward from Landsat and Sentinel-2 time series through generalizing endmember selection based on machine learning regression (Frantz et al., 2021; Schug et al., 2020).

### 3.4. Surface radiation balance

The partitioning of incoming radiation at the land surface is a key factor in regulating climate and Earth system processes. Incident radiation from the sun ( $S_d$ ) and downwelling longwave radiation from the atmosphere ( $L_d$ ) can be reflected, absorbed and re-emitted at the land surface, defining the net radiation energy ( $R_{net}$ ) available at the surface:

$$R_{net} = S_{net} + L_{net} = (1 - \alpha) * S_d + L_d - \epsilon_s \sigma T_s^4 - (1 - \epsilon_s) * L_d \quad (1)$$

here  $S_{net}$  and  $L_{net}$ , are net shortwave and longwave radiation energy, respectively,  $\alpha$  is the broad-band albedo,  $S_d$  and  $L_d$  are the incoming (downward) shortwave and longwave radiation, respectively,  $\epsilon_s$  is surface emissivity,  $T_s$  is surface temperature (ST), and  $\sigma$  is the Stefan-Boltzmann constant. The precise balance defined in Eq. 1 depends on local surface conditions and governs the rate of heating or cooling of the surface and surrounding air layer. The reflectance of the Earth surface in discrete wavelength bands is a primary satellite observable, conveying information including about properties of soils, plants, urban cover, and surface water. Satellite-based surface reflectance, albedo, and surface temperature products are collectively critical to understanding how factors regulating surface radiation balance respond to changes in land-use and land-cover, as well as the role humans play in modifying their environment.

#### 3.4.1. Surface reflectance

Atmospheric correction of top of atmosphere (TOA) reflectance to surface reflectance is a fundamental pre-processing step required for the majority of land products (Roy et al., 2014a). The influence of the atmosphere in scattering and absorbing incoming solar radiation as well as reflected and emitted surface radiation, is well established (Fraser and Kaufman, 1985). This influence, like the weather, is highly variable in

space and time, particularly for aerosol constituents that significantly scatter and absorb at shorter wavelengths (Dubovik et al., 2002). For example, the mean absolute difference between TOA reflectance and atmospherically corrected (i.e., surface) reflectance, expressed as a percentage of the surface reflectance, was documented as 45%, 22%, and 12% for the Landsat ETM+ visible blue, green and red bands across the United States (Roy et al., 2014a).

Modern atmospheric correction algorithms use radiative transfer models in conjunction with ancillary data that characterize the atmospheric constituents, and usually an image-based aerosol retrieval methodology. The LaSRC (Land Surface Reflectance Code) is a generic atmospheric correction algorithm that accounts for gaseous absorption along with molecular scattering and aerosol extinction. LaSRC is based on the inversion of the “6SV” vectorial radiative transfer code (Kotchenova and Vermote, 2007; Kotchenova et al., 2008). Although LaSRC was originally developed for MODIS and VIIRS (Vermote et al., 2014; Vermote and Saleous, 2002), it has been adapted to Landsat-8 and 9 (Vermote et al., 2016) and Sentinel-2 (Doxani et al., 2018). LaSRC provides per-pixel quality assessment data and an internal cloud and shadow mask (Skakun et al., 2019). When both Landsat and Sentinel-2 observations are combined, other approaches to atmospheric correction can also be considered. Given that the primary bands of Landsat-8 and 9 are very similar to Sentinel-2, and that their data together provide several observations per week, time series approaches such as the Multi-Angle Implementation of the Atmospheric Correction (MAIAC) algorithm (Lyapustin et al., 2018) are possible. The use of the dynamic covariance technique, where the latest image is correlated with earlier images, helps establish a reproducible spatial surface pattern and develop a clear-sky reference image for improved cloud and cloud shadow detection (Lyapustin et al., 2008). Other algorithms, such as the Sensor Invariant Atmospheric Correction (SIAC) algorithm, that uses the MODIS BRDF/Albedo product (Schaaf et al., 2002) and Copernicus Atmosphere Monitoring Service (CAMS) operational forecasts of aerosol optical thickness and column water vapor (Benedetti et al., 2009; Morcrette et al., 2009) have been developed to atmospherically correct Landsat and other sensor imagery (Yin et al., 2022) with per-pixel surface reflectance uncertainties that are helpful for propagation into higher level product generation algorithms.

Validation of surface reflectance is challenging due to the dynamic nature of the atmosphere and has typically relied on the use of AERONET data (Holben et al., 1998) to characterize atmospheric constituents at sites selected to capture a wide range of surface and atmospheric conditions (Ju et al., 2012; Vermote and Kotchenova, 2008; Wang et al., 2009). Recent community exercises including the Atmospheric Correction Intercomparison eXercise (ACIX) provide a forum for surface reflectance validation and atmospheric correction algorithm intercomparison (Doxani et al., 2018; Doxani et al., 2023). Notably, the most recent ACIX exercise included the use of reference data from instrumented sites, such as ROSAS (Meygret et al., 2011) and RadCalNet (Bouvet et al., 2019), that directly and continuously measure surface reflectance. New systems, such as CAMSIS that use imaging systems mounted on stationary towers to measure heterogeneous vegetated sites (Vermote et al., 2022), are being developed and will enable meaningful validation of corrections to account for surface heterogeneity (i.e., adjacency effects) (Liang et al., 2001; Lyapustin, 2001; Ouaidrari and Vermote, 1999).

### 3.4.2. Albedo

Land surface albedo is also considered an essential climate variable (CEOS, 2015) necessary to monitor the surface energy budget. Medium-resolution albedo measures, retrieved daily or every couple of days, provide the details required to fully capture variability of the surface energy budget.

Land surface albedo ( $\alpha$ ) is a hemispherical reflective quantity, representing the proportion of the incoming solar radiation that is reflected as a function of surface cover and structure, and ranges from 0.0 for the

most absorptive surfaces, such as water, to almost 1.0 for the brightest reflective surfaces, such as fresh snow. Surface albedo can vary rapidly in time, for example, due to snowfall, snow melt, vegetation phenology, harvesting, and wildfires (Wang et al., 2017; Zhang et al., 2017), and at scales that may not be resolved at coarse spatial resolution. If sufficient directional surface observations are available to adequately model the character of the surface reflectance anisotropy (defined by the bidirectional reflectance distribution function (BRDF)), then robust measures of intrinsic surface albedo can be estimated from satellite observed reflectances. Note that intrinsic measures of surface albedo, commonly called white sky albedo (bihemispherical reflectance, or wholly diffuse albedo) and black sky albedo (directional hemispherical reflectance, or wholly direct albedo) can be combined as a function of aerosol optical depth to generate an instantaneous albedo at a specific time (also known as blue-sky albedo) as would be measured by tower albedometers (Roman et al., 2010).

Coarse spatial resolution land surface BRDF and albedo products have been generated at global scale on a systematic daily to weekly basis, including from MODIS and VIIRS (Roujean et al., 1992; Schaaf et al., 2002; Schaaf et al., 2011; Wang et al., 2019; Wang et al., 2017) and from multi-angle sensors such as MISR (Lyapustin et al., 2006; Martonchik et al., 1998), POLDER (Bacour and Breon, 2005; Hautecoeur and Leroy, 1998) and AATRS (Sayer et al., 2012). Sensors that have narrow fields of view and lower revisit cycles, such as Landsat and Sentinel-2, do not provide sufficient angular sampling of the surface to be able to characterize the BRDF reliably at time scales where the surface can be assumed to be unchanged (Roy et al., 2016b). Recently, medium-resolution surface albedos have been determined by coupling medium-resolution surface reflectance with surface anisotropy information derived from coincident more frequent but lower spatial resolution sensors. For example, a Landsat albedo algorithm has been developed that relies on daily MODIS/VIIRS BRDF retrievals from concurrent or nearby locations and couples these with each Landsat observation to generate 30-m albedo products (Fig. 3) (Elmes et al., 2021; Erb et al., 2022). Ideally, Landsat and Sentinel-2 based albedo products should be produced at near-daily to weekly time steps to capture rapid surface changes. This is especially needed to capture snowfall and rapid melting of snow cover, which can result in significant radiative forcing changes due to markedly different snow and non-snow covered surface albedo and changes in the snow characteristics (Betts, 2000; Erb et al., 2022). Thus, the temporal dynamism of snow covered surfaces will be better captured by combined Landsat and Sentinel-2 observations and this will be particularly true at higher latitudes because of low illumination conditions in the shoulder and winter seasons (despite more frequent overpasses).

Satellite albedo product accuracy has been quantified by albedo product comparison with tower radiometer observations, such as measured by the US National Ecological Observation Network (NEON), the Baseline Surface Radiation Network (BSRN), the Greenland Climate Network (GC-Net), and the international FLUXNET (Wang et al., 2019). Accuracy assessment has typically been limited to comparisons with instrumented towers, but field measurements and uncrewed aerial vehicles UAVs and airborne data are also possible (Lyapustin et al., 2010; Wright et al., 2014; Wulder et al., 2022). Tower data provide long time series validation opportunities. The tower height governs how spatially representative the tower data are of the satellite footprint. For Landsat and Sentinel-2, even the short GC-Net towers are sufficient (Elmes et al., 2021). All albedo products produced by space agencies internationally have per-pixel quality assessment information, for example, indicating the confidence in the albedo retrieval, and whether the albedo is a snow-free, and it is important that this information be examined by product users.

### 3.4.3. Land surface temperature

Land surface temperature ( $T_s$ ) is a critical diagnostic of the surface energy balance, evaporative fluxes, and vegetation stress.  $T_s$  can vary

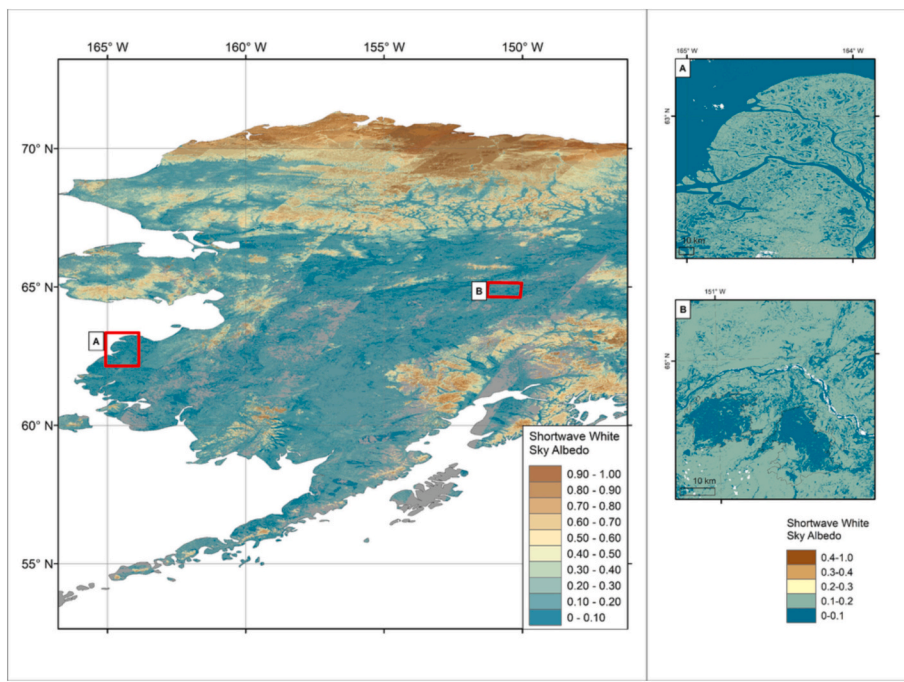


**Fig. 3.** Landsat-8 derived Shortwave White Sky Albedo for May and June 2018 over Alaska USA. The 30-m resolution albedo values are generated by combining Landsat surface reflectances (C1) with temporally coincident BRDF information from MODIS (C6.1). The insets highlight the detail provided by 30-m albedo data including A) albedo values over the small waterbodies and wetlands in the Yukon River Delta in June 2018, and B) the decrease in albedo occurring over the Mooseheart (left) and Zitziana River (right) fires scars which occurred in 2018. For further details see Erb et al. (2022).

rapidly in space and time: for example, the diurnal variation in land  $T_s$  can be markedly different between a road and an adjacent crop field.  $T_s$  does not mix linearly with scale, and medium-resolution estimates are needed to capture many aspects of the landscape that are not resolved at coarse resolution. Medium-resolution land  $T_s$  has a wide range of uses including estimating net radiation, crop water use and evapotranspiration (see section 3.8), and quantifying urban heat island effects (Weng et al., 2004). That is why we consider medium-resolution land  $T_s$  to be an essential product.

There is a long history of algorithms developed to retrieve land surface temperature ( $T_s$ ) from coarse global coverage sensors with thermal wavelength detectors. Notably, the NOAA AVHRR sensors have  $\sim 11\text{-}\mu\text{m}$  and  $\sim 12\text{-}\mu\text{m}$  thermal bands and more recent sensors have an additional  $\sim 4\text{ }\mu\text{m}$  band, and MODIS and VIIRS continue these configurations. Split-window  $T_s$  algorithms take advantage of these bands to reduce differential atmospheric absorption (Gerace et al., 2020; Wan and Dozier, 1996).

The Sentinel-2A and -2B sensors do not have thermal wavelength detectors and so land  $T_s$  and  $\epsilon_s$  products would need to be derived from Landsat only. Landsat's thermal sensors are unique for their excellent calibration ( $<0.3\text{ K RMSE}$ ) and routine global medium-resolution coverage (Barsi et al., 2014; Hook et al., 2020; Schott et al., 2012). The Landsat TM and ETM+ sensors had a single  $\sim 11.5\text{-}\mu\text{m}$  thermal band and although land  $T_s$  can be derived using atmospheric data, this requires the emissivity to be pre-defined or assumed to be constant (Malakar et al., 2018). Landsat-8 and 9 carry the TIRS sensors with two thermal bands (10.8 and 12  $\mu\text{m}$ ) that enable retrieval of land  $T_s$  after compensation of the measured radiance for atmospheric effects using a split-window correction (Gerace et al., 2020). However, the  $\epsilon_s$  must be specified *a priori*, for example, based on the ASTER Global Emissivity Dataset (Hulley et al., 2015). The goal for satellite-retrieved land  $T_s$  is an uncertainty of 1 K based on user-driven baseline requirements and approved by the Committee on Earth Observation (CEOS) Satellites Working Group on Calibration and Validation (WGCV) Land Production Validation subgroup (Guillevic et al., 2018). The WGCV has further defined a protocol for best practices for the validation of surface

temperature products. These include a temperature-based validation, radiance-based validation, multi-sensor inter-comparisons, and time-series analyses (Guillevic et al., 2018). Quality Assessment flags in land  $T_s$  products should include information related to the input data quality, cloud flags, and other algorithm performance metrics.

Land  $\epsilon_s$  is a desirable product. However, at least three thermal bands are necessary to physically retrieve emissivity. Planning for the next generation of Landsat therefore includes five thermal bands (Wulder et al., 2022) specifically to facilitate temperature-emissivity separation (Hulley and Hook, 2011). In this case, emissivity could be dynamically retrieved and supplied as an independent product such as in the current standard MODIS, VIIRS, and ECOSystem Spaceborne Thermal Radiometer Experiment on Space Station (ECOSTRESS) surface temperature products (Hulley et al., 2022; Hulley et al., 2018). Furthermore, net radiation (Eq. 1) should be considered as an aspirational product, combining albedo, temperature, emissivity, and gridded insolation and longwave data from reanalysis.

### 3.5. Biodiversity and faunal habitat

Biodiversity declines are a major societal concern because of resulting threats to ecosystem services, and because of the inherent value that many people place on natural ecosystems and the species that inhabit them. However, assessing the full diversity of life is challenging. Satellite data and derived products have an important role in informing efforts to conserve species' habitat and safeguard biodiversity. Land cover classifications, for example, are good predictors of habitat quality and species distributions (Skidmore et al., 2021; Turner et al., 2003). Similarly, land cover change analyses highlight threats to protected areas (DeFries et al., 2005; Falcucci et al., 2007) or ecosystem services (Andrew et al., 2014). In addition, satellite data can characterize the underlying environmental conditions that affect biodiversity (Duro et al., 2007).

Coarse-resolution satellite data can predict biodiversity at global to continental scales (Fjeldsa et al., 1997; Waring et al., 2006). For example, the 1-km MODIS-based Dynamic Habitat Indices (DHIs),

explain two thirds of the variation in species richness of amphibians, birds, and mammals globally (Radeloff et al., 2019). Similarly, image texture measures derived from MODIS vegetation indices provide a proxy for habitat heterogeneity (Tuanmu and Jetz, 2015; Wallis et al., 2016), and MODIS-based winter habitat indices capture patterns of snow and frozen ground (Gudex-Cross et al., 2021), making such indices useful, for example, for bird species richness predictions (Carroll et al., 2022).

Medium-resolution satellite data are best suited for assessments of biodiversity and faunal habitat (Farwell et al., 2021; Pettorelli et al., 2014; Turner et al., 2003) because those data capture both variability in environmental condition within an animal's territory (Pettorelli et al., 2005; St-Louis et al., 2010) and heterogeneity in vegetation structure (Cohen and Goward, 2004; Liu et al., 2001). Furthermore, medium-resolution satellite data capture conservation threats, such as urban development and agricultural expansion, well.

There are several metrics that can be retrieved from satellite data to act as proxies or predictors of biodiversity. The DHIs summarize three aspects of the annual phenology of vegetation productivity and were originally proposed by Berry et al. (2007) and Mackey et al. (2004), and further developed by Coops et al. (2009), Hobi et al. (2017) and Radeloff et al. (2019). *Cumulative productivity* is a measure of available energy. *Minimum productivity* is a measure of resource limitations. Lastly, *Variation in productivity* captures seasonality. The DHIs correlate well with biodiversity, but currently are only available globally at coarse resolution (e.g., silvis.forest.wisc.edu/data/dhis).

We suggest to produce the three DHIs globally as an essential medium-resolution product for biodiversity applications (Fig. 4). The DHIs can be derived from any proxy for vegetation productivity (Hobi et al., 2017), so 30-m EVI data would be adequate until more direct measures of productivity, such as FPAR were available. For the composite DHIs, which summarize long-term averages and are best for analyses of multi-year biodiversity data, such as species richness estimates derived from range maps, we suggest to analyze one decade of Landsat and Sentinel-2 observations, and calculate the median monthly vegetation indices among years. For the annual DHIs, which are best when analyzing annual biodiversity data from field survey, missing monthly values need to be filled after curve fitting (Hobi et al., 2021).

The DHIs cannot be measured directly on the ground, and are unitless, which precludes their direct validation. However, quality

assessment flags for the DHIs need to propagate uncertainties inherent in the EVI (or FPAR), and uncertainties related to sparse observations. For both composite and annual DHIs, it would be valuable to report the number of observations available in each month, their standard deviation, the months for which missing values had to be filled, and the longest stretch of subsequent months for which data was missing. In addition, a categorical quality flag that summarizes the detailed quality-related information into three classes of high-, medium-, and low-quality DHIs would be useful.

### 3.6. Snow and glaciers

We suggest that snow cover extent is an essential data product to support climate change investigations and snow hydrology applications. Although most land cover remote sensing classifications include permanent snow and ice thematic classes, there is a need to map inter- and intra-annual variability in snow cover. Trends in the perennial land ice extent relate to local climate trends and the impacts of warming, water resources during the dry season, and contributions to sea level rise as glaciated areas continue to recede globally.

Satellite-based cryospheric products, primarily derived from active and passive microwave data, and in a few cases Landsat, emerged in the late 1980s with imaging of ice sheet margins, sea ice, snow cover, albedo, and surface melting (Cavalieri et al., 2003; Key and Haefliger, 1992; Key et al., 2016). Mapping snow cover extent was based on thresholding spectral indices such as the Normalized Difference Snow Index (NDSI), which is the normalized ratio of the green and SWIR bands (Dozier, 1989). Landsat snow cover extent mapping was limited by visible band saturation in the pre-Landsat-8 era (Crawford et al., 2013; Hall et al., 1986) and Landsat's low temporal resolution, which prohibited the mapping of fast-changing snow cover conditions that occur, for example, in mountainous regions and ephemeral mid-latitude melt zones (Crawford, 2015; Selkowitz and Forster, 2016a). In the 1990s and early 2000s, snow mapping algorithms were developed using Landsat and MODIS with refinements using other indices such as the NDVI to reduce NDSI thresholding sensitivity to forest cover (Hall et al., 2019; Riggs and Hall, 2020; Riggs et al., 2017). Spectral unmixing methods were developed that retrieved the sub-pixel fractional snow cover by unmixing end-member snow spectra from various background surface types such as rock, soil, or vegetation (Dozier et al., 2009; Painter et al.,

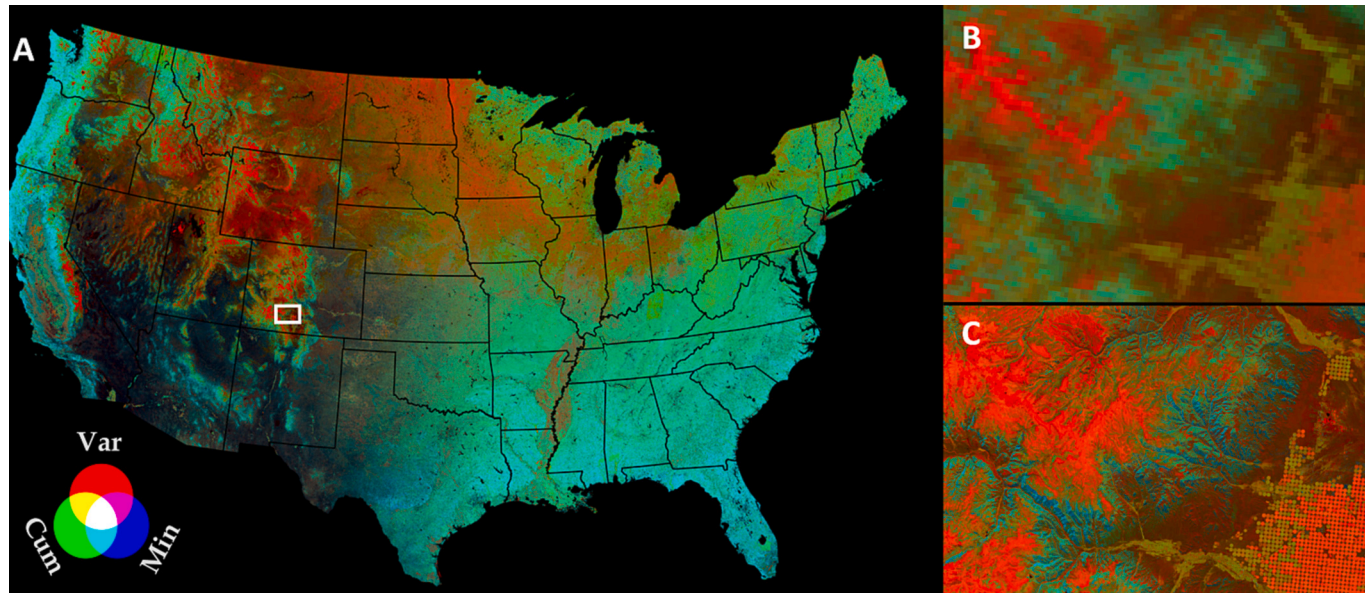


**Fig. 4.** The three Dynamic Habitat Indices (DHIs) from Landsat for the conterminous US (A) as a color composite with the cumulative, minimum and variability DHIs in GBR, and a zoom-in for parts of Colorado highlighting differences between MODIS (B) and Landsat DHIs (C).

2003; Painter et al., 2009). The improved radiometric resolution of the Landsat-8 and 9 optical wavelength sensors (12- and 14-bit, respectively, versus 8-bit for previous Landsat sensors) greatly increases the efficacy of the spectral unmixing approach for snow cover mapping (Crawford et al., 2019). For example, spectral unmixing is the basis for the current USGS fSCA algorithm (Selkowitz and Forster, 2016b; Selkowitz et al., 2017).

A second essential product is perennial ice extent, which has been developed using MODIS and VIIRS by tracking the seasonal minimum snow extent, and spectrally determining the extent of exposed bare ice and snow-covered glacier ice, and excluding debris-covered areas (ice with heavy debris cover, or rock glaciers, or ice pods within permafrost, are not typically considered in the mapping) (Rittger et al., 2021; Rittger et al., 2013). Perennial ice extent mapping is also possible with the current Landsat and Sentinel-2 constellation using existing algorithms that together have daily coverage >50° latitude and sub-daily coverage near the poles (Li and Roy, 2017). Although past algorithms based on MODIS and VIIRS have succeeded in mapping the snow cover minimum and its interannual variability, mapping the trend of perennial land ice cover will require the medium-resolution scale of the Landsat and Sentinel-2 sensors because extent changes are small from one year to the next.

For snow cover extent, validation and quality data will need to address retrieval uncertainties that propagate from atmospheric correction artifacts, cloud and cloud shadow contamination (Crawford et al., 2013), and terrain shadowing (Rittger et al., 2021). For accuracy assessments, especially of fractional snow cover maps, high-resolution satellite imagery is necessary. Just as Landsat data were used to develop and validate snow cover products from MODIS (Crawford, 2015; Hall et al., 2001; Rittger et al., 2013), Landsat snow cover algorithms can be validated using high spatial resolution WorldView or PlanetScope imagery (Bair et al., 2020; Stillinger et al., 2019). To validate perennial ice cover, Worldview stereo imagery and other sources of high-resolution topographic data can be used to identify the surface slope break along debris-covered glacier boundaries relative to the adjacent non-ice or low-ice content material.

As a desirable product, we recommend glacier and ice sheet velocity data in addition to snow albedo (Section 3.4.2) and cover extent. Glacier and ice sheet flow velocity measurement by VNIR image-pair correlation to map ice feature displacement is quite mature (Bindschadler and Scambos, 1991; Fahnestock et al., 2016). These approaches became feasible thanks to the improved radiometric sensitivity of Landsat-8 and Sentinel-2, which allows ice flow tracking by estimating displacement based on decameter-scale roughness features (sastrugi fields, (Bindschadler, 2003)), even in the absence of higher-contrast crevasses or debris cover.

### 3.7. Inland and coastal water extent and condition

#### 3.7.1. Surface water extent and dynamics

Surface water greatly affects climate, ecosystem processes, and human activity (Arnell, 2004; Shiklomanov, 1998). Surface water extent is highly dynamic due to both natural processes such as precipitation and evaporation, and human activities such as damming and irrigation. Information on surface water presence is a key variable in numerical weather prediction and climate models (IPCC, 2013) (Subin et al., 2012). The Global Climate Observing System (GCOS) has identified lake area as an Essential Climate Variable, and surface water occurrence change is one of the relevant indicators of change in the climate system (Adrian et al., 2009). Natural lakes and free-flowing rivers are among the world's most species-rich ecosystems (Dudgeon et al., 2006), making surface water habitat an Essential Biodiversity Variable (Pereira et al., 2013; Pettorelli et al., 2016). Similarly, the UN Sustainable Development Target 6.6 calls for protection and restoration of water-related ecosystems and for the monitoring of change in their extent over time as a key environmental indicator (UN Environment, 2019). Humanity

depends on water for drinking (WHO, 2016), sanitation (Hutton et al., 2004), food production (Khan and Hanjra, 2009; Luseno et al., 2003), energy (Spang et al., 2014), and industry (Florke et al., 2013), while waterborne diseases such as malaria, and dengue pose substantial health risks (Birley, 1991).

Given the critical importance of surface water for climate, biodiversity, and humanity, it is necessary to map surface water occurrence reliably and consistently worldwide over several decades, with the highest possible spatial and temporal resolution. This means capturing seasonal and inter-annual changes of waterbodies, as well as their persistence over time (Belward et al., 2020). While surface water is often included in land cover maps, such maps do not capture surface water dynamics, which require mapping surface water extent ideally on a daily basis, but at least weekly. There are various methods for mapping surface water using optical remote sensing, with distinct trade-offs in terms of spatial and temporal resolution (Huang et al., 2018). The necessary first step in retrieving a range of downstream derivatives is identifying surface water presence or absence with very low commission and omission error for each single observation ('pixel level'). Such higher-level derivatives are available in the Global Surface Water Explorer and include products such as occurrence, occurrence change intensity, maximum extent, recurrence, seasonality, and transition (Fig. 5), which describe both short- and long-term global surface water dynamics (Pekel et al., 2016). Landsat data allow to map surface water seasonality at 5- to 10-year intervals (Yamazaki et al., 2015), and over multiple decades at sub-continental (Tulbure et al., 2016), continental (Mueller et al., 2016), and global scales (Pekel et al., 2016; Pickens et al., 2020). However, Landsat's 30-m resolution and relatively low observation frequency induce omission errors for smaller water bodies, which can be widespread (Downing et al., 2006) and precludes mapping of surface hydrological connectivity (Wu et al., 2021) making it advantageous to also analyze 10-20 m Sentinel-2 or Sentinel-1 data.

The identification of surface water presence or absence with low commission and omission error is the necessary first step before deriving temporally resolved water parameters, such as the maximum surface water extent, water recurrence and seasonality, needed to describe short- and long-term global surface water dynamics (Pekel et al., 2016). Inland water's small area (<3% of the global land area) and high spatio-temporal variability pose particular challenges to assess accuracy globally across different sensors and over several decades (Pekel et al., 2016; Pickens et al., 2020) while adhering to best statistical practices (Olofsson et al., 2014; Olofsson et al., 2012).

The validation design for water surface evaluation must address the inherent challenges of small spatial extent and spatio-temporal variation of inland water (Pekel et al., 2016). Obtaining a comprehensive global reference dataset for validation purposes is challenging due to the limited availability of high spatial resolution imagery archives. Furthermore, the frequent cloud coverage in certain regions restricts the availability of suitable observation. However, to meet the requirements of best statistical practices, a substantial number of samples is necessary. For instance, the validation of the Global Surface Water Explorer conducted by Pekel et al. (2016) utilized a comprehensive set of 40,124 control points. A confidence measure of the class assignment (i.e., water, land, or non-valid observation) should be provided as per pixel QA flags, and propagated into parameters that document the long-term surface water dynamics.

#### 3.7.2. Surface water quality

Just as important as the presence or absence of surface water is its quality, which is directly related to the ecosystem services waterbodies offer. Water quality is usually defined in terms of the physical, chemical, or biological properties of the water column. Global human change and rising temperature together with more frequent severe weather events threaten water quality in lakes, rivers, reservoirs, and coastal environments (Vörösmarty et al., 2000; Whitehead et al., 2009). Optical remote sensing allows for monitoring surface water quality indicators such as

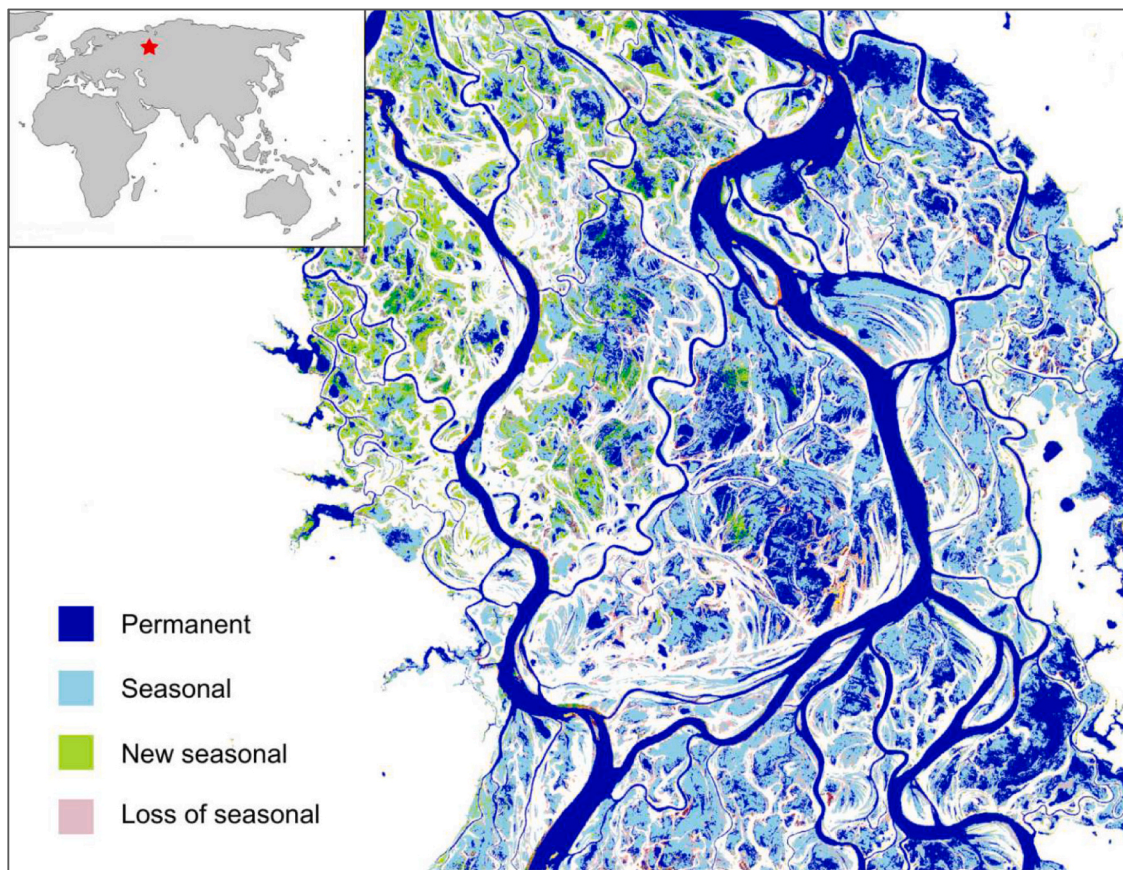


**Fig. 5.** An example of the water transition extracted from the Global Surface Water Extent dataset (Pekel et al., 2016) focusing on the River Ob in western Siberia, Russia. This change map offers comprehensive documentation of transitions taking place between permanent water bodies and seasonal ones, and is based on an analysis of the entire Landsat archive.

the concentration of chlorophyll-a (Chla), which is the primary pigment in phytoplankton (Carpenter and Carpenter, 1983). MODIS Chla products at 250- to 1000-m resolution have been utilized for studying and monitoring harmful algal blooms and trophic states in coastal waters (Park et al., 2010; Werdell et al., 2009) as well as in large African or North American lakes (Binding et al., 2010; Chavula et al., 2009). However, many water bodies are too small to be reliably monitored with MODIS or MERIS data. For instance, Clark et al. (2017) showed that only < 10% of the U.S. water bodies (e.g., drinking water supplies, recreational waters) are resolvable through a nominal 300 m spatial resolution.

Since the mid-1980s, Landsat data analyses of small waterbodies demonstrated the feasibility for determining turbidity and total suspended solids (TSS) (Carpenter and Carpenter, 1983; Mertes et al., 1993; Montanher et al., 2014), harmful algal blooms (Ho et al., 2017) and water clarity (Kloiber et al., 2002). The utility of Landsat-5 and 7 data, however, remained largely exploratory, due to their low temporal resolution, low radiometric resolution, and sparse spectral bands in the visible and NIR needed to monitor dynamic water quality parameters (Mouw et al., 2017). The improved radiometric quality and spectral coverage of the Landsat-8 and 9 OLI and OLI-2 (Masek et al., 2020) combined with Sentinel-2A and -2B MSIs with similar radiometric capabilities but improved spectral resolution in the NIR, has spurred research efforts to assess the feasibility of generating harmonious water quality products from the two missions (Kuhn et al., 2019; Pahlevan et al., 2019).

Combined Landsat and Sentinel-2 water quality products would enable the monitoring of naturally dynamic aquatic ecosystems, impacts of episodic events such as extended wet/dry periods (Gámez et al., 2019; Sinha et al., 2017), illegal spills and discharges (Dethier et al., 2019),

and harmful algal blooms (Bresciani et al., 2018). Indeed, the shellfish industry is using this virtual constellation for site selection, and to devise risk mitigation strategies in the event of harmful algal blooms (Gernez et al., 2017; Snyder et al., 2017). The UNEP as the custodian agency for Sustainable Development Goal 6.3.2 indicator (i.e., the proportion of waterbodies with good ambient waters) is leveraging such data products to report on the global near-surface water quality conditions on a global scale. Estimating essential near-surface water quality variables including Chla, TSS, turbidity, and Secchi disk depth (or transparency) requires consistent satellite TOA reflectance data with reliable cloud screening and atmospheric correction (Pahlevan et al., 2021), and retrieval algorithms that, to date, rely mostly on empirical or semi-analytical models (IOCCG, 2000, 2018).

Given the state of the knowledge and the availability of adequate *in situ* training datasets, global TSS, turbidity, and transparency products from both Landsat and Sentinel-2 observations are feasible for a range of aquatic conditions (Balasubramanian et al., 2020; Kuhn et al., 2019). With its red-edge band, Sentinel-2 is capable of resolving Chla in highly turbid/eutrophic waters whereas, similar to coarse-resolution imagers like VIIRS that are missing this band, Landsat can be used to retrieve Chla in less trophic waters (i.e., Chla < 8 mg m<sup>-3</sup>) (Jiang et al., 2020; Pahlevan et al., 2022; Smith et al., 2021). Progress on compensating for atmospheric effects will reduce the uncertainties in surface water quality products although atmospheric correction algorithms over aquatic environments are still underway (Pahlevan et al., 2021).

Validation of surface water quality products has been demonstrated (Pahlevan et al., 2022; Warren et al., 2021). However, high spatio-temporal dynamics of aquatic ecosystems, in particular in estuaries or larger lakes, present a major challenge when comparing satellite retrievals with field measurements. Frequent cloud cover, haze, sunglint

effects, and unfavorable environmental conditions (e.g., high winds) further diminish validation opportunities particularly in low and high latitudes. Lastly, validation data in developing countries are scarce, requiring a more cautious approach for the interpretation of products there. Surface water quality products should include pixel-level quality assessment flags, ideally in the form of continuous variables that quantify the confidence in a given estimate, rather than just categorical variables separating, for example, high-, medium- and low-quality pixels.

### 3.8. Evapotranspiration

Evapotranspiration (ET) is the net transfer of water from the land to the atmosphere, via both transpiration from plants and evaporation from soil and other surfaces. ET is the second largest component of the water budget, after precipitation, and a measure of the water that is consumed and lost from a watershed and therefore unavailable for other uses. Irrigated agriculture accounts for 70% of human water use globally, and water demand is expected increase further by 20% by 2050 due to increased irrigation needs (AQUASTAT, 2016; WWAP, 2012). Thus, accurate information on ET is required to balance water supply and water demand, and to ensure adequate water supplies for agricultural production, ecosystem needs, and other uses. Satellite observations in the thermal infrared and reflectance bands can be used to assess surface moisture and vegetation status governing evaporative losses over both natural and managed landscapes.

MODIS 8 and 16-day ET products are systematically generated globally at 500-m resolution based on the Penman-Monteith model, and used in regional water use assessments (Abolafia-Rosenzweig et al.,

2021; Mu et al., 2011). However, for many water resource applications, satellite data and derived ET products at <100-m resolution are required to capture variations in water use and plant stress at the stand or field scale (Anderson et al., 2012) (Fig. 6). Landsat is optimal for developing field-scale ET products because it provides well-calibrated, co-registered, and contemporaneous TIR and optical data at medium resolution (30–100 m). The aforementioned lack of Sentinel-2A and -2B TIR bands limits the use of their imagery standalone for ET estimation.

A variety of remote sensing approaches with different spectral and ancillary inputs, computational demands, and varying levels of complexity have been developed to map ET from Landsat data. Approaches that rely only on optical data commonly use crop type information and crop-specific NDVI transformations to estimate fractional cover, and ultimately instantaneous and 24 hr ET (Melton et al., 2012; Pereira et al., 2020). Another class of models use surface energy balance approaches (Allen et al., 2007; Anderson et al., 2007), which account for the energy used to transform liquid water in plants and soil into vapor, and rely on thermal, optical, and weather data to estimate net radiation, sensible heat flux, ground heat flux, and latent heat flux, or ET. Simplified surface energy balance approaches that rely on thermal and optical data are sometimes preferred for computational efficiency, but in these, certain components of the energy balance are not estimated (Fisher et al., 2008; Senay, 2018). In each of these approaches, instantaneous ET retrieved at the time of the satellite overpass is typically upscaled to a daily (24 hr total) value through the use of a scaling flux such as solar radiation, net radiation, or standardized reference ET, where daily ET = F \* ET<sub>f</sub>, and F is the daily scaling flux (L/T) and ET<sub>f</sub> (unitless) is the instantaneous fraction of the daily scaling flux. When reference ET is used for F, ET<sub>f</sub> is analogous to a crop coefficient used by

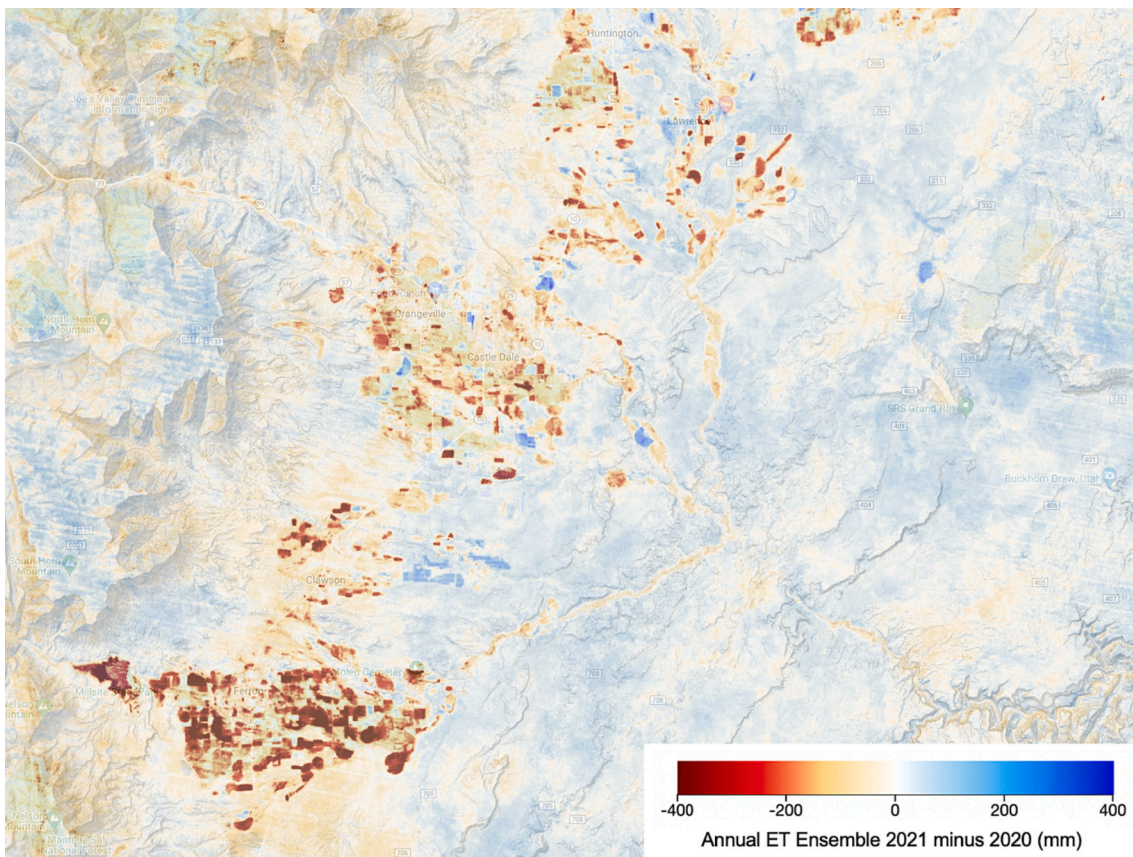


**Fig. 6.** Landsat-based OpenET ensemble average ET (Melton et al., 2021) difference between 2021 and 2020 annual ET for Ferron and Castle Dale, Utah, in the Upper Colorado River Basin. Agricultural areas in the region are primarily flood irrigated from mountain front streams, and low winter precipitation in 2020–2021 negatively impacted irrigation deliveries as seen by reduced field-scale ET in 2021. Growing season precipitation was higher in 2021, resulting in higher ET within dryland areas than in 2020. Figure created using ClimateEngine.org, basemap Google.

the agricultural engineering community (Hobbs and Huntington, 2016), but is representative of actual field conditions instead of well-watered conditions that traditional crop coefficients assume.

To gain credibility within the user community, Landsat ET products require comprehensive and rigorous evaluation over a range of vegetation cover types (e.g., croplands, grasslands, forests, shrublands), climate conditions (humid to arid), and land-management strategies (e.g., irrigated and rainfed crops). Validation data sources range from “point measurements” (meter to kilometer scale) from lysimeters and eddy covariance (EC) flux towers to larger scale (e.g., watershed) estimates obtained via water balance. Each type of measurement requires careful treatment and consideration of potential sources of measurement uncertainty. EC tower fluxes must undergo rigorous post-processing and energy budget closure assessment with station flux footprints identified to pair with respective satellite fluxes (Volk et al., 2023). Water balance requires high quality precipitation and streamflow data, and good understanding of watershed dynamics. The model intercomparison study conducted under the OpenET project makes use of all types of measurements, and may serve as an example for future remote sensing ET product validation and benchmark efforts (Melton et al., 2021; Volk et al., 2023). QA flags should propagate from thermal and VSWIR inputs to the ET model, as well as quality of gridded input meteorological inputs if available. Errors in ST retrieval due to undetected clouds or cloud fringes will be a major source of non-algorithmic error to ET estimates.

Although ETf and 24hr ET on Landsat overpass dates are essential products, land managers often require time-continuous information at daily, weekly or monthly time-steps. Gap-filling ET between Landsat overpasses can be accomplished by interpolating the instantaneous ETf retrieval on the overpass date to time-continuous values, then recovering the ET time series values at each time step *i* from the scaling flux time series:  $ET(i) = F(i) \times ETf(i)$ . The time step for a desirable ET time series product will be constrained by computational capabilities and storage capacity. Errors in daily ET estimates due to temporal interpolation decrease as the interval between satellite overpasses decreases by about 20% on average between 16 days and 8 days. Therefore, use of multiple medium-resolution satellite platforms capable of simultaneous acquisition of thermal and optical data is ideal for increasing accuracy of monthly, seasonal, and annual ET estimates. QA flags would need to reflect the temporal density of direct retrievals used in the interpolation.

#### 4. Aspirational future products

In addition to the essential and the desirable products outlined above, there are opportunities for aspirational, future products, which will require further algorithms refinements, but could become feasible. What follows are a few examples of such products, not a comprehensive list.

For land cover, there is proof-of-concept for the mapping forest types, or dominant tree species at the genus level if stands are fairly uniform, for both boreal (Astola et al., 2019; Hermosilla et al., 2023) and temperate (Hemmerling et al., 2021) forests. Similarly, forest structure has been successfully mapped for selected regions. For all of Canada's forests, attributes including biomass, volume, canopy cover, and height, have been mapped using Landsat, with the generation of time series structural dynamics also demonstrated (Matasci et al., 2018a; Matasci et al., 2018b). In urban areas, medium-resolution satellite data can capture urban form and structure, and provide information on urban heterogeneity by using new spectral indices or subpixel mapping to characterize inter-urban variation (Chen et al., 2020; Zhu et al., 2019c).

For forest disturbances, insect defoliation of forests has been successfully mapped in case studies (Goodwin et al., 2008; Ye et al., 2021b). Similarly, medium-resolution satellite data capture wind-throw in forests well (Baumann et al., 2014), but distinguishing disturbance agents correctly is an area of active research (Sebald et al., 2021; Senf and Seidl, 2021). For burned area mapping, retrieval of the fraction of the pixel that burned and the combustion completeness is of interest for pyrogenic

emission estimation, but they may be challenging to retrieve reliably over heterogeneous vegetation canopies and after post-fire exposure of soil (Roy et al., 2019).

In terms of vegetation condition, crop yield estimates are fairly mature for some crops (e.g., maize, (Kang and Ozdogan, 2019)) and in some areas (e.g., North America (Johnson, 2014)), indicating that their yields could be monitored globally with Landsat and Sentinel-2 data, and yields of other crops may be possible to monitor routinely as well (Ferencz et al., 2004; Gao et al., 2019). Similarly, the combination of Landsat and Sentinel-2 is frequent enough to capture mowing of temperate grasslands (Griffiths et al., 2020; Schwieder et al., 2022), thereby extending the mapping of grassland cover into grassland use. Using HLS data and a within-season emergence algorithm (Gao et al., 2020), crop emergence dates were mapped over the U.S. corn belt (Gao et al., 2021), inspiring early-season crop monitoring for a large area.

For biodiversity, habitat heterogeneity as captured by image texture is an aspirational product. Habitat texture captures small-scale variability in reflectance among nearby pixels resulting from the heterogeneity in the vegetation (Kayitakire et al., 2006; Wood et al., 2012), and high image texture is correlated with high species richness (Culbert et al., 2013; Hepinstall and Sader, 1997), and species occurrences (Estes et al., 2008; St-Louis et al., 2010). A second aspirational product for biodiversity is the set of three winter habitat indices capturing spatio-temporal patterns of snow (Gudex-Cross et al., 2021; Zhu et al., 2019a). The duration of snow cover, and variability of snow cover are both good predictors of species richness (Gudex-Cross et al., 2022), and high thermal heterogeneity of land surface temperature in winter is a proxy for the availability of thermal refugia (Elsen et al., 2020).

For the cryosphere, melt ponds on glaciers and sea ice are captured by Landsat data (Kingslake et al., 2017) because ponds have low NIR and SWIR reflectance. Other aspirational products are snow grain size (Fily et al., 1997; Painter et al., 2009), and ice front position for ice sheet outlet glaciers (Howat and Eddy, 2011; Moon and Joughin, 2008).

Regarding the biology and biogeochemical cycles of aquatic ecosystems, aspirational products include absorption by colored dissolved organic matter, source and fate of dissolved organic matter (Fichot and Benner, 2011), phytoplankton types (Mouw et al., 2017), organic and inorganic particle properties (Bukata et al., 1995; Estapa et al., 2012; Woźniak et al., 2010), and harmful algal bloom quantifications (i.e., estimating cyanobacterial biomass) (Matthews and Odermatt, 2015; Mishra et al., 2013).

Furthermore, the combination of Landsat and Sentinel-2 data with other types of satellite data, offers exciting opportunities for more aspirational products. The suite of essential global Landsat and Sentinel-2 data products systematically generated with production QA and validation, combined with the availability of a global ARD, would accelerate the development of fusion products. For example, there is potential to gap-fill and perhaps improve forest structure retrieval by integration of Landsat and Sentinel-2 data with lidar (e.g., GEDI, ICESat-2), and radar (e.g., Sentinel-1 and upcoming NISAR) data.

Ultimately, most of these and other aspirational products could be feasible for systematic production in the next decade given further research and algorithm refinement. The list of aspirational products is likely to grow as innovation and ingenuity devises new applications for Landsat and Sentinel-2 data.

#### 5. Discussion

The time is right for the production of a suite of essential medium-resolution, global, systematic products. With an observation opportunity almost every second day, the current constellation of two Landsat and two Sentinel-2 satellites provide temporal frequency that is unparalleled and comes close to the daily observations that coarse-resolution satellites provide. The high frequency at which medium-resolution satellite data are now available offers major opportunities to generate timely information for many pressing global problems. There are clear

and growing information needs related to a range of global change challenges that require a suite of medium-resolution products. Currently, these information needs are not met, which is detrimental to both, global change science and environmental management, and means that many of the potential benefits of the substantial investments into satellite sensors and ground segments have not yet been realized.

Ultimately, the goal is to provide a broad suite of scientifically robust and socially relevant data products that are policy informative, not policy prescriptive. The information needs are greatest for the relatively short list of essential products (Table 2). These products should be the highest priority, and include land cover, land cover change, burned area, forest loss, vegetation indices, phenology, dynamic habitat indices, albedo, land surface temperature, snow cover, ice extent, surface water extent, and evapotranspiration. We recommend that all of these products are produced globally and at least annually, and some of them, for example, evapotranspiration, surface water extent, and burned area, should be produced at finer temporal resolution. The reason why we deem these products as essential is that there is a well-established and high level of demand from large and varied user communities. Furthermore, all of these essential products pertain to multiple global change challenges including climate change, biodiversity conservation, food security, sustainable natural resource management and ecosystem services, and natural hazards (Table 1). Furthermore, for the essential products, algorithms are mature, lessening technological hurdles towards production.

In addition, we identified a longer list of desirable products because global change has many dimensions (Table 2). Examples of desirable products include leaf area index, land surface emissivity, ice sheet velocity, and surface water quality. Clearly, the desirable products meet many important information needs, and if sufficient resources were available, their production would be highly beneficial. However, the desirable projects either have currently a smaller user community or their algorithms are not as mature as the essential product algorithms.

### 5.1. Institutional and computational settings for product generation

There are different institutional approaches via which these products could be generated, and we do not advocate for a specific one. Successful models for the generation of terrestrial satellite products include partnerships between science agencies and academia (e.g., NASA's MODIS product suite), or by government research agencies (e.g., the NLCD by the USGS) or between public and private entities (e.g., EU's Copernicus Program). Research groups in academia play an important role developing algorithms, and demonstrating aspirational products, but such groups often struggle to maintain continuous funding to ensure the necessary long-term consistency and production of data products. Given that the combination of Landsat and Sentinel-2 satellite data will result in products with the most desired spatial and categorical features for applications of global interest, value could be found in an international collaboration to support the generation of these products. CEOS could be one organization to foster such a collaboration.

Independent of the approach, multi-decadal funding is required to maintain product continuity, including support for routine quality assessment, periodic validation, and product reprocessing. Products should have sufficient algorithm and product documentation, including information on the upstream and ancillary data used in the product generation, to allow verification of scientific claims and allow others to reproduce the products. Sharing algorithms openly will foster the involvement of user communities in the generation and review of the products, which in turn will foster wider product use. User communities will embrace medium-resolution products more readily if their long-term availability is guaranteed. This is likely if products are generated with government agency support, or the support from multiple governments in an international collaboration. Indeed, laws and policy frameworks increasingly require the use of Earth observation data as compliance and performance tools, and once the essential medium-

resolution products that we propose here become readily available, that trend will further accelerate. In this regard, rigorous and independent accuracy assessments of all products are also key, because they instill trust in the quality of the products and provide numeric estimates of the uncertainty in the products that are necessary to make informed decisions.

The products should be hosted in long-term guaranteed archives and made freely and easily available. Both the Landsat and Sentinel-2 satellite programs have plans for future launches and a commitment to continue with current open data policies. Although commercial satellite constellations do not provide a consistent global acquisition strategy and are not openly distributed without cost, the ability to request high-resolution acquisitions provides value-added information complementing long-term, medium resolution global data that are freely and openly distributed.

In terms of the computing environment, cloud-computing makes the generation and reprocessing of high-level products more feasible. For example, the USGS recently used commercial cloud computing to efficiently reprocess the Landsat archive and enable direct cloud access of Landsat images including global surface reflectance and land surface temperature (Crawford et al., 2023). Similarly, Google Earth Engine has enabled a new community to process medium-resolution satellite data at continental to global scales. However, cloud computing does not change the need for systematic product generation, and we do not advocate for an on-demand-processing model. Aside from the computational overhead, systematically generated products are needed for governmental reporting needs, and to ensure that scientific results are reproducible. Furthermore, there is little research so far on how to conduct valid accuracy assessments or quality assessments for on-demand-processed products. The aforementioned reporting needs and need for reproducible results necessitates a well-designed collection strategy and versioning control due to the implications of changes in upstream products on those further downstream.

## 6. Conclusions

We developed here a list of products to be derived from medium-resolution Landsat and Sentinel-2 data, which include land cover, land cover change, burned area, forest loss, vegetation indices, phenology, dynamic habitat indices, albedo, land surface temperature, snow cover, ice extent, surface water extent, and evapotranspiration. To create the proposed suite of essential products is a major undertaking, and requires that major challenges will have to be overcome, both in terms of securing long-term funding, creating the appropriate institutional and organizational setting, designing robust and efficient algorithms, and processing and storing very large volumes of data. However, producing these essential products would be a small undertaking in comparison to launching and operating the current constellation of medium-resolution satellites, and greatly leverage their value for much larger user communities. Serving these user communities, in turn, provides the strongest possible justification for future medium-resolution satellite missions, and the continuation of the Landsat and Sentinel-2 legacy. Two decades since MODIS products became available, and five decades after the first Landsat images were recorded, there is now the opportunity to produce freely available, standardized, and consistent products based on medium-resolution satellite imagery, which would be another major steps towards what inspired and sustained the Landsat program throughout its history.

## Declaration of Competing Interest

The authors declare that they have no known competing financial interests or personal relationships that could have appeared to influence the work reported in this paper.

## Data availability

No data was used for the research described in the article.

## Acknowledgments

We gratefully acknowledge the NASA-USGS-industry Landsat development team for their efforts to ensure the continuity of the Landsat mission, and we thank the USGS for co-sponsoring and funding the USGS–NASA Landsat Science Team (<https://www.usgs.gov/landsat-missions/landsat-science-teams>). We also acknowledge the significant contributions of Dr. Jeff Masek (NASA/GSFC, retired), who was instrumental in supporting the Landsat Science Team and the development of multi-sensor products, John Dwyer (USGS, deceased, 2022) who in particular contributed to the development of operational Landsat products, and Dr. Thomas Loveland (USGS, deceased 2022) whose breadth of knowledge, leadership, and dedication to this and the previous Landsat Science Teams contributed greatly to the long-term success of the Landsat mission. Thanks also to Dr. Angela Erb, who assisted with figure preparation. Any use of trade, firm, or product names is for descriptive purposes only and does not imply endorsement by the U.S. Government.

## References

- Abolafia-Rosenzweig, R., Pan, M., Zeng, J.L., Livneh, B., 2021. Remotely sensed ensembles of the terrestrial water budget over major global river basins: An assessment of three closure techniques. *Remote Sens. Environ.* 252, 112191.
- Adrian, R., O'Reilly, C.M., Zagarese, H., Baines, S.B., Hessen, D.O., Keller, W., Livingstone, D.M., Sommaruga, R., Straile, D., Van Donk, E., Weyhenmeyer, G.A., Winder, M., 2009. Lakes as sentinels of climate change. *Limnol. Oceanogr.* 54, 2283–2297.
- Allen, R.G., Tasumi, M., Trezza, R., 2007. Satellite-based energy balance for mapping evapotranspiration with internalized calibration (METRIC) - Model. *J. Irrig. Drain. Eng.* 133, 380–394.
- Anderson, M.C., Norman, J.M., Mecikalski, J.R., Otkin, J.A., Kustas, W.P., 2007. A climatological study of evapotranspiration and moisture stress across the continental United States based on thermal remote sensing: 1. Model formulation. *J. Geophys. Res.-Atmos.* 112, D10117.
- Anderson, M.C., Allen, R.G., Morse, A., Kustas, W.P., 2012. Use of Landsat thermal imagery in monitoring evapotranspiration and managing water resources. *Remote Sens. Environ.* 122, 50–65.
- Andrew, M.E., Wulder, M.A., Nelson, T.A., 2014. Potential contributions of remote sensing to ecosystem service assessments. *Prog. Phys. Geogr.* 38, 328–353.
- AQUASTAT, F., 2016. Water withdrawal by section, around 2010. In: In: Food and Agriculture Organization of the United Nations, Rome.
- Arino, O., Piccolini, I., Kasischke, E., Siegert, F., Chuvieco, E., Martin, P., Li, Z., Fraser, R. H., Eva, H., Stroppiana, D., Pereira, J.M.C., Silva, J.M.N., Roy, D., Barbosa, P., 2001. Methods of mapping surfaces burned in vegetation fires. In: Ahern, F.J., Goldammer, J.G., Justice, C. (Eds.), Global and Regional Fire Monitoring from Space: Planning a Coordinated International Effort. SPB Publishing, The Hague, pp. 227–255.
- Arnell, N.W., 2004. Climate change and global water resources: SRES emissions and socio-economic scenarios. *Glob. Environ. Change* 14, 31–52.
- Astola, H., Hame, T., Sirro, L., Molinier, M., Kilpi, J., 2019. Comparison of Sentinel-2 and Landsat 8 imagery for forest variable prediction in boreal region. *Remote Sens. Environ.* 223, 257–273.
- Azzari, G., Grassini, P., Edreira, J.I.R., Conley, S., Mourtzinis, S., Lobell, D.B., 2019. Satellite mapping of tillage practices in the North Central US region from 2005 to 2016. *Remote Sens. Environ.* 221, 417–429.
- Bacour, C., Breon, F.M., 2005. Variability of biome reflectance directional signatures as seen by POLDER. *Remote Sens. Environ.* 98, 80–95.
- Bair, E.H., Rittger, K., Ahmad, J.A., Chabot, D., 2020. Comparison of modeled snow properties in Afghanistan, Pakistan, and Tajikistan. *Cryosphere* 14, 331–347.
- Balasubramanian, S.V., Pahlevan, N., Smith, B., Binding, C., Schalles, J., Loisel, H., Gurlin, D., Greb, S., Alikas, K., Randa, M., Bunkei, M., Moses, W., Ha, N., Lehmann, M.K., O'Donnell, D., Ondrusek, M., Han, T.H., Fichot, C.G., Moore, T., Boss, E., 2020. Robust algorithm for estimating total suspended solids (TSS) in inland and nearshore coastal waters. *Remote Sens. Environ.* 246, 111768.
- Baret, F., Morissette, J.T., Fernandes, R.A., Champeaux, J.L., Myneni, R.B., Chen, J., Plummer, S., Weiss, M., Bacour, C., Garrigues, S., Nickeson, J.E., 2006. Evaluation of the representativeness of networks of sites for the global validation and intercomparison of land biophysical products: Proposition of the CEOS-BELMANIP. *IEEE Trans. Geosci. Remote Sens.* 44, 1794–1803.
- Barlow, J., Martin, Y., Franklin, S.E., 2003. Detecting translational landslide scars using segmentation of Landsat ETM+ and DEM data in the northern Cascade Mountains, British Columbia. *Can. J. Remote. Sens.* 29, 510–517.
- Barsi, J.A., Schott, J.R., Hook, S.J., Raqueno, N.G., Markham, B.L., Radocinski, R.G., 2014. Landsat-8 thermal infrared sensor (TIRS) vicarious radiometric calibration. *Remote Sens.* 6, 11607–11626.
- Baumann, M., Ozdogan, M., Wolter, P.T., Krylov, A., Vladimirova, N., Radeloff, V.C., 2014. Landsat remote sensing of forest windfall disturbance. *Remote Sens. Environ.* 143, 171–179.
- Baumann, M., Ozdogan, M., Richardson, A.D., Radeloff, V.C., 2017. Phenology from Landsat when data is scarce: Using MODIS and dynamic time-warping combine multi-year Landsat imagery to derive annual phenology curves. *J. Appl. Earth Obs. Geoinform.* 54, 72–83.
- Belward, A., Pekel, J., Cottam, A., Gorelick, N., De Felice, L., Wen, Q., Dewsbury, I., 2020. *Atlas of Global Surface Water Dynamics*. Luxembourg.
- Benedetti, A., Morcrette, J.J., Boucher, O., Dethof, A., Engelen, R.J., Fisher, M., Flentje, H., Huneeus, N., Jones, L., Kaiser, J.W., Kinne, S., Mangold, A., Razinger, M., Simmons, A.J., Suttie, M., 2009. Aerosol analysis and forecast in the European Centre for Medium-Range Weather Forecasts Integrated Forecast System: 2. Data assimilation. *J. Geophys. Res.-Atmos.* 114, D13205.
- Berner, L.T., Massey, R., Jantz, P., Forbes, B.C., Macias-Fauria, M., Myers-Smith, I., Kumpula, T., Gauthier, G., Andreu-Hayles, L., Gaglioti, B.V., Burns, P., Zetterberg, P., D'Arrigo, R., Goetz, S.J., 2020. Summer warming explains widespread but not uniform greening in the Arctic tundra biome. *Nat. Commun.* 11 (4621), 4621.
- Berry, S., Mackey, B.G., Brown, T., 2007. Potential applications of remotely sensed vegetation greenness to habitat analysis and the conservation of dispersive fauna. *Pac. Conserv. Biol.* 13, 12–127.
- Betts, R.A., 2000. Offset of the potential carbon sink from boreal forestation by decreases in surface albedo. *Nature* 408, 187–190.
- de Beurs, K.M., Henebry, G.M., 2004. Land surface phenology, climatic variation, and institutional change: Analyzing agricultural land cover change in Kazakhstan. *Remote Sens. Environ.* 89, 497–509.
- Binding, C.E., Jerome, J.H., Bukata, R.P., Booty, W.G., 2010. Suspended particulate matter in Lake Erie derived from MODIS aquatic colour imagery. *Int. J. Remote Sens.* 31, 5239–5255.
- Bindschadler, R., 2003. Tracking subpixel-scale sastrugi with advanced land imager. *IEEE Trans. Geosci. Remote Sens.* 41, 1373–1377.
- Bindschadler, R.A., Scambos, T.A., 1991. Satellite-image-derived velocity-field of an Antarctic ice stream. *Science* 252, 242–246.
- Birley, M.H., 1991. Guidelines for forecasting the vector-borne disease implications of water resources development.
- Bojinski, S., Verstraete, M., Peterson, T.C., Richter, C., Simmons, A., Zemp, M., 2014. The concept of essential climate variables in support of climate research, applications, and policy. *Bull. Am. Meteorol. Soc.* 95, 1431–1443.
- Bolton, D.K., Friedl, M.A., 2013. Forecasting crop yield using remotely sensed vegetation indices and crop phenology metrics. *Agric. For. Meteorol.* 173, 74–84.
- Bolton, D.K., Gray, J.M., Melaas, E.K., Moon, M., Eklundh, L., Friedl, M.A., 2020. Continental-scale land surface phenology from harmonized Landsat 8 and Sentinel-2 imagery. *Remote Sens. Environ.* 240, 111685.
- Boryan, C., Yang, Z.W., Mueller, R., Craig, M., 2011. Monitoring US agriculture: the US Department of Agriculture, National Agricultural Statistics Service, Cropland Data Layer Program. *Geocarto Int.* 26, 341–358.
- Boschetti, L., Roy, D.P., Justice, C.O., Humber, M.L., 2015. MODIS-Landsat fusion for large area 30 m burned area mapping. *Remote Sens. Environ.* 161, 27–42.
- Boschetti, L., Roy, D.P., Giglio, L., Huang, H.Y., Zubkova, M., Humber, M.L., 2019. Global validation of the collection 6 MODIS burned area product. *Remote Sens. Environ.* 235, 111490.
- Bouvet, M., Thome, K., Berthelot, B., Bialek, A., Czapla-Myers, J., Fox, N.P., Goryl, P., Henry, P., Ma, L.L., Marcq, S., Meygret, A., Wenny, B.N., Woolliams, E.R., 2019. RadCalNet: a radiometric calibration network for earth observing imagers operating in the visible to shortwave infrared spectral range. *Remote Sens.* 11, 2401.
- Breiman, L., 2001. Random forests. *Mach. Learn.* 45, 5–32.
- Bresciani, M., Cazzaniga, I., Austoni, M., Sforzi, T., Buzzi, F., Morabito, G., Giardino, C., 2018. Mapping phytoplankton blooms in deep subalpine lakes from Sentinel-2A and Landsat-8. *Hydrobiologia* 824, 197–214.
- Brown, J.F., Tollerud, H.J., Barber, C.P., Zhou, Q., Dwyer, J.L., Vogelmann, J.E., Loveland, T.R., Woodcock, C.E., Stehman, S.V., Zhu, Z., Pengra, B.W., Smith, K., Horton, J.A., Xian, G., Auch, R.F., Sohl, T.L., Sayler, K.L., Gallant, A.L., Zelenak, D., Reker, R.R., Rover, J., 2020a. Lessons learned implementing an operational continuous United States national land change monitoring capability: The Land Change Monitoring, Assessment, and Projection (LCMAP) approach. *Remote Sens. Environ.* 238, 111356.
- Brown, L.A., Meier, C., Morris, H., Pastor-Guzman, J., Bai, G., Lerebourg, C., Gobron, N., Lanconelli, C., Clerici, M., Dash, J., 2020b. Evaluation of global leaf area index and fraction of absorbed photosynthetically active radiation products over North America using Copernicus Ground Based Observations for Validation data. *Remote Sens. Environ.* 247, 111935.
- Brown, C.F., Brumby, S.P., Guzder-Williams, B., Birch, T., Hyde, S.B., Mazzariello, J., Czerwinski, W., Pasquarella, V.J., Haertel, R., Ilyushchenko, S., Schwehr, K., Weisse, M., Stolle, F., Hanson, C., Guinan, O., Moore, R., Tait, A.M., 2022. Dynamic World, Near real-time global 10 m land use land cover mapping. *Sci. Data* 9, 251.
- Bukata, R.P., Jerome, J.H., Kondratyev, K.Y., Pozdnyakov, D.V., 1995. *Optical Properties and Remote Sensing of Inland and Coastal Waters*. CRC Press, New York.
- Bullock, E.L., Woodcock, C.E., Souza, C., Olofsson, P., 2020. Satellite-based estimates reveal widespread forest degradation in the Amazon. *Glob. Chang. Biol.* 26, 2956–2969.
- Büttner, G., Feranec, J., Jaffrain, G., Mari, L., Maucha, G., Soukup, T., 2004. The CORINE land cover 2000 project. In: EARSEL, pp. 331–346.

- Carpenter, D., Carpenter, S., 1983. Modeling inland water quality using Landsat data. *Remote Sens. Environ.* 13, 345–352.
- Carroll, K.A., Farwell, L.S., Pidgeon, A.M., Razenkova, E., Gudex-Cross, D., Helmers, D. P., Lewińska, K.E., Elsen, P.R., Radeloff, V.C., 2022. Mapping breeding bird species richness at management-relevant resolutions across the United States. *Ecol. Appl.* e2624.
- Castaneda, C., Herrero, J., Casterad, M.A., 2005. Landsat monitoring of playa-lakes in the Spanish Monegros desert. *J. Arid Environ.* 63, 497–516.
- Cavalieri, D.J., Parkinson, C.L., Vinnikov, K.Y., 2003. 30-Year satellite record reveals contrasting Arctic and Antarctic decadal sea ice variability. *Geophys. Res. Lett.* 30, 1970.
- CEOS, 2015. Earth Satellite Observations in Support of Climate Information Challenges, p. 37.
- Chastain, R., Housman, I., Goldstein, J., Finco, M., Tenneson, K., 2019. Empirical cross sensor comparison of Sentinel-2A and 2B MSI, Landsat-8 OLI, and Landsat-7 ETM + top of atmosphere spectral characteristics over the conterminous United States. *Remote Sens. Environ.* 221, 274–285.
- Chavula, G., Brezonik, P., Thenkabail, P., Johnson, T., Bauer, M., 2009. Estimating chlorophyll concentration in Lake Malawi from MODIS satellite imagery. *Phys. Chem. Earth* 34, 755–760.
- Chen, J., Liao, A.P., Cao, X., Chen, L.J., Chen, X.H., He, C.Y., Han, G., Peng, S., Lu, M., Zhang, W.W., Tong, X.H., Mills, J., 2015. Global land cover mapping at 30 m resolution: A POK-based operational approach. *ISPRS J. Photogramm. Remote Sens.* 103, 7–27.
- Chen, G., He, Y.N., De Santis, A., Li, G.S., Cobb, R., Meentemeyer, R.K., 2017. Assessing the impact of emerging forest disease on wildfire using Landsat and KOMPSAT-2 data. *Remote Sens. Environ.* 195, 218–229.
- Chen, T.H.K., Prishchepov, A.V., Fensholt, R., Sabel, C.E., 2019. Detecting and monitoring long-term landslides in urbanized areas with nighttime light data and multi-seasonal Landsat imagery across Taiwan from 1998 to 2017. *Remote Sens. Environ.* 225, 317–327.
- Chen, T.H.K., Qiu, C.P., Schmitt, M., Zhu, X.X., Sabel, C.E., Prishchepov, A.V., 2020. Mapping horizontal and vertical urban densification in Denmark with Landsat time-series from 1985 to 2018: A semantic segmentation solution. *Remote Sens. Environ.* 251, 112096.
- Chiabai, A., Travisi, C.M., Markandya, A., Ding, H., Nunes, P., 2011. Economic assessment of forest ecosystem services losses: cost of policy inaction. *Environ. Resour. Econ.* 50, 405–445.
- Chuvieco, E., Martin, M.P., Palacios, A., 2002. Assessment of different spectral indices in the red-near-infrared spectral domain for burned land discrimination. *Int. J. Remote Sens.* 23, 5103–5110.
- Chuvieco, E., Mouillet, F., van der Werf, G.R., San Miguel, J., Tanase, M., Koutsias, N., Garcia, M., Yebra, M., Padilla, M., Gitas, I., Heil, A., Hawbaker, T.J., Giglio, L., 2019. Historical background and current developments for mapping burned area from satellite Earth observation. *Remote Sens. Environ.* 225, 45–64.
- Cihlar, J., 2000. Land cover mapping of large areas from satellites: status and research priorities. *Int. J. Remote Sens.* 21, 1093–1114.
- Clark, J.M., Schaeffer, B.A., Darling, J.A., Urquhart, E.A., Johnston, J.M., Ignatius, A.R., Myer, M.H., Loftin, K.A., Werdell, P.J., Stumpf, R.P., 2017. Satellite monitoring of cyanobacterial harmful algal bloom frequency in recreational waters and drinking water sources. *Ecol. Indic.* 80, 84–95.
- Claverie, M., Ju, J., Masek, J.G., Dungan, J.L., Vermote, E.F., Roger, J.C., Skakun, S.V., Justice, C., 2018. The Harmonized Landsat and Sentinel-2 surface reflectance data set. *Remote Sens. Environ.* 219, 145–161.
- Cohen, W.B., Goward, S.N., 2004. Landsat's role in ecological applications of remote sensing. *Bioscience* 54, 535–545.
- Cohen, W.B., Healey, S.P., Yang, Z., Stehman, S.V., Brewer, C.K., Brooks, E.B., Gorelick, N., Huang, C., Hughes, M.J., Kennedy, R.E., Loveland, T.R., Moisen, G.G., Schroeder, T.A., Vogelmann, J.E., Woodcock, C.E., Yang, L., Zhu, Z., 2017. How similar are forest disturbance maps derived from different landsat time series algorithms? *Forests* 8, 98.
- Coops, N.C., Waring, R.H., Wulder, M.A., Pidgeon, A.M., Radeloff, V.C., 2009. Bird diversity: a predictable function of satellite-derived estimates of seasonal variation in canopy light absorbance across the United States. *J. Biogeogr.* 36, 905–918.
- Coops, N.C., Shang, C., Wulder, M.A., White, J.C., Hermosilla, T., 2020. Change in forest condition: Characterizing non-random replacing disturbances using time series satellite imagery. *For. Ecol. Manag.* 474, 118370.
- Cracknell, A.P., 1997. Advanced Very High Resolution Radiometer AVHRR. CRC Press.
- Crawford, C.J., 2015. MODIS Terra Collection 6 fractional snow cover validation in mountainous terrain during spring snowmelt using Landsat TM and ETM. *Hydroclim. Process.* 29, 128–138.
- Crawford, C.J., Manson, S.M., Bauer, M.E., Hall, D.K., 2013. Multitemporal snow cover mapping in mountainous terrain for Landsat climate data record development. *Remote Sens. Environ.* 135, 224–233.
- Crawford, C.J., van den Bosch, J., Brunt, K.M., Hom, M.G., Cooper, J.W., Harding, D.J., Butler, J.J., Dabney, P.W., Neumann, T.A., Cleckner, C.S., Markus, T., 2019. Radiometric calibration of a non-imaging airborne spectrometer to measure the Greenland ice sheet surface. *Atmos. Meas. Tech.* 12, 1913–1933.
- Crawford, C.J., Roy, D.P., Arab, S., Barnes, C., Vermote, E., Hulley, G., Gerace, A., Choate, M., Engebreton, C., Micijevic, E., Schmidt, G., Anderson, C., Anderson, M., Bouchard, M., Cook, B., Dittmeier, R., Howard, D., Jenkerson, C.B., Kim, M., Kleyians, T., Maiersperger, T., Muller, C., Neigh, C., Owen, L., Page, B., Pahlevan, N., Rengarajan, R., Roger, J.-C., Sayler, K.L., Scaramuzza, P., Skakun, S., Yan, L., Zhang, H.K., Zhe, Z., Zahn, S., 2023. The 50-year Landsat collection 2 archive. *Sci. Remote Sens.* 8, 100103.
- Culbert, P.D., Radeloff, V.C., Flather, C.H., Kellndorfer, J.M., Rittenhouse, C.D., Pidgeon, A.M., 2013. The influence of vertical and horizontal habitat structure on nationwide patterns of avian biodiversity. *Auk* 130, 656–665.
- Dara, A., Baumann, M., Kuemmerle, T., Pfugmacher, D., Rabe, A., Griffiths, P., Holzel, N., Kamp, J., Freitag, M., Hostert, P., 2018. Mapping the timing of cropland abandonment and recultivation in northern Kazakhstan using annual Landsat time series. *Remote Sens. Environ.* 213, 49–60.
- DeFries, R.S., Townshend, J.R.G., 1994. NDVI-derived land cover classifications at a global scale. *Int. J. Remote Sens.* 15, 3567–3586.
- DeFries, R.S., Townshend, J.R.G., Hansen, M.C., 1999. Continuous fields of vegetation characteristics at the global scale at 1-km resolution. *J. Geophys. Res.* 104, 16,911–9123.
- DeFries, R., Hansen, A., Newton, A.C., Hansen, M.C., 2005. Increasing isolation of protected areas in tropical forests over the past twenty years. *Ecol. Appl.* 15, 19–26.
- Deines, J.M., Kendall, A.D., Hyndman, D.W., 2017. Annual irrigation dynamics in the US Northern high plains derived from landsat satellite data. *Geophys. Res. Lett.* 44, 9350–9360.
- Dethier, E.N., Sartain, S.L., Lutz, D.A., 2019. Heightened levels and seasonal inversion of riverine suspended sediment in a tropical biodiversity hot spot due to artisanal gold mining. *Proc. Natl. Acad. Sci.* 116, 23936–23941.
- Di Gregorio, A., 2016. Land Cover Classification System - Classification Concepts Software Version 3.
- Disney, M.I., Lewis, P., Gomez-Dans, J., Roy, D., Wooster, M.J., Lajas, D., 2011. 3D radiative transfer modelling of fire impacts on a two-layer savanna system. *Remote Sens. Environ.* 115, 1866–1881.
- Downing, J.A., Prairie, Y.T., Cole, J.J., Duarte, C.M., Tranvik, L.J., Striegl, R.G., McDowell, W.H., Kortelainen, P., Caraco, N.F., Melack, J.M., Middelburg, J.J., 2006. The global abundance and size distribution of lakes, ponds, and impoundments. *Limnol. Oceanogr.* 51, 2388–2397.
- Doxani, G., Vermote, E., Roger, J.C., Gascon, F., Adriaensen, S., Frantz, D., Hagolle, O., Hollstein, A., Kirches, G., Li, F.Q., Louis, J., Mangin, A., Pahlevan, N., Pflug, B., Vanhelmont, Q., 2018. Atmospheric correction inter-comparison exercise. *Remote Sens.* 10, 352.
- Doxani, G., Vermote, E.F., Roger, J.C., Skagen, S.K., Gascon, F., Collison, A., De Keukelaere, L., Desjardins, C., Frantz, D., Hagolle, O., Kim, M., Louis, J., Pacifici, F., Pflug, B., Poilve, H., Ramon, D., Richter, R., Yin, F., 2023. Atmospheric Correction Inter-comparison eXercise, ACIX-II Land: An assessment of atmospheric correction processors for Landsat 8 and Sentinel-2 over land. *Remote Sens. Environ.* 285, 113412.
- Dozier, J., 1989. Spectral signature of alpine snow cover from the Landsat Thematic Mapper. *Remote Sens. Environ.* 28, 9.
- Dozier, J., Green, R.O., Nolin, A.W., Painter, T.H., 2009. Interpretation of snow properties from imaging spectrometry. *Remote Sens. Environ.* 113, S25–S37.
- Drusch, M., Del Bello, U., Carlier, S., Colin, O., Fernandez, V., Gascon, F., Hoersch, B., Isola, C., Laberinti, P., Martimort, P., Meygret, A., Spoto, F., Sy, O., Marchese, F., Bargellini, P., 2012. Sentinel-2: ESA's optical high-resolution mission for GMES operational services. *Remote Sens. Environ.* 120, 25–36.
- Dubovik, O., Holben, B., Eck, T.F., Smirnov, A., Kaufman, Y.J., King, M.D., Tanre, D., Slutsker, I., 2002. Variability of absorption and optical properties of key aerosol types observed in worldwide locations. *J. Atmos. Sci.* 59, 590–608.
- Dudgeon, D., Arthington, A.H., Gessner, M.O., Kawabata, Z.I., Knowler, D.J., Leveque, C., Naiman, R.J., Prieur-Richard, A.H., Soto, D., Stiassny, M.L.J., Sullivan, C.A., 2006. Freshwater biodiversity: importance, threats, status and conservation challenges. *Biol. Rev.* 81, 163–182.
- Duro, D., Coops, N.C., Wulder, M.A., Han, T., 2007. Development of a large area biodiversity monitoring system driven by remote sensing. *Prog. Phys. Geogr.* 31, 235–260.
- Dwyer, J.L., Roy, D.P., Sauer, B., Jenkerson, C.B., Zhang, H.K.K., Lymburner, L., 2018. Analysis ready data: enabling analysis of the landsat archive. *Remote Sens.* 10, 1363.
- Egorov, A., Roy, D.P., Boschetti, L., 2023. Generation and comprehensive validation of 30 m conterminous United States Landsat percent tree cover and forest cover loss annual products. *Sci. Remote Sens.* 7, 100084.
- Egorov, A.V., Roy, D.P., Zhang, H.K.K., Li, Z.B., Yan, L., Huang, H.Y., 2019. Landsat 4, 5 and 7 (1982 to 2017) Analysis Ready Data (ARD) Observation Coverage over the Conterminous United States and Implications for Terrestrial Monitoring. *Remote Sens.* 11, 447.
- Elmes, A., Levy, C., Erb, A., Hall, D.K., Scambos, T.A., DiGirolamo, N., Schaaf, C., 2021. Consequences of the 2019 Greenland Ice Sheet Melt Episode on Albedo. *Remote Sens.* 13, 227.
- Elmore, A.J., Guinn, S.M., Minsley, B.J., Richardson, A.D., 2012. Landscape controls on the timing of spring, autumn, and growing season length in mid-Atlantic forests. *Glob. Chang. Biol.* 18, 656–674.
- Elsen, P.R., Farwell, L.S., Pidgeon, A.M., Radeloff, V.C., 2020. Landsat 8 TIRS-derived relative temperature and thermal heterogeneity predict winter bird species richness patterns across the conterminous United States. *Remote Sens. Environ.* 236, 111514, 111514.
- Erb, K.H., Luyssaert, S., Meyfroidt, P., Pongratz, J., Don, A., Kloster, S., Kuemmerle, T., Fetz, T., Fuchs, R., Herold, M., Haberl, H., Jones, C.D., Marin-Spiotta, E., McCallum, I., Robertson, E., Seufert, V., Fritz, S., Valade, A., Wiltshire, A., Dolman, A.J., 2017. Land management: data availability and process understanding for global change studies. *Glob. Chang. Biol.* 23, 512–533.
- Erb, K.H., Kastner, T., Plutnar, C., Bais, A.L.S., Carvalhais, N., Fetz, T., Gingrich, S., Haberl, H., Lauk, C., Niedertscheider, M., Pongratz, J., Thurner, M., Luyssaert, S., 2018. Unexpectedly large impact of forest management and grazing on global vegetation biomass. *Nature* 553, 73–+.

- Erb, A.M., Li, Z., Sun, Q.S., Paynter, I., Wang, Z.S., Schaaf, C., 2022. Evaluation of the Landsat-8 Albedo Product across the Circumpolar Domain. *Remote Sens.* 14, 5320.
- Esch, T., Heldens, W., Hirner, A., Keil, M., Marconcini, M., Roth, A., Zeidler, J., Dech, S., Strano, E., 2017. Breaking new ground in mapping human settlements from space - The Global Urban Footprint. *ISPRS J. Photogramm. Remote Sens.* 134, 30–42.
- Estapa, M.L., Boss, E., Mayer, L.M., Roesler, C.S., 2012. Role of iron and organic carbon in mass-specific light absorption by particulate matter from Louisiana coastal waters. *Limnol. Oceanogr.* 57, 97–112.
- Estes, L.D., Okin, G.S., Mwangi, A.G., Shugart, H.H., 2008. Habitat selection by a rare forest antelope: A multi-scale approach combining field data and imagery from three sensors. *Remote Sens. Environ.* 112, 2033–2050.
- Fahnestock, M., Scambos, T., Moon, T., Gardner, A., Haran, T., Klinger, M., 2016. Rapid large-area mapping of ice flow using Landsat 8. *Remote Sens. Environ.* 185, 84–94.
- Falucci, A., Maiorano, L., Boitani, L., 2007. Changes in land-use/land-cover patterns in Italy and their implications for biodiversity conservation. *Landscape Ecol.* 22, 617–631.
- Farwell, L.S., Gudex-Cross, D., Anise, I.E., Bosch, M.J., Olah, A.M., Radeloff, V.C., Razenková, E., Rogova, N., Silveira, E.M.O., Smith, M.M., Pidgeon, A.M., 2021. Satellite image texture captures vegetation heterogeneity and explains patterns of bird richness. *Remote Sens. Environ.* 253, 112175.
- Felipe-Lucia, M.R., Soliveres, S., Penone, C., Fischer, M., Ammer, C., Boch, S., Boeddinghaus, R.S., Bonkowski, M., Buscot, F., Fiore-Donno, A.M., Franki, K., Goldmann, K., Gossner, M.M., Holzel, N., Jochum, M., Kandeler, E., Klaus, V.H., Kleinebecker, T., Leimer, S., Manning, P., Oelmann, Y., Saiz, H., Schall, P., Schlotter, M., Schoning, I., Schrumpf, M., Solly, E.F., Stempfhuber, B., Weisser, W.W., Wilcke, W., Wubet, T., Allan, E., 2020. Land-use intensity alters networks between biodiversity, ecosystem functions, and services. *Proc. Natl. Acad. Sci. U. S. A.* 117, 28140–28149.
- Feng, Y., Zeng, Z.Z., Searchinger, T.D., Ziegler, A.D., Wu, J., Wang, D.S., He, X.Y., Elsen, P.R., Ciais, P., Xu, R.R., Guo, Z.L., Peng, L.Q., Tao, Y.H., Spracklen, D.V., Holden, J., Liu, X.P., Zheng, Y., Xu, P., Chen, J., Jiang, X., Song, X.P., Lakshmi, V., Wood, E.F., Zheng, C.M., 2022. Doubling of annual forest carbon loss over the tropics during the early twenty-first century. *Nat. Sustain.* 5, 444–451.
- Terencz, C., Bognar, P., Lichtenberger, J., Hamar, D., Tarsczi, G., Timar, G., Molnar, G., Pasztor, S., Steinbach, P., Szekely, B., Ferencz, O.E., Ferencz-Arkos, I., 2004. Crop yield estimation by satellite remote sensing. *Int. J. Remote Sens.* 25, 4113–4149.
- Fernandes, R., Weiss, M., Camacho, F., Berthelot, B., Baret, F., Duca, R., IEEE, 2014. Development and assessment of leaf area index algorithms for the Sentinel-2 multispectral imager. In: *IEEE Joint International Geoscience and Remote Sensing Symposium (IGARSS) / 35th Canadian Symposium on Remote Sensing*, pp. 3922–3925. Quebec City, CANADA.
- Fichot, C.G., Benner, R., 2011. A novel method to estimate DOC concentrations from CDOM absorption coefficients in coastal waters. *Geophys. Res. Lett.* 38, L03610.
- Filipponi, F., Valentini, E., Xuan, A.N., Guerra, C.A., Wolf, F., Andrzejak, M., Taramelli, A., 2018. Global MODIS fraction of green vegetation cover for monitoring abrupt and gradual vegetation changes. *Remote Sens. Environ.* 10, 653.
- Fily, M., Bourdelle, B., Dedieu, J.P., Sergent, C., 1997. Comparison of in situ and Landsat thematic mapper derived snow grain characteristics in the Alps. *Remote Sens. Environ.* 59, 452–460.
- Fisher, J.I., Mustard, J.F., Vadéboncoeur, M.A., 2006. Green leaf phenology at Landsat resolution: Scaling from the field to the satellite. *Remote Sens. Environ.* 100, 265–279.
- Fisher, J.B., Tu, K.P., Baldocchi, D.D., 2008. Global estimates of the land-atmosphere water flux based on monthly AVHRR and ISLSCP-II data, validated at 16 FLUXNET sites. *Remote Sens. Environ.* 112, 901–919.
- Fjeldså, J., Ehrlich, D., Lambin, E., Prins, E., 1997. Are biodiversity 'hotspots' correlated with current ecoclimatic stability? A pilot study using the NOAA-AVHRR remote sensing data. *Biodivers. Conserv.* 6, 401–422.
- Florké, M., Kynast, E., Barlund, I., Eisner, S., Wimmer, F., Alcamo, J., 2013. Domestic and industrial water uses of the past 60 years as a mirror of socio-economic development: A global simulation study. *Glob. Environ. Change* 23, 144–156.
- Foley, J.A., DeFries, R., Asner, G.P., Barford, C., Bonan, G., Carpenter, S.R., Chapin, F.S., Coe, M.T., Daily, G.C., Gibbs, H.K., Helkowski, J.H., Holloway, T., Howard, E.A., Kucharik, C.J., Monfreda, C., Patz, J.A., Prentice, I.C., Ramankutty, N., Snyder, P.K., 2005. Global consequences of land use. *Science* 309, 570–574.
- Frantz, D., Schug, F., Okujeni, A., Navacchi, C., Wagner, W., van der Linden, S., Hostert, P., 2021. National-scale mapping of building height using Sentinel-1 and Sentinel-2 time series. *Remote Sens. Environ.* 252, 112128.
- Fraser, R.S., Kaufman, Y.J., 1985. The relative importance of aerosol scattering and absorption in remote sensing. *IEEE Trans. Geosci. Remote Sens.* 23, 625–633.
- French, N.H.F., Kasischke, E.S., Hall, R.J., Murphy, K.A., Verbyla, D.L., Hoy, E.E., Allen, J.L., 2008. Using Landsat data to assess fire and burn severity in the North American boreal forest region: an overview and summary of results. *Int. J. Wildland Fire* 17, 443–462.
- Friedl, M.A., McIver, D.K., Hodges, J.C.F., Zhang, X.Y., Muchoney, D., Strahler, A.H., Woodcock, C.E., Gopal, S., Schneider, A., Cooper, A., Baccini, A., Gao, F., Schaaf, C., 2002. Global land cover mapping from MODIS: algorithms and early results. *Remote Sens. Environ.* 83, 287–302. pii s0034-4257(02)00078-0.
- Friedl, M.A., Gray, J.M., Melas, E.K., Richardson, A.D., Hufkens, K., Keenan, T.F., Bailey, A., O'Keefe, J., 2014. A tale of two springs: using recent climate anomalies to characterize the sensitivity of temperate forest phenology to climate change. *Environ. Res. Lett.* 9, 054006.
- Friedl, M.A., Woodcock, C.E., Olofsson, P., Zhu, Z., Loveland, T., Stanićirova, R., Arevalo, P., Bullock, E., Hu, K.-T., Zhang, Y., Turlej, K., Tarrio, K., McAvoy, K., Gorelick, N., Wang, J.A., Barber, C.P., Souza, C., 2022. Medium spatial resolution mapping of global land cover and land cover change across multiple decades from Landsat. *Front. Remote Sens.* 3, 894571.
- Fritz, S., See, L., McCallum, I., You, L.Z., Bun, A., Moltchanova, E., Duerauer, M., Albrecht, F., Schill, C., Perger, C., Havlik, P., Mosnier, A., Thornton, P., Woods, S., Sichra, U., Herrero, M., Becker-Reshef, I., Justice, C., Hansen, M., Gong, P., Aziz, S., A., Cipriani, A., Cumani, R., Cecchi, G., Conchedda, G., Ferreira, S., Gomez, A., Haffani, M., Kayitakire, F., Malanding, J., Mueller, R., Newby, T., Nonguierma, A., Olusegun, A., Ortner, S., Rajak, D.R., Rocha, J., Schepaschenko, D., Schepaschenko, M., Terekhov, A., Tiangwa, A., Vancutsem, C., Vintrou, E., Wu, W., B., van der Velde, M., Dunwoody, A., Kraxner, F., Obersteiner, M., 2015. Mapping global cropland and field size. *Glob. Chang. Biol.* 21, 1980–1992.
- Fritz, S., See, L., Bayas, J.C.L., Waldner, F., Jacques, D., Becker-Reshef, I., Whitcraft, A., Baruth, B., Bonifacio, R., Crutchfield, J., Rembold, F., Rojas, O., Schucknecht, A., Van der Velde, M., Verdin, J., Wu, B.F., Yan, N.N., You, L.Z., Gilliams, S., Mucher, S., Tetrault, R., Moorthy, I., McCallum, I., 2019. A comparison of global agricultural monitoring systems and current gaps. *Agric. Syst.* 168, 258–272.
- Gámez, T.E., Benton, L., Manning, S.R., 2019. Observations of two reservoirs during a drought in central Texas, USA: Strategies for detecting harmful algal blooms. *Ecol. Indic.* 104, 588–593.
- Ganguly, S., Nemani, R.R., Zhang, G., Hashimoto, H., Milesi, C., Michaelis, A., Wang, W., L., Votava, P., Samanta, A., Melton, F., Dungan, J.L., Vermote, E., Gao, F., Knyazikhin, Y., Myneni, R.B., 2012. Generating global Leaf Area Index from Landsat: Algorithm formulation and demonstration. *Remote Sens. Environ.* 122, 185–202.
- Gao, F., Anderson, M.C., Kustas, W.P., Wang, Y.J., 2012. Simple method for retrieving leaf area index from Landsat using MODIS leaf area index products as reference. *J. Appl. Remote. Sens.* 6, 063554.
- Gao, F., Anderson, M.C., Zhang, X.Y., Yang, Z.W., Alfieri, J.G., Kustas, W.P., Mueller, R., Johnson, D.M., Prueger, J.H., 2017. Toward mapping crop progress at field scales through fusion of Landsat and MODIS imagery. *Remote Sens. Environ.* 188, 9–25.
- Gao, F., Anderson, M., Daughtry, C., Karniel, A., Hively, D., Kustas, W., 2020. A within-season approach for detecting early growth stages in corn and soybean using high temporal and spatial resolution imagery. *Remote Sens. Environ.* 242, 111752.
- Gao, F., Anderson, M.C., Johnson, D.M., Seffrin, R., Wardlow, B., Suyker, A., Diao, C.Y., Browning, D.M., 2021. Towards Routine Mapping of Crop Emergence within the Season Using the Harmonized Landsat and Sentinel-2 Dataset. *Remote Sens.* 13, 5074.
- Gaso, D.V., Berger, A.G., Ciganda, V.S., 2019. Predicting wheat grain yield and spatial variability at field scale using a simple regression or a crop model in conjunction with Landsat images. *Comput. Electron. Agric.* 159, 75–83.
- GBIF, 2022. Global Biodiversity Information Facility.
- GCOS, 2016. The Global Observing System for Climate, Implementation Needs. Report adopted by the Conference of the Parties to the UNFCCC, 2016 session. WMO, Geneva.
- GCOS, 2021. The Status of the Global Climate Observing System 2021: The GCOS Status Report.
- GCOS, 2022. The 2022 GCOS Implementation Plan. World Meteorological Organization, Geneva, Switzerland.
- GEO-BON, 2022. Essential Biodiversity Variables.
- Gerace, A., Kleynhans, T., Eon, R., Montanaro, M., 2020. Towards an operational, split window-derived surface temperature product for the thermal infrared sensors onboard Landsat 8 and 9. *Remote Sens.* 12, 224.
- Gernez, P., Doxaran, D., Barillé, L., 2017. Shellfish aquaculture from space: potential of Sentinel2 to monitor tide-driven changes in turbidity, chlorophyll concentration and oyster physiological response at the scale of an oyster farm. *Front. Mar. Sci.* 4, 137.
- Giglio, L., Roy, D.P., 2020. On the outstanding need for a long-term, multi-decadal, validated and quality assessed record of global burned area: Caution in the use of Advanced Very High Resolution Radiometer data. *Sci. Remote Sens.* 2, 100007.
- Giglio, L., Boschetti, L., Roy, D.P., Humber, M.L., Justice, C.O., 2018. The Collection 6 MODIS burned area mapping algorithm and product. *Remote Sens. Environ.* 217, 72–85.
- Goldeijk, K.K., 2001. Estimating global land use change over the past 300 years: The HYDE Database. *Glob. Biogeochim. Cycles* 15, 417–433.
- Gong, P., Wang, J., Yu, L., Zhao, Y.C., Zhao, Y.Y., Liang, L., Niu, Z.G., Huang, X.M., Fu, H., H., Liu, S., Li, C.C., Li, X.Y., Fu, W., Liu, C.X., Xu, Y., Wang, X.Y., Cheng, Q., Hu, L.Y., Yao, W.B., Zhang, H., Zhu, P., Zhao, Z.Y., Zhang, H.Y., Zheng, Y.M., Ji, L.Y., Zhang, Y.W., Chen, H., Yan, A., Guo, J.H., Wang, L., Liu, X.J., Shi, T.T., Zhu, M.H., Chen, Y.L., Yang, G.W., Tang, P., Xu, B., Giri, C., Clinton, N., Zhu, Z.L., Chen, J., 2013. Finer resolution observation and monitoring of global land cover: first mapping results with Landsat TM and ETM+ data. *Int. J. Remote Sens.* 34, 2607–2654.
- Goodwin, N.R., Coops, N.C., Wulder, M.A., Gillanders, S., Schroeder, T.A., Nelson, T., 2008. Estimation of insect infestation dynamics using a temporal sequence of Landsat data. *Remote Sens. Environ.* 112, 3680–3689.
- Goward, S.N., Williams, D.L., Arvidson, T., Rocchio, L.E.P., Irons, J.R., Russell, C.A., Johnston, S.S., 2017. Landsat's Enduring Legacy: Pioneering Global Land Observations from Space. American Society for Photogrammetry and Remote Sensing, Bethesda.
- Griffiths, P., Nendel, C., Hostert, P., 2019. Intra-annual reflectance composites from Sentinel-2 and Landsat for national-scale crop and land cover mapping. *Remote Sens. Environ.* 220, 135–151.
- Griffiths, P., Nendel, C., Pickert, J., Hostert, P., 2020. Towards national-scale characterization of grassland use intensity from integrated Sentinel-2 and Landsat time series. *Remote Sens. Environ.* 238, 111124.
- Grogan, K., Pflugmacher, D., Hostert, P., Kennedy, R., Fensholt, R., 2015. Cross-border forest disturbance and the role of natural rubber in mainland Southeast Asia using annual Landsat time series. *Remote Sens. Environ.* 169, 438–453.

- Gudex-Cross, D., Keyser, S.R., Zuckerberg, B., Fink, D., Zhu, L., Pauli, J.N., Radeloff, V.C., 2021. Winter Habitat Indices (WHIs) for the contiguous US and their relationship with winter bird biodiversity. *Remote Sens. Environ.* 255, 112309.
- Gudex-Cross, D., Zhu, L., Keyser, S.R., Zuckerberg, B., Pauli, J.N., Radeloff, V.C., 2022. Winter conditions structure extratropical patterns of species richness of amphibians, birds and mammals globally. *Glob. Ecol. Biogeogr.* 31, 1366–1380.
- Guillevic, P., Gottsche, F., Nickeson, J., Hulley, G., Ghent, D., Yu, Y., Trigo, I.F., Hook, S., Sobrino, J.A., Remedios, J., Roman, M.O., Camacho, F., 2018. Land surface temperature product validation best practice protocol. Version 1.1. In: Guillevic, P., Götsche, F., Nickeson, J., Román, M. (Eds.), Best Practice for Satellite Derived Land Product Validation: Land Product Validation Subgroup. Committee on Earth Observation Satellites.
- Gutman, G., Byrnes, R., Masek, J., Covington, S., Justice, C., Franks, S., Headley, R., 2008. Towards monitoring land-cover and land-use changes at a global scale: The Global Land Survey 2005. *Photogramm. Eng. Remote. Sens.* 74, 6–10.
- Haines-Young, R., 2009. Land use and biodiversity relationships. *Land Use Policy* 26, S178–S186.
- Hall, D.K., Ormsby, J.P., Johnson, L., Brown, J., 1980. Landsat digital analysis of the initial recovery of burned tundra at Kokolik River, Alaska. *Remote Sens. Environ.* 10, 263–272.
- Hall, D.K., Chang, A.T.C., Foster, J.L., 1986. Detection of the depth-hoar layer in the snow-pack of the Arctic coastal-plain of Alaska, USA, using satellite data. *J. Glaciol.* 32, 87–94.
- Hall, D.K., Foster, J.L., Salomonson, V.V., Klein, A.G., Chien, J.Y.L., 2001. Development of a technique to assess snow-cover mapping errors from space. *IEEE Trans. Geosci. Remote Sens.* 39, 432–438.
- Hall, D.K., Riggs, G.A., DiGirolamo, N.E., Roman, M.O., 2019. Evaluation of MODIS and VIIRS cloud-gap-filled snow-cover products for production of an Earth science data record. *Hydroclim. Earth Sci. Cl.* 23, 5227–5241.
- Hansen, M.C., Loveland, T.R., 2012. A review of large area monitoring of land cover change using Landsat data. *Remote Sens. Environ.* 122, 66–74.
- Hansen, M.C., Reed, B., 2000. A comparison of the IGBP DISCover and University of Maryland 1km global land cover products. *Int. J. Remote Sens.* 21, 1365–1373.
- Hansen, M.C., Defries, R.S., Townshend, J.R.G., Sohlberg, R., 2000. Global land cover classification at 1km spatial resolution using a classification tree approach. *Int. J. Remote Sens.* 21, 1331–1364.
- Hansen, M.C., Stehman, S.V., Potapov, P.V., Loveland, T.R., Townshend, J.R.G., DeFries, R.S., Pittman, K.W., Arunarwati, B., Stolle, F., Steininger, M.K., Carroll, M., DiMiceli, C., 2008. Humid tropical forest clearing from 2000 to 2005 quantified by using multitemporal and multiresolution remotely sensed data. *Proc. Natl. Acad. Sci. U. S. A.* 105, 9439–9444.
- Hansen, M.C., Egorov, A., Roy, D.P., Potapov, P., Ju, J.C., Turubanova, S., Kommareddy, I., Loveland, T.R., 2011. Continuous fields of land cover for the conterminous United States using Landsat data: first results from the Web-Enabled Landsat Data (WELD) project. *Remote Sens. Lett.* 2, 279–288.
- Hansen, M.C., Potapov, P.V., Moore, R., Hancher, M., Turubanova, S.A., Tyukavina, A., Thau, D., Stehman, S.V., Goetz, S.J., Loveland, T.R., Kommareddy, A., Egorov, A., Chini, L., Justice, C.O., Townshend, J.R.G., 2013. High-resolution global maps of 21st-century forest cover change. *Science* 342, 850–853.
- Hansen, M.C., Krylov, A., Tyukavina, A., Potapov, P.V., Turubanova, S., Zutta, B., Ifo, S., Margono, B., Stolle, F., Moore, R., 2016. Humid tropical forest disturbance alerts using Landsat data. *Environ. Res. Lett.* 11, 034008.
- Hautecoeur, O., Leroy, M.M., 1998. Surface bidirectional reflectance distribution function observed at global scale by POLDER/ADEOS. *Geophys. Res. Lett.* 25, 4197–4200.
- Hawbaker, T.J., Vanderhoof, M.K., Beal, Y., Takacs, J.D., Schmidt, G.L., Fargout, J.T., Willimas, B., Brunner, N.M., Caldwell, M.K., Picotte, J.J., Howard, S.M., Stitt, S., Dwyer, J.L., 2017. Mapping burned areas using dense time-series of Landsat data. *Remote Sens. Environ.* 198, 504–522.
- Hawbaker, T.J., Vanderhoof, M.K., Schmidt, G.L., Beal, Y.J., Picotte, J.J., Takacs, J.D., Falgout, J.T., Dwyer, J.L., 2020. The Landsat Burned Area algorithm and products for the conterminous United States. *Remote Sens. Environ.* 244, 111801.
- He, Y.A., Chen, G., Potter, C., Meentemeyer, R.K., 2019. Integrating multi-sensor remote sensing and species distribution modeling to map the spread of emerging forest disease and tree mortality. *Remote Sens. Environ.* 231, 111238.
- Healey, S.P., Yang, Z.Q., Cohen, W.B., Pierce, D.J., 2006. Application of two regression-based methods to estimate the effects of partial harvest on forest structure using Landsat data. *Remote Sens. Environ.* 101, 115–126.
- Healey, S.P., Cohen, W.B., Yang, Z.Q., Brewer, C.K., Brooks, E.B., Gorelick, N., Hernandez, A.J., Huang, C.Q., Hughes, M.J., Kennedy, R.E., Loveland, T.R., Moisen, G.G., Schroeder, T.A., Stehman, S.V., Vogelmann, J.E., Woodcock, C.E., Yang, L.M., Zhu, Z., 2018. Mapping forest change using stacked generalization: An ensemble approach. *Remote Sens. Environ.* 204, 717–728.
- Hegglin, M.I., Bastos, A., Bovenmann, H., Buchwitz, M., Fawcett, D., Ghent, D., Kulk, G., Sathyendranath, S., Shepherd, T.G., Quegan, S., Rothlisberger, R., Briggs, S., Buontempo, C., Cazenave, A., Chuvieco, E., Ciais, P., Crisp, D., Engelen, R., Fadnavis, S., Herold, M., Horwath, M., Jonsson, O., Kpaka, G., Merchant, C.J., Mielke, C., Nagler, T., Paul, F., Popp, T., Quaife, T., Rayner, N.A., Robert, C., Schroder, M., Sitch, S., Venturini, S., van der Schalie, R., van der Vliet, M., Wigneron, J.P., Woolway, R.I., 2022. Space-based Earth observation in support of the UNFCCC Paris Agreement. *Front. Environ. Sci.* 10, 941490.
- Heimhuber, V., Tulbure, M.G., Broich, M., 2018. Addressing spatio-temporal resolution constraints in Landsat and MODIS-based mapping of large-scale floodplain inundation dynamics. *Remote Sens. Environ.* 211, 307–320.
- Hemmerling, J., Pflugmacher, D., Hostert, P., 2021. Mapping temperate forest tree species using dense Sentinel-2 time series. *Remote Sens. Environ.* 267, 112743.
- Hepinstall, J.A., Sader, S.A., 1997. Using bayesian statistics, thematic mapper satellite imagery, and breeding bird survey data to model bird species probability of occurrence in maine. *Photogramm. Eng. Remote. Sens.* 63, 1231–1237.
- Hermosilla, T., Wulder, M.A., White, J.C., Coops, N.C., Hobart, G.W., 2015. An integrated Landsat time series protocol for change detection and generation of annual gap-free surface reflectance composites. *Remote Sens. Environ.* 158, 220–234.
- Hermosilla, T., Bastyar, A., Coops, N.C., White, J.C., Wulder, M.A., 2023. Mapping the presence and distribution of tree species in Canada's forested ecosystems. *Remote Sens. Environ.* 282, 113276.
- Ho, J.C., Stumpf, R.P., Bridgeman, T.B., Michalak, A.M., 2017. Using Landsat to extend the historical record of lacustrine phytoplankton blooms: A Lake Erie case study. *Remote Sens. Environ.* 191, 273–285.
- Hobbins, M.T., Huntington, J.L., 2016. Evapotranspiration and Evaporative Demand. In: Singh, V.P. (Ed.), *Handbook of Applied Hydrology*. McGraw-Hill Education, New York.
- Hobi, M.L., Dubinin, M., Graham, C.H., Coops, N.C., Clayton, M.K., Pidgeon, A.M., Radeloff, V.C., 2017. A comparison of Dynamic Habitat Indices derived from different MODIS products as predictors of avian species richness. *Remote Sens. Environ.* 195, 142–152.
- Hobi, M.L., Farwell, L.S., Dubinin, M., Kolesov, D., Pidgeon, A.M., Coops, N., Radeloff, V.C., 2021. Patterns of bird species richness explained by annual variation in remotely sensed Dynamic Habitat Indices. *Ecol. Indic.* 127, 107774.
- Holben, B.N., Eck, T.F., Slutsker, I., Tanre, D., Buis, J.P., Setzer, A., Vermote, E., Reagan, J.A., Kaufman, Y.J., Nakajima, T., Lavenu, F., Jankowiak, I., Smirnov, A., 1998. AERONET - A federated instrument network and data archive for aerosol characterization. *Remote Sens. Environ.* 66, 1–16.
- Homer, C., Dewitz, J., Jin, S.M., Xian, G., Costello, C., Danielson, P., Gass, L., Funk, M., Wickham, J., Stehman, S., Auch, R., Riitters, K., 2020. Conterminous United States land cover change patterns 2001–2016 from the 2016 National Land Cover Database. *ISPRS J. Photogramm. Remote Sens.* 162, 184–199.
- Hook, S.J., Cawse-Nicholson, K., Barsi, J., Radocinski, R., Hulley, G.C., Johnson, W.R., Rivera, G., Markham, B., 2020. In-Flight Validation of the ECOSTRESS, Landsats 7 and 8 Thermal Infrared Spectral Channels Using the Lake Tahoe CA/NV and Salton Sea CA Automated Validation Sites. *IEEE Trans. Geosci. Remote Sens.* 58, 1294–1302.
- Houghton, R.A., 2013. The emissions of carbon from deforestation and degradation in the tropics: past trends and future potential. *Carbon Manag.* 4, 539–546.
- Howat, I.M., Eddy, A., 2011. Multi-decadal retreat of Greenland's marine-terminating glaciers. *J. Glaciol.* 57, 389–396.
- Huang, C., Chen, Y., Zhang, S.Q., Wu, J.P., 2018. Detecting, extracting, and monitoring surface water from space using optical sensors: a review. *Rev. Geophys.* 56, 333–360.
- Huete, A., Didan, K., Miura, T., Rodriguez, E.P., Gao, X., Ferreira, L.G., 2002. Overview of the radiometric and biophysical performance of the MODIS vegetation indices. *Remote Sens. Environ.* 83, 195–213. pii s0034-4257(02)00096-2.
- Hulley, G.C., Hook, S.J., 2011. Generating Consistent Land Surface Temperature and Emissivity Products Between ASTER and MODIS Data for Earth Science Research. *IEEE Trans. Geosci. Remote Sens.* 49, 1304–1315.
- Hulley, G.C., Hook, S.J., Abbott, E., Malakar, N., Islam, T., Abrams, M., 2015. The ASTER Global Emissivity Dataset (ASTER GED): Mapping Earth's emissivity at 100 meter spatial scale. *Geophys. Res. Lett.* 42, 7966–7976.
- Hulley, G.C., Malakar, N.K., Islam, T., Freepartner, R.J., 2018. NASA's MODIS and VIIRS Land Surface Temperature and Emissivity Products: A Long-Term and Consistent Earth System Data Record. *IEEE J. Sel. Top. Appl. Earth Obs. Remote Sens.* 11, 522–535.
- Hulley, G.C., Gottsche, F.M., Rivera, G., Hook, S.J., Freepartner, R.J., Martin, M.A., Cawse-Nicholson, K., Johnson, W.R., 2022. Validation and Quality Assessment of the ECOSTRESS Level-2 Land Surface Temperature and Emissivity Product. *IEEE Trans. Geosci. Remote Sens.* 60.
- Hutton, G., Haller, L., Water, S., 2004. Evaluation of the Costs and Benefits of Water and Sanitation Improvements at the Global Level. World Health Organization, Geneva.
- Inglada, J., Vincent, A., Arias, M., Tardy, B., Morin, D., Rodes, I., 2017. Operational high resolution land cover map production at the country scale using satellite image time series. *Remote Sens.* 9, 95.
- IOCCG, 2000. Remote sensing of ocean colour in coastal, and other optically-complex, waters. In: Sathyendranath, S. (Ed.), Dartmouth. Reports of the International Ocean Colour Coordinating Group, Canada.
- IOCCG, 2018. Earth observations in support of global water quality monitoring. In: Greb, S., Dekker, A., Binding, C. (Eds.), IOCCG Report Series. International Ocean Colour Coordinating Group, Dartmouth, Canada.
- IPCC (2013). Climate Change: The Physical Science Basis. Contribution of Working Group I to the Fifth Assessment Report of the Intergovernmental Panel on Climate Change. T.F. Stocker, D. Qin, G.-K. Plattner, M. Tignor, S.K. Allen, J. Boschung, A. Nauels, Y. Xia, V. Bex, & P.M. Midgley Cambridge, United Kingdom and New York, NY, USA.
- IPCC, 2021. Summary for Policymakers. In: Masson-Delmotte, V. (Ed.), *The Physical Science Basis. Contribution of Working Group I to the Sixth Assessment Report of the Intergovernmental Panel on Climate Change*.
- Jiang, G.J., Loiselle, S.A., Yang, D.T., Ma, R.H., Su, W., Gao, C.J., 2020. Remote estimation of chlorophyll a concentrations over a wide range of optical conditions based on water classification from VIIRS observations. *Remote Sens. Environ.* 241, 111735.
- Jin, S.M., Yang, L.M., Zhu, Z., Homer, C., 2017. A land cover change detection and classification protocol for updating Alaska NLCD 2001 to 2011. *Remote Sens. Environ.* 195, 44–55.

- Johnson, D.M., 2014. An assessment of pre- and within-season remotely sensed variables for forecasting corn and soybean yields in the United States. *Remote Sens. Environ.* 141, 116–128.
- Ju, J.C., Roy, D.P., Vermote, E., Masek, J., Kovalskyy, V., 2012. Continental-scale validation of MODIS-based and LEDAPS Landsat ETM plus atmospheric correction methods. *Remote Sens. Environ.* 122, 175–184.
- Justice, C.O., Townshend, J.R.G., Holben, B.N., Tucker, C.J., 1985. Analysis of the phenology of global vegetation using meteorological satellite data. *Int. J. Remote Sens.* 6, 1271–1318.
- Justice, C.O., Vermote, E., Townshend, J.R.G., Defries, R., Roy, D.P., Hall, D.K., Salomonson, V.V., Privette, J.L., Riggs, G., Strahler, A., Lucht, W., Myeni, R.B., Knyazikhin, Y., Running, S.W., Nemani, R.R., Wan, Z.M., Huete, A.R., van Leeuwen, W., Wolfe, R.E., Giglio, L., Muller, J.P., Lewis, P., Barnsley, M.J., 1998. The Moderate Resolution Imaging Spectroradiometer (MODIS): Land remote sensing for global change research. *IEEE Trans. Geosci. Remote Sens.* 36, 1228–1249.
- Kang, Y.H., Ozdogan, M., 2019. Field-level crop yield mapping with Landsat using a hierarchical data assimilation approach. *Remote Sens. Environ.* 228, 144–163.
- Kang, Y.H., Ozdogan, M., Gao, F., Anderson, M.C., White, W.A., Yang, Y., Erickson, T.A., 2021. A data-driven approach to estimate leaf area index for Landsat images over the contiguous US. *Remote Sens. Environ.* 258, 112383.
- Karra, K., Kontgis, C., Statman-Weil, Z., Mazzarriello, J.C., Mathis, M., Brumby, S.P., 2021. Global land use/land cover with Sentinel 2 and deep learning. In: 2021 IEEE International Geoscience and Remote Sensing Symposium IGARSS, pp. 4704–4707. Brussels, Belgium.
- Kaufman, Y.J., Herring, D.D., Ranson, K.J., Collatz, G.J., 1998. Earth Observing System AM1 mission to earth. *IEEE Trans. Geosci. Remote Sens.* 36, 1045–1055.
- Kayitakire, F., Hamel, C., Defourny, P., 2006. Retrieving forest structure variables based on image texture analysis and IKONOS-2 imagery. *Remote Sens. Environ.* 102, 390–401.
- Keenan, T.F., Gray, J., Friedl, M.A., Toomey, M., Bohrer, G., Hollinger, D.Y., Munger, J.W., O'Keefe, J., Schmid, H.P., SueWing, I., Yang, B., Richardson, A.D., 2014. Net carbon uptake has increased through warming-induced changes in temperate forest phenology. *Nat. Clim. Chang.* 4, 598–604.
- Kennedy, R.E., Yang, Z.G., Cohen, W.B., 2010. Detecting trends in forest disturbance and recovery using yearly Landsat time series: 1. LandTrendr - Temporal segmentation algorithms. *Remote Sens. Environ.* 114, 2897–2910.
- Kennedy, R.E., Yang, Z.Q., Braaten, J., Copass, C., Antonova, N., Jordan, C., Nelson, P., 2015. Attribution of disturbance change agent from Landsat time-series in support of habitat monitoring in the Puget Sound region, USA. *Remote Sens. Environ.* 166, 271–285.
- Key, J., Haefliger, M., 1992. Arctic ice surface-temperature retrieval from AVHRR thermal channels. *J. Geophys. Res.-Atmos.* 97, 5885–5893.
- Key, J., Wang, X.J., Liu, Y.H., Dworak, R., Letterly, A., 2016. The AVHRR polar pathfinder climate data records. *Remote Sens.* 8, 167.
- Khan, S., Hanjra, M.A., 2009. Footprints of water and energy inputs in food production - global perspectives. *Food Policy* 34, 130–140.
- Kim, D.H., Sexton, J.O., Noojipady, P., Huang, C.Q., Anand, A., Channan, S., Feng, M., Townshend, J.R., 2014. Global, Landsat-based forest-cover change from 1990 to 2000. *Remote Sens. Environ.* 155, 178–193.
- Kingslake, J., Ely, J.C., Das, I., Bell, R.E., 2017. Widespread movement of meltwater onto and across Antarctic ice shelves. *Nature* 544, 349–352.
- Kloiber, S.N., Brezonik, P.L., Olmanson, L.G., Bauer, M.E., 2002. A procedure for regional lake water clarity assessment using Landsat multispectral data. *Remote Sens. Environ.* 82, 38–47. doi:10.1016/S0034-4252(02)00022-6.
- Kokaly, R.F., Rockwell, B.W., Haire, S.L., King, T.V.V., 2007. Characterization of post-fire surface cover, soils, and burn severity at the Cerro Grande Fire, New Mexico, using hyperspectral and multispectral remote sensing. *Remote Sens. Environ.* 106, 305–325.
- Korner, C., Basler, D., 2010. Phenology under global warming. *Science* 327, 1461–1462.
- Kotchenova, S.Y., Vermote, E.F., 2007. Validation of a vector version of the 6S radiative transfer code for atmospheric correction of satellite data. Part II. Homogeneous Lambertian and anisotropic surfaces. *Appl. Opt.* 46, 4455–4464.
- Kotchenova, S.Y., Vermote, E.F., Levy, R., Lyapustin, A., 2008. Radiative transfer codes for atmospheric correction and aerosol retrieval: intercomparison study. *Appl. Opt.* 47, 2215–2226.
- Kovalskyy, V., Roy, D.P., 2013. The global availability of Landsat 5 TM and Landsat 7 ETM + land surface observations and implications for global 30 m Landsat data product generation. *Remote Sens. Environ.* 130, 280–293.
- Kuhn, C., Valerio, A.D., Ward, N., Loken, L., Sawakuchi, H.O., Karnpelt, M., Richey, J., Stadler, P., Crawford, J., Strieg, R., Vermote, E., Pahlevan, N., Butman, D., 2019. Performance of Landsat-8 and Sentinel-2 surface reflectance products for river remote sensing retrievals of chlorophyll-a and turbidity. *Remote Sens. Environ.* 224, 104–118.
- Kumar, S.S., Roy, D.P., 2018. Global operational land imager Landsat-8 reflectance-based active fire detection algorithm. *Int. J. Digit. Earth* 11, 154–178.
- Kussul, N., Lavreniuk, M., Skakun, S., Shelestov, A., 2017. Deep learning classification of land cover and crop types using remote sensing data. *IEEE Geosci. Remote Sens. Lett.* 14, 778–782.
- Lacroix, P., Araujo, G., Hollingsworth, J., Taipe, E., 2019. Self-entrainment motion of a slow-moving landslide inferred from Landsat-8 time series. *J. Geophys. Res. Earth Surf.* 124, 1201–1216.
- Lentile, L.B., Holden, Z.A., Smith, A.M.S., Falkowski, M.J., Hudak, A.T., Morgan, P., Lewis, S.A., Gessler, P.E., Benson, N.C., 2006. Remote sensing techniques to assess active fire characteristics and post-fire effects. *Int. J. Wildland Fire* 15, 319–345.
- Lesiv, M., Schepashchenko, D., Molchanova, E., Bun, R., Durauer, M., Prishchepov, A.V., Schiernhorn, F., Estel, S., Kuemmerle, T., Alcantara, C., Kussul, N., Shchepashchenko, M., Kutovaya, O., Martynenko, O., Karminov, V., Shvidenko, A., Havlik, P., Kraxner, F., See, L., Fritz, S., 2018. Spatial distribution of arable and abandoned land across former Soviet Union countries. *Sci. Data* 5, 180056.
- Li, J., Roy, D.P., 2017. A global analysis of Sentinel-2A, Sentinel-2B and Landsat-8 data revisit intervals and implications for terrestrial monitoring. *Remote Sens.* 9, 902.
- Li, K.Y., Coe, M.T., Ramankutty, N., De Jong, R., 2007. Modeling the hydrological impact of land-use change in West Africa. *J. Hydrol.* 337, 258–268.
- Liang, S.L., Fang, H.L., Chen, M.Z., 2001. Atmospheric correction of landsat ETM+ land surface imagery - Part I: methods. *IEEE Trans. Geosci. Remote Sens.* 39, 2490–2498.
- Liu, J.G., Linderman, M., Ouyang, Z.Y., An, L., Yang, J., Zhang, H.M., 2001. Ecological degradation in protected areas: The case of Wolong Nature Reserve for giant pandas. *Science* 292, 98–101.
- Liu, H., Gong, P., Wang, J., Wang, X., Ning, G., Xu, B., 2021. Production of global daily seamless data cubes and quantification of global land cover change from 1985 to 2020-iMap World 1.0. *Remote Sens. Environ.* 258, 112364.
- López García, M.J., Caselles, V., 1991. Mapping burns and natural reforestation using thematic mapper data. *Geocarto Int.* 1, 31–37.
- Loveland, T.R., Reed, B.C., Brown, J.F., Ohlen, D.O., Zhu, Z., Yang, L., Merchant, J.W., 2000. Development of a global land cover characteristics database and IGBP DISCover from 1 km AVHRR data. *Int. J. Remote Sens.* 21, 1303–1330.
- Luseno, W.K., McPeak, J.G., Barrett, C.B., Little, P.D., Gebru, G., 2003. Assessing the value of climate forecast information for pastoralists: Evidence from southern Ethiopia and northern Kenya. *World Dev.* 31, 1477–1494.
- Lyapustin, A.I., 2001. Three-dimensional effects in the remote sensing of surface albedo. *IEEE Trans. Geosci. Remote Sens.* 39, 254–263.
- Lyapustin, A., Wang, Y., Martonchik, J., Privette, J.L., Holben, B., Slutsker, I., Sinyuk, A., Smirnov, A., 2006. Local analysis of MISR surface BRF and albedo over GSFC and Mongu AERONET sites. *IEEE Trans. Geosci. Remote Sens.* 44, 1707–1718.
- Lyapustin, A., Wang, Y., Frey, R., 2008. An automatic cloud mask algorithm based on time series of MODIS measurements. *J. Geophys. Res.-Atmos.* 113, D16207.
- Lyapustin, A., Gatebe, C.K., Kahn, R., Brandt, R., Redemann, J., Russell, P., King, M.D., Pedersen, C.A., Gerland, S., Poudyal, R., Marshak, A., Wang, Y., Schaaf, C., Hall, D., Kokhanovsky, A., 2010. Analysis of snow bidirectional reflectance from ARCTAS Spring-2008 Campaign. *Atmos. Chem. Phys.* 10, 4359–4375.
- Lyapustin, A., Wang, Y.J., Korkin, S., Huang, D., 2018. MODIS collection 6 MAIAC algorithm. *Atmos. Meas. Tech.* 11, 5741–5765.
- MA, 2005. Millennium Ecosystem Assessment - Ecosystems and Human Well-being: Biodiversity Synthesis. Island Press, Washington, D.C.
- Mackey, B.G., Bryan, J., Randall, L., 2004. Australia's dynamic habitat template. In: MODIS Vegetation Workshop II Missoula, Montana.
- Malakar, N.K., Hulley, G.C., Hook, S.J., Laraby, K., Cook, M., Schott, J.R., 2018. An operational land surface temperature product for landsat thermal data: methodology and validation. *IEEE Trans. Geosci. Remote Sens.* 56, 5717–5735.
- Martonchik, J.V., Diner, D.J., Kahn, R.A., Ackerman, T.P., Verstraete, M.E., Pinty, B., Gordon, H.R., 1998. Techniques for the retrieval of aerosol properties over land and ocean using multiangular imaging. *IEEE Trans. Geosci. Remote Sens.* 36, 1212–1227.
- Masek, J.G., Huang, C., Wolfe, R., Cohen, W., Hall, F., Kutler, J., Nelson, P., 2008. North American forest disturbance mapped from a decadal Landsat record. *Remote Sens. Environ.* 112, 2914–2926.
- Masek, J.G., Wulder, M.A., Markham, B., McCorkel, J., Crawford, C.J., Storey, J., Jenstrom, D., 2020. Landsat 9: Empowering open science and applications through continuity. *Remote Sens. Environ.* 248, 111968.
- Matasci, G., Hermosilla, T., Wulder, M.A., White, J.C., Coops, N.C., Hobart, G.W., Bolton, D.K., Tompaliski, P., Bater, C.W., 2018a. Three decades of forest structural dynamics over Canada's forested ecosystems using Landsat time-series and lidar plots. *Remote Sens. Environ.* 216, 697–714.
- Matasci, G., Hermosilla, T., Wulder, M.A., White, J.C., Coops, N.C., Hobart, G.W., Zald, H.S.J., 2018b. Large-area mapping of Canadian boreal forest cover, height, biomass and other structural attributes using Landsat composites and lidar plots. *Remote Sens. Environ.* 209, 90–106.
- Matricardi, E.A.T., Skole, D.L., Costa, O.B., Pedlowski, M.A., Samek, J.H., Miguel, E.P., 2020. Long-term forest degradation surpasses deforestation in the Brazilian Amazon. *Science* 369, 1378–1379.
- Matthews, M.W., Odermatt, D., 2015. Improved algorithm for routine monitoring of cyanobacteria and eutrophication in inland and near-coastal waters. *Remote Sens. Environ.* 156, 374–382.
- Melaas, E.K., Sulla-Menache, D., Gray, J.M., Black, T.A., Morin, T.H., Richardson, A.D., Friedl, M.A., 2016. Multisite analysis of land surface phenology in North American temperate and boreal deciduous forests from Landsat. *Remote Sens. Environ.* 186, 452–464.
- Melchiorre, A., Boschetti, L., 2018. Global analysis of burned area persistence time with MODIS data. *Remote Sens.* 10, 750.
- Melton, F.S., Johnson, L.F., Lund, C.P., Pierce, L.L., Michaelis, A.R., Hiatt, S.H., Guzman, A., Adhikari, D.D., Purdy, A.J., Rosevelt, C., Votava, P., Trout, T.J., Temesgen, B., Frame, K., Sheffner, E.J., Nemani, R.R., 2012. Satellite irrigation management support with the terrestrial observation and prediction system: a framework for integration of satellite and surface observations to support improvements in agricultural water resource management. *IEEE J. Sel. Top. Appl. Earth Obs. Remote Sens.* 5, 1709–1721.
- Melton, F.S., Huntington, J., Grimm, R., Herring, J., Hall, M., Rollison, D., Erickson, T., Allen, R., Anderson, M., Fisher, J.B., Kilic, A., Senay, G.B., Volk, J., Hain, C., Johnson, L., Ruhoff, A., Blankenau, P., Bromley, M., Carrara, W., Daudert, B., Doherty, C., Dunkerly, C., Friedrichs, M., Guzman, A., Halverson, G., Hansen, J., Harding, J., Kang, Y.H., Ketchum, D., Minor, B., Morton, C., Ortega-Salazar, S., Ott, T., Ozdogan, M., ReVelle, P.M., Schull, M., Wang, C., Yang, Y., Anderson, R.G.,

2021. OpenET: filling a critical data gap in water management for the Western United States. *J. Am. Water Resour. Assoc.* 58, 971–994.
- Mertes, L.A., Smith, M.O., Adams, J.B., 1993. Estimating suspended sediment concentrations in surface waters of the Amazon River wetlands from Landsat images. *Remote Sens. Environ.* 43, 281–301.
- Meygret, A., Santer, R.P., Berthelot, B., 2011. ROSAS: a robotic station for atmosphere and surface characterization dedicated to on-orbit calibration. In: *Earth Observing Systems XVI*. Society of Photo-Optical Instrumentation Engineers, p. 815311.
- Milne, R., Jallow, B.P., Arrouays, C., Drichi, I., Beets, P., Harun, I.B., Hrubovcak, J., Huffman, T., Irving, W., Koehl, M., Lin, E., 2003. Basis for consistent representation of land areas. In: Penman, J., et al. (Eds.), *Good Practice Guidance for Land Use, Land-Use Change and Forestry*. The Intergovernmental Panel on Climate Change (IPCC), Kanagawa, Japan.
- Minnich, R.A., 1983. Fire mosaics in southern California and northern Baja California. *Science* 219, 1287–1294.
- Mishra, S., Mishra, D.R., Lee, Z., Tucker, C.S., 2013. Quantifying cyanobacterial phycocyanin concentration in turbid productive waters: A quasi-analytical approach. *Remote Sens. Environ.* 133, 141–151.
- Moffette, F., Alix-Garcia, J., Shea, K., Pickens, A.H., 2021. The impact of near-real-time deforestation alerts across the tropics. *Nat. Clim. Chang.* 11.
- Montanher, O.C., Novo, E.M., Barbosa, C.C., Rennó, C.D., Silva, T.S., 2014. Empirical models for estimating the suspended sediment concentration in Amazonian white water rivers using Landsat 5/TM. *Int. J. Appl. Earth Obs. Geoinf.* 29, 67–77.
- Moon, T., Joughin, I., 2008. Changes in ice front position on Greenland's outlet glaciers from 1992 to 2007. *J. Geophys. Res. Earth Surf.* 113, F02022.
- Morcrette, J.J., Boucher, O., Jones, L., Salmon, D., Bechtold, P., Beljaars, A., Benedetti, A., Bonet, A., Kaiser, J.W., Razinger, M., Schulz, M., Serrar, S., Simmons, A.J., Sofiev, M., Sutcliffe, M., Tompkins, A.M., Untch, A., 2009. Aerosol analysis and forecast in the European Centre for Medium-Range Weather Forecasts Integrated Forecast System: Forward modeling. *J. Geophys. Res.-Atmos.* 114, D06206.
- Morisette, J.T., Privette, J.L., Justice, C.O., 2002. A framework for the validation of MODIS Land products. *Remote Sens. Environ.* 83, 77–96. pii s0034-4257(02)00088-3.
- Mouw, C.B., Hardman-Mountford, N.J., Alvain, S., Bracher, A., Brewin, R.J.W., Bricaud, A., Ciotti, A.M., Devred, E., Fujiwara, A., Hirata, T., Hirawake, T., Kostadinov, T.S., Roy, S., Uitz, J., 2017. A consumer's guide to satellite remote sensing of multiple phytoplankton groups in the global ocean. *Front. Mar. Sci.* 4, 41.
- Mu, Q.Z., Zhao, M.S., Running, S.W., 2011. Improvements to a MODIS global terrestrial evapotranspiration algorithm. *Remote Sens. Environ.* 115, 1781–1800.
- Mueller, N., Lewis, A., Roberts, D., Ring, S., Melrose, R., Sixsmith, J., Lymburner, L., McIntyre, A., Tan, P., Curnow, S., Ip, A., 2016. Water observations from space: Mapping surface water from 25 years of Landsat imagery across Australia. *Remote Sens. Environ.* 174, 341–352.
- NASA, Council, A., Committee, E.S.S., 1986. Earth system science overview: a program for global change.
- Nelson, B.W., Kapos, V., Adams, J.B., Oliveira, W.J., Braun, O.P.G., Doamaral, I.L., 1994. Forest disturbance by large blowdowns in the Brazilian Amazon. *Ecology* 75, 853–858.
- NRC, 1990. Research strategies for the US global change research program.
- NRC, 2018. Thriving on Our Changing Planet: A Decadal Strategy for Earth Observation from Space. Washington, DC.
- Ochiai, O., Poultier, B., Seifert, F.M., Ward, S., Jarvis, I., Whitcraft, A., Sahajpal, R., Gilliams, S., Herold, M., Carter, S., Duncanson, L.I., Kay, H., Lucas, R., Wilson, S.N., Melo, J., Post, J., Briggs, S., Quegan, S., Dowell, M., Cescatti, A., Crisp, D., Saatchi, S., Tadono, T., Steventon, M., Rosenqvist, A., 2023. Towards a roadmap for space-based observations of the land sector for the UNFCCC global stocktake. *Iscience* 26, 106489.
- Olofsson, P., Stehman, S.V., Woodcock, C.E., Sulla-Menashe, D., Sibley, A.M., Newell, J. D., Friedl, M.A., Herold, M., 2012. A global land-cover validation data set, part I: fundamental design principles. *Int. J. Remote Sens.* 33, 5768–5788.
- Olofsson, P., Foody, G.M., Herold, M., Stehman, S.V., Woodcock, C.E., Wulder, M.A., 2014. Good practices for estimating area and assessing accuracy of land change. *Remote Sens. Environ.* 148, 42–57.
- Otkin, J.A., Anderson, M.C., Hain, C., Mladenova, I.E., Basara, J.B., Svoboda, M., 2013. Examining rapid onset drought development using the thermal infrared-based evaporative stress index. *J. Hydrometeorol.* 14, 1057–1074.
- Ouaidrari, H., Vermote, E.F., 1999. Operational atmospheric correction of Landsat TM data. *Remote Sens. Environ.* 70, 4–15.
- Padilla, M., Stehman, S.V., Chuvieco, E., 2014. Validation of the 2008 MODIS-MCD45 global burned area product using stratified random sampling. *Remote Sens. Environ.* 144, 187–196.
- Pahlevan, N., Chittimalli, S.K., Balasubramanian, S.V., Vellucci, V., 2019. Sentinel-2/Landsat-8 product consistency and implications for monitoring aquatic systems. *Remote Sens. Environ.* 220, 19–29.
- Pahlevan, N., Mangin, A., Balasubramanian, S.V., Smith, B., Alikas, K., Arai, K., Barbosa, C., Bélanger, S., Binding, C., Bresciani, M., Giardino, C., Gurlin, D., Fan, Y., Harmel, T., Hunter, P., Ishikaza, J., Kratzer, S., Lehmann, M.K., Ligi, M., Ma, R., Martin-Lauzer, F.-R., Olmanson, L., Oppelt, N., Pan, Y., Peters, S., Reynaud, N., Sander de Carvalho, L.A., Simis, S., Spyrikos, E., Steinmetz, F., Stelzer, K., Sterckx, S., Tormos, T., Tyler, A., Vanhellemont, Q., Warren, M., 2021. ACIX-Aqua: A global assessment of atmospheric correction methods for Landsat-8 and Sentinel-2 over lakes, rivers, and coastal waters. *Remote Sens. Environ.* 258, 112366.
- Pahlevan, N., Smith, B., Alikas, K., Anstee, J., Barbosa, C., Binding, C., Bresciani, M., Cremella, B., Giardino, C., Gurlin, D., Fernandez, V., Jamet, C., Kangro, K., Lehmann, M.K., Loisel, H., Matsushita, B., Ha, N., Olmanson, L., Potvin, G., Simis, S., G.H., VanderWoude, A., Vantrepotte, V., Ruiz-Verdu, A., 2022. Simultaneous retrieval of selected optical water quality indicators from Landsat-8, Sentinel-2, and Sentinel-3. *Remote Sens. Environ.* 270, 112860.
- Painter, T.H., Dozier, J., Roberts, D.A., Davis, R.E., Green, R.O., 2003. Retrieval of subpixel snow-covered area and grain size from imaging spectrometer data. *Remote Sens. Environ.* 85, 64–77.
- Painter, T.H., Rittger, K., McKenzie, C., Slaughter, P., Davis, R.E., Dozier, J., 2009. Retrieval of subpixel snow covered area, grain size, and albedo from MODIS. *Remote Sens. Environ.* 113, 868–879.
- Park, Y.-J., Ruddick, K., Lacroix, G., 2010. Detection of algal blooms in European waters based on satellite chlorophyll data from MERIS and MODIS. *Int. J. Remote Sens.* 31, 6567–6583.
- Pasquarella, V.J., Bradley, B.A., Woodcock, C.E., 2017. Near-Real-Time Monitoring of Insect Defoliation Using Landsat Time Series. *Forests* 8, 275.
- Pekel, J.F., Cottam, A., Gorelick, N., Belward, A.S., 2016. High-resolution mapping of global surface water and its long-term changes. *Nature* 540, 418–+.
- Penman, J., Gyartay, M., Hiraishi, T., Krug, T., Kruger, D., 2003. *Good Practice Guidance for Land Use, Land-Use Change and Forestry*. Hayama, Japan.
- Penuelas, J., Rutishauser, T., Filella, I., 2009. Phenology feedbacks on climate change. *Science* 324, 887–888.
- Pereira, H.M., Ferrier, S., Walters, M., Geller, G.N., Jongman, R.H.G., Scholes, R.J., Bruford, M.W., Brummitt, N., Butchart, S.H.M., Cardoso, A.C., Coops, N.C., Dulloo, E., Faith, D.P., Freyhof, J., Gregory, R.D., Heip, C., Hoft, R., Hurt, G., Jetz, W., Karp, D.S., McGeoch, M.A., Obura, D., Onoda, Y., Pettorelli, N., Reyers, M., Sayre, R., Schaeffer, J.P.W., Stuart, S.N., Turak, E., Walpole, M., Wegmann, M., 2013. Essential biodiversity variables. *Science* 339, 277–278.
- Pereira, L.S., Paredes, P., Melton, F., Johnson, L., Wang, T., Lopez-Urrea, R., Cancela, J. J., Allen, R.G., 2020. Prediction of crop coefficients from fraction of ground cover and height. Background and validation using ground and remote sensing data. *Agric. Water Manag.* 241, 106197.
- Pettorelli, N., Vik, J.O., Mysterud, A., Gaillard, J.M., Tucker, C.J., Stenseth, N.C., 2005. Using the satellite-derived NDVI to assess ecological responses to environmental change. *Trends Ecol. Evol.* 20, 503–510.
- Pettorelli, N., Safi, K., Turner, W., 2014. Satellite remote sensing, biodiversity research and conservation of the future. *Phil. Trans. R. Soc. B* 369, 20130190.
- Pettorelli, N., Wegmann, M., Skidmore, A., Mücher, S., Dawson, T.P., Fernandez, M., Lucas, R., Schaepman, M.E., Wang, T., O'Connor, B., Jongman, R.H.G., Kempeiers, P., Sonnenschein, R., Leidner, A.K., Böhm, M., He, K.S., Nagendra, H., Dubois, G., Fatoyinbo, T., Hansen, M.C., Paganini, M., de Klerk, H.M., Asner, G.P., Kerr, J.T., Estes, A.B., Schmeller, D.S., Heiden, U., Rocchini, D., Pereira, H.M., Turak, E., Fernandez, N., Lausch, A., Cho, M.A., Alcaraz-Segura, D., McGeoch, M.A., Turner, W., Mueller, A., St-Louis, V., Penner, J., Vihervaara, P., Belward, A., Reyers, B., Geller, G.N., 2016. Framing the concept of satellite remote sensing essential biodiversity variables: challenges and future directions. *Remote Sens. Ecol. Conserv.* 2, 122–131.
- Pflugmacher, D., Cohen, W.B., Kennedy, R.E., Yang, Z.Q., 2014. Using Landsat-derived disturbance and recovery history and lidar to map forest biomass dynamics. *Remote Sens. Environ.* 151, 124–137.
- Piao, S.L., Liu, Q., Chen, A.P., Janssens, I.A., Fu, Y.S., Dai, J.H., Liu, L.L., Lian, X., Shen, M.G., Zhu, X.L., 2019. Plant phenology and global climate change: Current progresses and challenges. *Glob. Chang. Biol.* 25, 1922–1940.
- Pickens, A.H., Hansen, M.C., Hancher, M., Stehman, S.V., Tyukavina, A., Potapov, P., Marroquin, B., Sherani, Z., 2020. Mapping and sampling to characterize global inland water dynamics from 1999 to 2018 with full Landsat time-series. *Remote Sens. Environ.* 243, 111792.
- Picotte, J.J., Bhattacharai, K., Howard, D., Lecker, J., Epting, J., Quayle, B., Benson, N., Nelson, K., 2020. Changes to the Monitoring Trends in Burn Severity program mapping production procedures and data products. *Fire Ecol.* 16, 16.
- Potapov, P.V., Turubanova, S.A., Tyukavina, A., Krylov, A.M., McCarty, J.L., Radeloff, V. C., Hansen, M.C., 2015. Eastern Europe's forest cover dynamics from 1985 to 2012 quantified from the full Landsat archive. *Remote Sens. Environ.* 159, 28–43.
- Potapov, P., Hansen, M.C., Kommareddy, I., Kommareddy, A., Turubanova, S., Pickens, A., Adusei, B., Tyukavina, A., Ying, Q., 2020. Landsat analysis ready data for global land cover and land cover change mapping. *Remote Sens.* 12, 426.
- Powers, R.P., Jetz, W., 2019. Global habitat loss and extinction risk of terrestrial vertebrates under future land-use-change scenarios. *Nat. Clim. Chang.* 9, 323–+.
- Qiu, S., Zhu, Z., Olofsson, P., Woodcock, C.E., Jin, S.M., 2023. Evaluation of Landsat image compositing algorithms. *Remote Sens. Environ.* 285, 113375.
- Radeloff, V.C., Dubinin, M., Coops, N.C., Allen, A.M., Brooks, T.M., Clayton, M.K., Costa, G.C., Graham, C.H., Helmers, D.P., Ives, A.R., Kolesov, D., Pidgeon, A.M., Rapacciuolo, G., Razenkov, E., Suttidate, N., Young, B.E., Zhu, L., Hobi, M.L., 2019. The Dynamic Habitat Indices (DHIs) from MODIS and global biodiversity. *Remote Sens. Environ.* 222, 204–214.
- Radeloff, V.C., Mockrin, M.H., Helmers, D., Carlson, A., Hawbaker, T.J., Martinuzzi, S., Schug, F., Alexandre, P.M., Kramer, H.A., Pidgeon, A.M., 2023. Rising wildfire risk to houses in the United States, especially in grasslands and shrublands. *Science* 382, 702–707.
- Ramankutty, N., Foley, J.A., 1999. Estimating historical changes in global land cover: Croplands from 1700 to 1992. *Glob. Biogeochem. Cycles* 13, 997–1027.
- Reiche, J., Mullissa, A., Slagter, B., Gou, Y.Q., Tsendbazar, N.E., Odongo-Braun, C., Vollrath, A., Weisse, M.J., Stolle, F., Pickens, A., Donchyts, G., Clinton, N., Gorelick, N., Herold, M., 2021. Forest disturbance alerts for the Congo Basin using Sentinel-1. *Environ. Res. Lett.* 16, 024005.
- Riggs, G., Hall, D., 2020. Continuity of MODIS and VIIRS snow cover extent data products for development of an Earth Science data record. *Remote Sens.* 12, 3781.

- Riggs, G.A., Hall, D.K., Roman, M.O., 2017. Overview of NASA's MODIS and Visible Infrared Imaging Radiometer Suite (VIIRS) snow-cover Earth System Data Records. *Earth Syst. Sci. Data* 9, 765–777.
- Rittger, K., Painter, T.H., Dozier, J., 2013. Assessment of methods for mapping snow cover from MODIS. *Adv. Water Resour.* 51, 367–380.
- Rittger, K., Krock, M., Kleiber, W., Bair, E.H., Brodzik, M.J., Stephenson, T.R., Rajagopalan, B., Bormann, K.J., Painter, T.H., 2021. Multi-sensor fusion using random forests for daily fractional snow cover at 30 m. *Remote Sens. Environ.* 264, 112608.
- Roe, S., Streck, C., Obersteiner, M., Frank, S., Griscom, B., Drouet, L., Fricko, O., Gusti, M., Harris, N., Hasegawa, T., Hausfather, Z., Havlik, P., House, J., Nabuurs, G. J., Popp, A., Sanchez, M.J.S., Sanderman, J., Smith, P., Stehfest, E., Lawrence, D., 2019. Contribution of the land sector to a 1.5 degrees C world. *Nat. Clim. Chang.* 9, 817–+.
- Roman, M.O., Schaaf, C.B., Lewis, P., Gao, F., Anderson, G.P., Privette, J.L., Strahler, A. H., Woodcock, C.E., Barnsley, M., 2010. Assessing the coupling between surface albedo derived from MODIS and the fraction of diffuse skylight over spatially-characterized landscapes. *Remote Sens. Environ.* 114, 738–760.
- Roteta, E., Bastarrika, A., Padilla, M., Storm, T., Chuvieco, E., 2019. Development of a Sentinel-2 burned area algorithm: Generation of a small fire database for sub-Saharan Africa. *Remote Sens. Environ.* 222, 1–17.
- Roujean, J.L., Leroy, M., Deschamps, P.Y., 1992. A bidirectional reflectance model of the Earth's surface for the correction of remote sensing data. *J. Geophys. Res.-Atmos.* 97, 20455–20468.
- Roy, D.P., Landmann, T., 2005. Characterizing the surface heterogeneity of fire effects using multi-temporal reflective wavelength data. *Int. J. Remote Sens.* 26, 4197–4218.
- Roy, D.P., Jin, Y., Lewis, P.E., Justice, C.O., 2005. Prototyping a global algorithm for systematic fire-affected area mapping using MODIS time series data. *Remote Sens. Environ.* 97, 137–162.
- Roy, D.P., Borak, J.S., Devadiga, S., Wolfe, R.E., Zheng, M., Descloitres, J., 2002. The MODIS Land product quality assessment approach. *Remote Sens. Environ.* 83, 62–76.
- Roy, D.R., Boschetti, L., Trigg, S.N., 2006. Remote sensing of fire severity: Assessing the performance of the normalized Burn ratio. *IEEE Geosci. Remote Sens. Lett.* 3, 112–116.
- Roy, D.P., Ju, J.C., Kline, K., Scaramuzza, P.L., Kovalskyy, V., Hansen, M., Loveland, T. R., Vermote, E., Zhang, C.S., 2010. Web-enabled Landsat Data (WELD): Landsat ETM plus composited mosaics of the conterminous United States. *Remote Sens. Environ.* 114, 35–49.
- Roy, D.P., Qin, Y., Kovalskyy, V., Vermote, E.F., Ju, J., Egorov, A., Hansen, M.C., Kommarreddy, I., Yan, L., 2014a. Conterminous United States demonstration and characterization of MODIS-based Landsat ETM plus atmospheric correction. *Remote Sens. Environ.* 140, 433–449.
- Roy, D.P., Wulder, M.A., Loveland, T.R., Woodcock, C.E., Allen, R.G., Anderson, M.C., Helder, D., Irons, J.R., Johnson, D.M., Kennedy, R., Scambos, T., Schaaf, C.B., Schott, J.R., Sheng, Y., Vermote, E.F., Belward, A.S., Bindschadler, R., Cohen, W.B., Gao, F., Hippel, J.D., Hostert, P., Huntington, J., Justice, C.O., Kilic, A., Kovalskyy, V., Lee, Z.P., Lymbumer, L., Masek, J.G., McCorkel, J., Shuai, Y., Trezza, R., Vogelmann, J., Wynne, R.H., Zhu, Z., 2014b. Landsat-8: Science and product vision for terrestrial global change research. *Remote Sens. Environ.* 145, 154–172.
- Roy, D.P., Kovalskyy, V., Zhang, H.K., Vermote, E.F., Yan, L., Kumar, S.S., Egorov, A., 2016a. Characterization of Landsat-7 to Landsat-8 reflective wavelength and normalized difference vegetation index continuity. *Remote Sens. Environ.* 185, 57–70.
- Roy, D.P., Zhang, H.K., Ju, J., Gomez-Dans, J.L., Lewis, P.E., Schaaf, C.B., Sun, Q., Li, J., Huang, H., Kovalskyy, V., 2016b. A general method to normalize Landsat reflectance data to nadir BRDF adjusted reflectance. *Remote Sens. Environ.* 176, 255–271.
- Roy, D.P., Huang, H.Y., Boschetti, L., Giglio, L., Yan, L., Zhang, H.K.H., Li, Z.B., 2019. Landsat-8 and Sentinel-2 burned area mapping - A combined sensor multi-temporal change detection approach. *Remote Sens. Environ.* 231, 111254.
- Roy, D.P., Huang, H.Y., Houborg, R., Martins, V.S., 2021. A global analysis of the temporal availability of PlanetScope high spatial resolution multi-spectral imagery. *Remote Sens. Environ.* 264, 112586.
- Sacks, W.J., Deryng, D., Foley, J.A., Ramankutty, N., 2010. Crop planting dates: an analysis of global patterns. *Glob. Ecol. Biogeogr.* 19, 607–620.
- Sahajpal, R., Zhang, X.S., Izaurralde, R.C., Gelfand, I., Hurtt, G.C., 2014. Identifying representative crop rotation patterns and grassland loss in the US Western Corn Belt. *Comput. Electron. Agric.* 108, 173–182.
- Saunier, S., Pflug, B., Lobos, I.M., Franch, B., Louis, J., De Los Reyes, R., Debaecker, V., Cadau, E.G., Boccia, V., Gascon, F., Kocaman, S., 2022. Sen2Like: Paving the Way towards Harmonization and Fusion of Optical Data. *Remote Sens.* 14, 3855.
- Sayer, A.M., Thomas, G.E., Grainger, R.G., Carboni, E., Poulsen, C., Siddans, R., 2012. Use of MODIS-derived surface reflectance data in the ORAC-AATSR aerosol retrieval algorithm: Impact of differences between sensor spectral response functions. *Remote Sens. Environ.* 116, 177–188.
- Schaaf, C.B., Gao, F., Strahler, A.H., Lucht, W., Li, X.W., Tsang, T., Strugnell, N.C., Zhang, X.Y., Jin, Y.F., Muller, J.P., Lewis, P., Barnsley, M., Hobson, P., Disney, M., Roberts, G., Dunderdale, M., Doll, C., d'Entremont, R.P., Hu, B.X., Liang, S.L., Privette, J.L., Roy, D., 2002. First operational BRDF, albedo nadir reflectance products from MODIS. *Remote Sens. Environ.* 83, 135–148. pii s0034-4257(02)00091-3.
- Schaaf, C.B., Liu, J., Gao, F., Strahler, A.H., 2011. Aqua and Terra MODIS albedo and reflectance anisotropy products. In: Ramachandran, B. (Ed.), NASA's Earth Observing System and the Science of ASTER and MODIS. Springer, New York, NY, pp. 549–561.
- Schneider, A., Friedl, M.A., Potere, D., 2009. A new map of global urban extent from MODIS satellite data. *Environ. Res. Lett.* 4, 044003.
- Scholes, R.J., Walters, M., Turak, E., Saarenmaa, H., Heip, C.H.R., Tuama, E.O., Faith, D. P., Mooney, H.A., Ferrier, S., Jongman, R.H.G., Harrison, I.J., Yahara, T., Pereira, H. M., Larigauderie, A., Geller, G., 2012. Building a global observing system for biodiversity. *Curr. Opin. Environ. Sustain.* 4, 139–146.
- Schott, J.R., Hook, S.J., Barsi, J.A., Markham, B.L., Miller, J., Padula, F.P., Raqueno, N. G., 2012. Thermal infrared radiometric calibration of the entire Landsat 4, 5, and 7 archive (1982–2010). *Remote Sens. Environ.* 122, 41–49.
- Schroeder, W., Oliva, P., Giglio, L., Quayle, B., Lorenz, E., Morelli, F., 2016. Active fire detection using Landsat-8/OLI data. *Remote Sens. Environ.* 185, 210–220.
- Schroeder, T.A., Schleeweis, K.G., Moisen, G.G., Toney, C., Cohen, W.B., Freeman, E.A., Yang, Z.Q., Huang, C.Q., 2017. Testing a Landsat-based approach for mapping disturbance causality in US forests. *Remote Sens. Environ.* 195, 230–243.
- Schug, F., Bar-Massada, A., Carlson, A.R., Cox, H., Hawbaker, T.J., Helmers, D., Hostert, P., Kaim, D., Kasraee, N.K., Martinuzzi, S., Mockrin, M.H., 2023. The global wildland–urban interface. *Nature* 621, 94–99.
- Schug, F., Frantz, D., Okujeni, A., Van der Linden, S., Hostert, P., 2020. Mapping urban-rural gradients of settlements and vegetation at national scale using Sentinel-2 spectral-temporal metrics and regression-based unmixing with synthetic training data. *Remote Sens. Environ.* 246.
- Schwaab, J., Meier, R., Mussetti, G., Seneviratne, S., Burgi, C., Davin, E.L., 2021. The role of urban trees in reducing land surface temperatures in European cities. *Nat. Commun.* 12, 6763.
- Schwieder, M., Wesemeyer, M., Frantz, D., Pföch, K., Erasmi, S., Pickert, J., Nendel, C., Hostert, P., 2022. Mapping grassland mowing events across Germany based on combined Sentinel-2 and Landsat 8 time series. *Remote Sens. Environ.* 269, 112795.
- Sebald, J., Senf, C., Seidl, R., 2021. Human or natural? Landscape context improves the attribution of forest disturbances mapped from Landsat in Central Europe. *Remote Sens. Environ.* 262, 112502.
- Selkowitz, D.J., Forster, R.R., 2016a. An automated approach for mapping persistent ice and snow cover over high latitude regions. *Remote Sens.* 8, 16.
- Selkowitz, D.J., Forster, R.R., 2016b. Automated mapping of persistent ice and snow cover across the western US with Landsat. *ISPRS J. Photogramm. Remote Sens.* 117, 126–140.
- Selkowitz, D.J., Painter, T.H., Rittger, K.E., Schmidt, G., Forster, R., 2017. The USGS landsat snow covered area products: methods and preliminary validation. In: Selkowitz, D.J. (Ed.), *Automated Approaches for Snow and Ice Cover Monitoring Using Optical Remote Sensing*. The University of Utah, Salt Lake City, Utah.
- Sellers, P.J., Meeson, B.W., Hall, F.G., Asrar, G., Murphy, R.E., Schiffer, R.A., Bretherton, F.P., Dickinson, R.E., Ellingson, R.G., Field, C.B., Huemmrich, K.F., Justice, C.O., Melack, J.M., Roulet, N.T., Schimel, D.S., Try, P.D., 1995. Remote-sensing of the land-surface for studies of global change - models, algorithms, experiments. *Remote Sens. Environ.* 51, 3–26.
- Senay, G.B., 2018. Satellite psychrometric formulations of the operational simplified surface energy balance (SSEBOP) model for quantifying and mapping evapotranspiration. *Appl. Eng. Agric.* 34, 555–566.
- Senf, C., Seidl, R., 2021. Mapping the forest disturbance regimes of Europe. *Nat. Sustain.* 4, 63–U102.
- Shiklomanov, I.A., 1998. The world's water resources A new appraisal and assessment for the 21 Century. UNESCO, Paris.
- Sinha, E., Michalak, A., Balaji, V., 2017. Eutrophication will increase during the 21st century as a result of precipitation changes. *Science* 357, 405–408.
- Skakun, S., Vermote, E.F., Roger, J.C., Justice, C.O., Masek, J.G., 2019. Validation of the lasrc cloud detection algorithm for landsat 8 images. *IEEE J. Sel. Top. Appl. Earth Obs. Remote Sens.* 12, 2439–2446.
- Skidmore, A.K., Coops, N.C., Neinavaz, E., Ali, A., Schaeppman, M.E., Paganini, M., Kissling, W.D., Vihervaara, P., Darvishzadeh, R., Feilhauer, H., Fernandez, M., Fernandez, N., Gorelick, N., Geizendorff, I., Heiden, U., Heurich, M., Hobern, D., Holzwarth, S., Muller-Karger, F.E., Van De Kerchove, R., Lausch, A., Leitau, P.J., Lock, M.C., Mucher, C.A., O'Connor, B., Rocchini, D., Turner, W., Vis, J.K., Wang, T. J., Wegmann, M., Wingate, V., 2021. Priority list of biodiversity metrics to observe from space. *Nat. Ecol. Evol.* 5, 896–906.
- Smith, B., Pahlevan, N., Schalles, J., Ruberg, S., Errera, R., Ma, R., Giardino, C., Bresciani, M., Barboso, C., Moore, R., Fernandes, V., Alikas, K., Kangro, K., 2021. A chlorophyll-a algorithm for Landsat-8 based on mixture density networks. *Front. Remote Sens.* 1, 623678.
- Snyder, J., Boss, E., Weatherbee, R., Thomas, A.C., Brady, D., Newell, C., 2017. Oyster aquaculture site selection using Landsat 8-derived sea surface temperature, turbidity, and chlorophyll-a. *Front. Mar. Sci.* 4, 190.
- Song, X.P., Hansen, M.C., Potapov, P., Adusei, B., Pickering, J., Adam, M., Lima, A., Zalles, V., Stehman, S.V., Di Bella, C.M., Conde, M.C., Copati, E.J., Fernandes, L.B., Hernandez-Serna, A., Jantz, S.M., Pickens, A.H., Turubanova, S., Tyukavina, A., 2021. Massive soybean expansion in South America since 2000 and implications for conservation. *Nat. Sustain.* 4, 784–792.
- Souza, C.M., Roberts, D.A., Cochrane, M.A., 2005. Combining spectral and spatial information to map canopy damage from selective logging and forest fires. *Remote Sens. Environ.* 98, 329–343.
- Spang, E.S., Moomaw, W.R., Gallagher, K.S., Kirshen, P.H., Marks, D.H., 2014. The water consumption of energy production: an international comparison. *Environ. Res. Lett.* 9, 105002.
- Spera, S.A., Galford, G.L., Coe, M.T., Macedo, M.N., Mustard, J.F., 2016. Land-use change affects water recycling in Brazil's last agricultural frontier. *Glob. Chang. Biol.* 22, 3405–3413.

- Steffen, W., Richardson, K., Rockstrom, J., Cornell, S.E., Fetzer, I., Bennett, E.M., Biggs, R., Carpenter, S.R., de Vries, W., de Wit, C.A., Folke, C., Gerten, D., Heinke, J., Mace, G.M., Persson, L.M., Ramanathan, V., Reyers, B., Sorlin, S., 2015. Planetary boundaries: Guiding human development on a changing planet. *Science* 347, 1259855.
- Stillinger, T., Roberts, D.A., Collar, N.M., Dozier, J., 2019. Cloud Masking for Landsat 8 and MODIS terra over snow-covered terrain: error analysis and spectral similarity between snow and cloud. *Water Resour. Res.* 55, 6169–6184.
- St-Louis, V., Pidgeon, A.M., Clayton, M.K., Locke, B.A., Bash, D., Radeloff, V.C., 2010. Habitat variables explain Loggerhead Shrike occurrence in the northern Chihuahuan Desert, but are poor correlates of fitness measures. *Landsl. Ecol.* 25, 643–654.
- Subin, Z.M., Riley, W.J., Mironov, D., 2012. An improved lake model for climate simulations: Model structure, evaluation, and sensitivity analyses in CESM1. *J. Adv. Model. Earth Syst.* 4, M02001.
- Sulla-Menashe, D., Gray, J.M., Abercrombie, S.P., Friedl, M.A., 2019. Hierarchical mapping of annual global land cover 2001 to present: The MODIS Collection 6 Land Cover product. *Remote Sens. Environ.* 222, 183–194.
- Thenkabail, P.S., Biradar, C.M., Noojipady, P., Dheeravath, V., Li, Y.J., Velpuri, M., Gumma, M., Gangalakunta, O.R.P., Tural, H., Cai, X.L., Vithanage, J., Schull, M.A., Dutta, R., 2009. Global irrigated area map (GIAM), derived from remote sensing, for the end of the last millennium. *Int. J. Remote Sens.* 30, 3679–3733.
- Townshend, J.R.G., 1994. Global datasets for land applications from the Advanced Very High Resolution Radiometer - An introduction. *Int. J. Remote Sens.* 15, 3319–3332.
- Townshend, J.R.G., Justice, C.O., 1988. Selecting the spatial resolution of satellite sensors required for global monitoring of land transformations. *Int. J. Remote Sens.* 9, 187–236.
- Townshend, J.R.G., Justice, C.O., Gurney, C., McManus, J., 1992. The impact of misregistration on change detection. *IEEE Trans. Geosci. Remote Sens.* 30, 1054–1060.
- Trigg, S., Flasse, S., 2000. Characterizing the spectral-temporal response of burned savannah using in situ spectroradiometry and infrared thermometry. *Int. J. Remote Sens.* 21, 3161–3168.
- Trigg, S.N., Roy, D.P., Flasse, S.P., 2005. An in situ study of the effects of surface anisotropy on the remote sensing of burned savannah. *Int. J. Remote Sens.* 26, 4869–4876.
- Tsutsumida, N., Comber, A.J., 2015. Measures of spatio-temporal accuracy for time series land cover data. *Int. J. Appl. Earth Obs. Geoinf.* 41, 46–55.
- Tuanmu, M.N., Jetz, W., 2015. A global, remote sensing-based characterization of terrestrial habitat heterogeneity for biodiversity and ecosystem modelling. *Glob. Ecol. Biogeogr.* 24, 1329–1339.
- Tubure, M.G., Broich, M., Stehman, S.V., Kommareddy, A., 2016. Surface water extent dynamics from three decades of seasonally continuous Landsat time series at subcontinental scale in a semi-arid region. *Remote Sens. Environ.* 178, 142–157.
- Tubure, M.G., Hostert, P., Kuemmerle, T., Broich, M., 2021. Regional matters: On the usefulness of regional land-cover datasets in times of global change. *Remote Sens. Ecol. Conserv.* 8, 272–283.
- Turner, M.G., 2010. Disturbance and landscape dynamics in a changing world. *Ecology* 91, 2833–2849.
- Turner, W., Spector, S., Gardiner, N., Fladeland, M., Sterling, E., Steininger, M., 2003. Remote sensing for biodiversity science and conservation. *Trends Ecol. Evol.* 18, 306–314.
- Tyukavina, A., Hansen, M.C., Potapov, P.V., Stehman, S.V., Smith-Rodriguez, K., Okpa, C., Aguilar, R., 2017. Types and rates of forest disturbance in Brazilian Legal Amazon, 2000–2013. *Sci. Adv.* 3, e1601047.
- Tyukavina, A., Hansen, M.C., Potapov, P., Parker, D., Okpa, C., Stehman, S.V., Kommareddy, I., Turubanova, S., 2018. Congo Basin forest loss dominated by increasing smallholder clearing. *Sci. Adv.* 4, eaat2993.
- UN, 2012. The Future We Want. United Nations Resolution following the Conference on Sustainable Development in Rio de Janeiro.
- UN, 2017. The 2030 Agenda for Sustainable Development. Resolution adopted by the General Assembly on 6 July 2017. Work of the Statistical Commission pertaining to the 2030 Agenda for Sustainable Development, United Nations.
- UN Environment, 2019. Water Related Ecosystems App.
- UNCBD, 2022. Kunming-Montreal Global Biodiversity Framework. UN Convention on Biological Diversity, Conference of Parties.
- UNCCD, 2013. Conference of Partners (COP) 11: Advice on how best to measure progress on strategic objectives 1, 2 and 3.
- Vancutsem, C., Achard, F., Pekel, J.F., Vieilledent, G., Carboni, S., Simonetti, D., Gallego, J., Aragao, L., Nasi, R., 2021. Long-term (1990–2019) monitoring of forest cover changes in the humid tropics. *Sci. Adv.* 7 eabe1603.
- Verbesselt, J., Hyndman, R., Newnham, G., Culvenor, D., 2010. Detecting trend and seasonal changes in satellite image time series. *Remote Sens. Environ.* 114, 106–115.
- Vermote, E.F., Kotchenova, S., 2008. Atmospheric correction for the monitoring of land surfaces. *J. Geophys. Res.-Atmos.* 113, D23s90.
- Vermote, E.F., Saleous, N.Z., 2002. Operational atmospheric correction of MODIS visible to middle infrared land surface data in the case of an infinite Lambertian target. In: 2nd Workshop of the Earth Science Satellite Remote Sensing. George Mason Univ, Fairfax, VA (pp. 123–+).
- Vermote, E., Justice, C., Csiszar, I., 2014. Early evaluation of the VIIRS calibration, cloud mask and surface reflectance Earth data records. *Remote Sens. Environ.* 148, 134–145.
- Vermote, E., Justice, C., Claverie, M., Franch, B., 2016. Preliminary analysis of the performance of the Landsat 8/OLI land surface reflectance product. *Remote Sens. Environ.* 185, 46–56.
- Vermote, E., McCorkel, J., Rountree, W.H., Santamaría-Artiga, A., Skakun, S., Franch, B., Roger, J.C., 2022. Validation of High Spatial Resolution Surface Reflectance using a Camera System (CAMSIS). In: IGARSS 2022 - 2022 IEEE International Geoscience and Remote Sensing Symposium, pp. 7729–7732. Kuala Lumpur, Malaysia.
- Volk, J.M., Huntington, J., Melton, F.S., Allen, R., Anderson, M.C., Fisher, J.B., Kilic, A., Senay, G., Halverson, G., Knipper, K., Minor, B., Pearson, C., Wang, T.X., Yang, Y., Everett, S., French, A.N., Jasoni, R., Kustas, W., 2023. Development of a benchmark Eddy flux evapotranspiration dataset for evaluation of satellite-driven evapotranspiration models over the CONUS. *Agric. For. Meteorol.* 331, 109307.
- Vörösmarty, C.J., Green, P., Salisbury, J., Lammers, R.B., 2000. Global water resources: vulnerability from climate change and population growth. *Science* 289, 284–288.
- Wallis, C.I.B., Paulsch, D., Zeilinger, J., Silva, B., Fernandez, G.F.C., Brandl, R., Farwig, N., Bendix, J., 2016. Contrasting performance of Lidar and optical texture models in predicting avian diversity in a tropical mountain forest. *Remote Sens. Environ.* 174, 223–232.
- Wan, Z.M., Dozier, J., 1996. A generalized split-window algorithm for retrieving land-surface temperature from space. *IEEE Trans. Geosci. Remote Sens.* 34, 892–905.
- Wang, Y.J., Lyapustin, A.I., Privette, J.L., Morisette, J.T., Holben, B., 2009. Atmospheric correction at AERONET locations: a new science and validation data set. *IEEE Trans. Geosci. Remote Sens.* 47, 2450–2466.
- Wang, Z.S., Schaaf, C.B., Sun, Q.S., Kim, J., Erb, A.M., Gao, F., Roman, M.O., Yang, Y., Petrov, S., Taylor, J.R., Masek, J.G., Morisette, J.T., Zhang, X.Y., Papuga, S.A., 2017. Monitoring land surface albedo and vegetation dynamics using high spatial and temporal resolution synthetic time series from Landsat and the MODIS BRDF/NBAR/albedo product. *Int. J. Appl. Earth Obs. Geoinf.* 59, 104–117.
- Wang, Z., Schaaf, C., Lattanzio, A., Carrer, D., Grant, I., Román, M., Camacho, F., Yu, Y., Sánchez-Zapero, J., Nickeson, J., 2019. Global surface albedo product validation best practices protocol. Version 1.0. In: Wang, Z., Nickeson, J., Román, M. (Eds.), Best Practice for Satellite Derived Land Product Validation. Land Product Validation Subgroup (WGCV/CEOS).
- Waring, R.H., Coops, N.C., Fan, W., Nightingale, J.M., 2006. MODIS enhanced vegetation index predicts tree species richness across forested ecoregions in the contiguous USA. *Remote Sens. Environ.* 103, 218–226.
- Warren, M.A., Simis, S.G.H., Selmes, N., 2021. Complementary water quality observations from high and medium resolution Sentinel sensors by aligning chlorophyll-a and turbidity algorithms. *Remote Sens. Environ.* 265, 112651.
- Weiss, M., Baret, F., 2016. S2ToolBox Level 2 products: LAI, FAPAR, FCOVER - Version 1.1. In: Sentinel-2 ToolBox Level2 Product.
- Weng, Q.H., Lu, D.S., Schubring, J., 2004. Estimation of land surface temperature-vegetation abundance relationship for urban heat island studies. *Remote Sens. Environ.* 89, 467–483.
- Werdell, P.J., Bailey, S.W., Franz, B.A., Harding Jr., L.W., Feldman, G.C., McClain, C.R., 2009. Regional and seasonal variability of chlorophyll-a in Chesapeake Bay as observed by SeaWiFS and MODIS-Aqua. *Remote Sens. Environ.* 113, 1319–1330.
- van der Werf, G.R., Randerson, J.T., Giglio, L., van Leeuwen, T.T., Chen, Y., Rogers, B.M., Mu, M.Q., van Marle, M.J.E., Morton, D.C., Collatz, G.J., Yokelson, R.J., Kasibhatla, P.S., 2017. Global fire emissions estimates during 1997–2016. *Earth Syst. Sci. Data* 9, 697–720.
- Whitcraft, A.K., Becker-Reshef, I., Justice, C.O., Jarvis, I., 2022. GEO global agricultural monitoring and global policy frameworks. In: Kavvada, A., Cripe, D., Friedl, L. (Eds.), Earth Observation Applications and Global Policy Frameworks. AGU, pp. 159–175.
- White, E.V., Roy, D.P., 2015. A contemporary decennial examination of changing agricultural field sizes using Landsat time series data. *Geo-Geogr. Environ.* 2, 33–54.
- White, J.C., Wulder, M.A., Hermosilla, T., Coops, N.C., Hobart, G.W., 2017. A nationwide annual characterization of 25 years of forest disturbance and recovery for Canada using Landsat time series. *Remote Sens. Environ.* 194, 303–321.
- White, J.C., Saarinen, N., Kankare, V., Wulder, M.A., Hermosilla, T., Coops, N.C., Pickell, P.D., Holopainen, M., Hyppä, J., Vaastaranta, M., 2018. Confirmation of post-harvest spectral recovery from Landsat time series using measures of forest cover and height derived from airborne laser scanning data. *Remote Sens. Environ.* 216, 262–275.
- Whitehead, P.G., Wilby, R.L., Battarbee, R.W., Kernan, M., Wade, A.J., 2009. A review of the potential impacts of climate change on surface water quality. *Hydrol. Sci. J.* 54, 101–123.
- WHO, 2016. Protecting surface water for health. In: Identifying, Assessing and Managing Drinking-Water Quality Risks in Surface-Water Catchments. World Health Organization.
- Wilson, E.H., Sader, S.A., 2002. Detection of forest harvest type using multiple dates of Landsat TM imagery. *Remote Sens. Environ.* 80, 385–396. pii s0034-4257(01)00318-2.
- Wood, E.M., Pidgeon, A.M., Radeloff, V.C., Keuler, N.S., 2012. Image texture as a remotely sensed measure of vegetation structure. *Remote Sens. Environ.* 121, 516–526.
- Woodcock, C.E., Loveland, T.R., Herold, M., Bauer, M.E., 2020. Transitioning from change detection to monitoring with remote sensing: A paradigm shift. *Remote Sens. Environ.* 238, 111558.
- Wooster, M.J., Roberts, G.J., Giglio, L., Roy, D.P., Freeborn, P.H., Boschetti, L., Justice, C., Ichoku, C., Schroeder, W., Davies, D., Smith, A.M.S., Setzer, A., Csizsar, I., Strydom, T., Frost, P., Zhang, T.R., Xu, W.D., De Jong, M.C., Johnston, J.M., Ellison, L., Vadrevu, K., Sparks, A.M., Nguyen, H., McCarty, J., Tanpitip, V., Schmidt, C., San-Miguel-Ayanz, J., 2021. Satellite remote sensing of active fires: History and current status, applications and future requirements. *Remote Sens. Environ.* 267, 112694.
- Wózniak, S.B., Stramski, D., Stramska, M., Reynolds, R.A., Wright, V.M., Miksic, E.Y., Cichocka, M., Cieplak, A.M., 2010. Optical variability of seawater in relation to particle concentration, composition, and size distribution in the nearshore marine environment at Imperial Beach, California. *J. Geophys. Res. Oceans* 115.

- Wright, P., Bergin, M., Dibb, J., Lefer, B., Domine, F., Carman, T., Carmagnola, C., Dumont, M., Courville, Z., Schaaf, C., Wang, Z.S., 2014. Comparing MODIS daily snow albedo to spectral albedo field measurements in Central Greenland. *Remote Sens. Environ.* 140, 118–129.
- Wu, L.L., Chen, Y.Q., Zhang, G.X., Xu, Y.J., Tan, Z.Q., 2021. Integrating the JRC monthly water history dataset and geostatistical analysis approach to quantify surface hydrological connectivity dynamics in an ungauged multi-lake system. *Water* 13, 497.
- Wulder, A.A., Skakun, R.S., Kurz, W.A., White, J.C., 2004. Estimating time since forest harvest using segmented Landsat ETM+ imagery. *Remote Sens. Environ.* 93, 179–187.
- Wulder, M.A., White, J.C., Loveland, T.R., Woodcock, C.E., Belward, A.S., Cohen, W.B., Fosnight, E.A., Shaw, J., Masek, J.G., Roy, D.P., 2016. The global Landsat archive: Status, consolidation, and direction. *Remote Sens. Environ.* 185, 271–283.
- Wulder, M.A., Coops, N.C., Roy, D.P., White, J.C., Hermosilla, T., 2018. Land cover 2.0. *Int. J. Remote Sens.* 39, 4254–4284.
- Wulder, M.A., Hermosilla, T., White, J.C., Hobart, G., Masek, J.G., 2021. Augmenting Landsat time series with Harmonized Landsat Sentinel-2 data products: Assessment of spectral correspondence. *Sci. Remote Sens.* 4, 100031.
- Wulder, M.A., Roy, D.P., Radeloff, V.C., Loveland, T.R., Anderson, M.C., Johnson, D.M., Healey, S., Zhu, Z., Scambos, T.A., Pahlevan, N., Hansen, M., Gorelick, N., Crawford, C.J., Masek, J.G., Hermosilla, T., White, J.C., Belward, A.S., Schaaf, C., Woodcock, C., Huntington, J.L., Lymburner, L., Hostert, P., Gao, F., Lyapustin, A., Pekel, J.-F., Strobl, P., Vermote, E., Cook, B.C., 2022. Fifty years of Landsat science and impacts. *Remote Sens. Environ.* 280, 113195.
- WWAP, 2012. The United Nations World Water Development Report 4: Managing Water under Uncertainty and Risk. World Water Assessment Programme, Paris.
- Xie, Y.H., Lark, T.J., 2021. Mapping annual irrigation from Landsat imagery and environmental variables across the conterminous United States. *Remote Sens. Environ.* 260, 112445.
- Yamazaki, D., Trigg, M.A., Ikeshima, D., 2015. Development of a global similar to 90 m water body map using multi-temporal Landsat images. *Remote Sens. Environ.* 171, 337–351.
- Yang, Y., Anderson, M.C., Gao, F., Johnson, D.M., Sun, L., Dulaney, W., Hain, C.R., Otkin, J.A., Prueger, J., Meyers, T.P., Bernacchi, C.J., Moore, C.E., 2021a. Phenological corrections to a field-scale, ET-based crop stress indicator: An application to yield forecasting across the US Corn Belt. *Remote Sens. Environ.* 257, 112337.
- Yang, Y., Anderson, M.C., Gao, F., Wood, J.D., Gu, L.H., Hain, C., 2021b. Studying drought-induced forest mortality using high spatiotemporal resolution evapotranspiration data from thermal satellite imaging. *Remote Sens. Environ.* 265, 112640.
- Ye, S., Rogan, J., Zhu, Z., Eastman, J.R., 2021a. A near-real-time approach for monitoring forest disturbance using Landsat time series: stochastic continuous change detection. *Remote Sens. Environ.* 252, 112167.
- Ye, S., Rogan, J., Zhu, Z., Hawbaker, T.J., Hart, S.J., Andrus, R.A., Meddens, A.J.H., Hicke, J.A., Eastman, J.R., Kulakowski, D., 2021b. Detecting subtle change from dense Landsat time series: Case studies of mountain pine beetle and spruce beetle disturbance. *Remote Sens. Environ.* 263, 112560.
- Yin, H., Brandão, A., Buchner, J., Helmers, D., Iuliano, B.G., Kimambo, N.E., Lewińska, K., E., Razenkova, E., Rizayeva, A., Rogova, N., Spawn, S.A., Xie, Y., Radeloff, V., 2020. Monitoring cropland abandonment with Landsat time series. *Remote Sens. Environ.* 246.
- Yin, F., Lewis, P.E., Gomez-Dans, J.L., 2022. Bayesian atmospheric correction over land: Sentinel-2/MSI and Landsat 8/OLI. *Geosci. Model Dev.* 15, 7933–7976.
- Yu, L., Wang, J., Clinton, N., Xin, Q.C., Zhong, L.H., Chen, Y.L., Gong, P., 2013. FROM-GC: 30 m global cropland extent derived through multisource data integration. *Int. J. Digit. Earth* 6, 521–533.
- Zanaga, D., Van De Kerchove, R., Daems, D., De Keersmaecker, W., Brockmann, C., Kirches, G., Wevers, J., Cartus, O., Santoro, M., Fritz, S., Lesiv, M., Herold, M., Tsendbazar, N.E., Xu, P., Ramoino, F., Arino, O., 2021. ESA WorldCover 10 m 2021 v200.
- Zhang, H.K.K., Roy, D.P., 2017. Using the 500 m MODIS land cover product to derive a consistent continental scale 30 m Landsat land cover classification. *Remote Sens. Environ.* 197, 15–34.
- Zhang, X.Y., Wang, J.M., Gao, F., Liu, Y., Schaaf, C., Friedl, M., Yu, Y.Y., Jayavelu, S., Gray, J., Liu, L.L., Yan, D., Henebry, G.M., 2017. Exploration of scaling effects on coarse resolution land surface phenology. *Remote Sens. Environ.* 190, 318–330.
- Zhang, X.Y., Liu, L.L., Liu, Y., Jayavelu, S., Wang, J.M., Moon, M., Henebry, G.M., Friedl, M.A., Schaaf, C.B., 2018. Generation and evaluation of the VIIRS land surface phenology product. *Remote Sens. Environ.* 216, 212–229.
- Zhang, D.J., Pan, Y.Z., Zhang, J.S., Hu, T.G., Zhao, J.H., Li, N., Chen, Q., 2020. A generalized approach based on convolutional neural networks for large area cropland mapping at very high resolution. *Remote Sens. Environ.* 247, 111912.
- Zhao, F., Huang, C.Q., Goward, S.N., Schleeweis, K., Rishmawi, K., Lindsey, M.A., Denning, E., Keddell, L., Cohen, W.B., Yang, Z.Q., Dungan, J.L., Michaelis, A., 2018. Development of Landsat-based annual US forest disturbance history maps (1986–2010) in support of the North American Carbon Program (NACP). *Remote Sens. Environ.* 209, 312–326.
- Zheng, B.J., Campbell, J.B., Serbin, G., Galbraith, J.M., 2014. Remote sensing of crop residue and tillage practices: Present capabilities and future prospects. *Soil Tillage Res.* 138, 26–34.
- Zhu, Z., 2017. Change detection using Landsat time series: A review of frequencies, preprocessing, algorithms, and applications. *ISPRS J. Photogramm. Remote Sens.* 130, 370–384.
- Zhu, Z., Woodcock, C.E., Olofsson, P., 2012. Continuous monitoring of forest disturbance using all available Landsat imagery. *Remote Sens. Environ.* 122, 75–91.
- Zhu, L., Ives, A.R., Zhang, C., Guo, Y., Radeloff, V.C., 2019a. Climate change causes functionally colder winters for snow cover-dependent organisms. *Nat. Clim. Chang.* 9, 886–893.
- Zhu, Z., Wulder, M.A., Roy, D.P., Woodcock, C.E., Hansen, M.C., Radeloff, V.C., Healey, S.P., Schaaf, C., Hostert, P., Strobl, P., 2019b. Benefits of the free and open Landsat data policy. *Remote Sens. Environ.* 224, 382–385.
- Zhu, Z., Zhou, Y.Y., Seto, K.C., Stokes, E.C., Deng, C.B., Pickett, S.T.A., Taubenbock, H., 2019c. Understanding an urbanizing planet: Strategic directions for remote sensing. *Remote Sens. Environ.* 228, 164–182.
- Zhu, Z., Qiu, S., Ye, S., 2022. Remote sensing of land change: A multifaceted perspective. *Remote Sens. Environ.* 282, 113266.